# SYNTHESIS AND EVALUATION OF NOVEL AMPHIPHILIC MACROMOLECULES AS DRUG CARRIERS AND THERAPEUTICS

By

JINZHONG WANG

A Dissertation submitted to the

Graduate School-New Brunswick

Rutgers, The State University of New Jersey

in partial fulfillment of the requirements

for the degree of

Doctor of Philosophy

Graduate Program in Chemistry

written under the direction of

KATHRYN E. UHRICH

and approved by

_____

_____

_____

_____

New Brunswick, New Jersey

October 2007

# ABSTRACT OF THE DISSERTATION

# SYNTHESIS AND EVALUATION OF NOVEL AMPHIPHILIC MACROMOLECULES AS DRUG CARRIERS AND THERAPEUTICS

**By JINZHONG WANG**

**Dissertation Director:**

**Professor Kathryn E. Uhrich**

Novel amphiphilic star-like macromolecules (ASM) and amphiphilic scorpion-like macromolecules (AScM) with double-chained and single-chained tails were synthesized and characterized. All macromolecules are composed of mucic acid-based hydrophobic "heads" and poly(ethylene glycol)-based hydrophilic "tails". Two different ASMs (**M12P5** and **M12P2x2**) and two different AScMs **(NC12P5** and **NC12P2x2**) were investigated to explore how branched PEG chains influence particle size, water-solubility, drug loading capacity, drug release rate and micelle stability. A hydrophobic, anti-inflammatory drug (indomethacin) was used to evaluate the encapsulation ability and release rate from the macromolecules. The double-chained macromolecules reduced the micellar sizes (10 nm for AScM, 22 nm for ASM) compared to single-chained macromolecules (18 nm for AScM, 48 nm for ASM). Through oil/water emulsion methods, drug-loading efficiency of ASM reached nearly 50%, higher than the self-assembled micelle AScMs, which display a drug-loading efficiency 30%. Indomethacin-loaded ASM released 52% of free drug within 50 hours, compared with 78% for AScM. Dynamic light scattering experiments showed that ASM minimized protein

interactions. Double-chained macromolecules perform as well or better than single-chained ones as drug delivery systems.

Several AScMs, which bear carboxylate groups on hydrophilic and hydrophobic domains, were also prepared. These macromolecules formed extremely stable micelles in aqueous solution with an average size of 20-35 nm and critical micelle concentration (CMC) as low as $10^{-7}$ M. Zeta potential values and micellar sizes in neutral buffer solutions correlated well with the carboxylate location and numbers. All macromolecules are capable of inhibiting unregulated uptake of highly-oxidized low density lipoproteins (LDL) by macrophages. This inhibition is caused by the interaction of scavenger receptors with negatively charged macromolecules, and closely responds to the number and location of negative charges. The AScM with one carboxylate at the hydrophobic domain and one carboxylate at hydrophilic domain exhibited the best LDL inhibition. To further enhance the treatment, a ligand GW 3965 was loaded into the AScM micelle.

## DEDICATION

This dissertation is dedicated to my father Mengen Wang, my mother Lianxiang Lu and my wife Lily Zhang.

## ACKNOWLEDGMENTS

I would like to give my first and special thanks to my affectionate PhD advisor, Dr. Kathryn E. Uhrich. The education she passed to me is the best through my life. She is a best friend, a kind mentor, a great scientist and an excellent communicator. I gained the most valuable attitude, thinking and manner to carry out scientific research. I also wish to thank my co-advisor, Dr. Prabhas Moghe. He often raises my interest and sparks inspiration in our research collaborations. His eagerness to help solve problems and move research forward greatly encouraged me. My deep appreciation also to my committee members, Dr. Edward Castner and Dr. Ralf Warmuth. Every time I had a conversation with them, I learned something to help publish my work.

I would like to thank the whole Uhrich research group, which feels like a big family. I want to thank my lab mates who shared my joys and struggles, Special thanks to Leilani de Rosario, a lady and a great mother who often cheers me up.

Finally, I thank my family. My father Mengen Wang and my mother Lianxiang Lu. They gave me extensive support in my studies towards a PhD degree. I would like to thank all the saints in the Franklin Park Church and my wife, Lily Zhang, who loves me deeply.

## TABLE OF CONTENTS

LIST OF SCHEMES

CHAPTER ONE



CHAPTER TWO



CHAPTER THREE

LIST OF TABLES

# CHAPTER ONE. OVERVIEW

## 1.1 Polymeric Micelle as Drug Carriers to Treat Cancers

### 1.1.1 Need for Drug Delivery Systems

Humans have utilized drugs to improve their health since early civilizations; beginning with the use of primary herbs, through the emergence of synthetic chemistry in the 20$^{th}$ century, and into the modern era of nanotechnology and combinatorial chemistry. Multiple natural and synthetic chemicals have been utilized as effective therapeutical drugs throughout history.[1] Historically, the method by which a drug is delivered gained less attention yet can have a significant effect on drug efficacy. Because of low water-solubility, poor membrane penetration and short *in vivo* half-life, a significant number of drugs molecules have been identified as poor therapeutic candidates.[2-4] With the potential to impact patients, a significant effort is currently made to overcome these problems.

### 1.1.2 Criteria for Drug Delivery Systems

Drug delivery systems are formulations or devices that improve the therapeutic efficiency of pharmaceuticals. The delivery system aims to control drug biodistribution profiles as well as drug concentration, release and targeting.[5] Drug delivery systems are designed to achieve several criteria: minimize drug degradation, prevent harmful side effects, increase drug bioavailability, and increase the fraction of drug accumulated in the required zone. The design for desirable drug delivery systems is summarized below.[6]

First, the drug delivery system should improve the drug's physiochemical properties, such as solubility and stability *in vivo*. Matrix encapsulation of poorly water-soluble drugs with a reservoir, in which the delivery system solubilizes the drugs and concurrently protects from macrophages and proteins is the most common delivery approach.[7, 8]

Second, a drug delivery system should transport the drug to the desired sites. Drug delivery systems may transport the therapeutic agents through the circulatory system or directly to a specific target such as an organ, tissue or cell. The delivery sysems should permeate physiological barriers such as the endothelial [9] and reticuloendothelial systems.[10] Thus, membrane permeability, delivery size and surface properties must be considered. Targeting strategies can be further utilized to direct the encapsulated drugs to a specific biological target.

Third, a drug delivery system should extend the drug's bioavailability.[11] For many treatments, the drug level in the circulatory system must be maintained within an effective concentration range. Often, delivery systems should provide sustained drug release within the optimum therapeutic concentration range for an extended period of time.

Last, a drug delivery system should be biocompatible.[12] The delivery system itself should not provoke undesired physiological effects such as toxicity.

### 1.1.3 Current Drug Delivery Developments

In the development of drug formulations, the goal is to optimize drug loading and release, prolong shelf-life and maintain low toxicity.[12] Liposomal delivery systems were first introduced as drug carriers over 40 years ago.[13, 14] A numbers of liposome-based delivery vehicles have been approved by the FDA for clinical applications.[14, 15] For the last three decades, researchers have specifically utilized nanotechnology to provide improvements in drug delivery and drug targeting.[13, 16] Most recently, colloidal drug carrier systems, including micellar solutions, [17] vesicle and liquid crystal dispersions[18, 19], as well as nanoparticle dispersions[20] show great promise.[11] Scheme 1-1 was adapted from Kaparissides's review article and outlines the classes of recently developed drug carriers.[11]

Other approaches to drug delivery are focused on crossing physical barriers, such as the blood-brain barrier, to better target the drug and improve its effectiveness.[21-23] Additional approaches address acceptable routes for the delivery of protein drugs other than via the gastro-intestinal tract, where protein degradation can occur.[24, 25]

### 1.1.4 Polymeric Micelles as Drug Delivery Systems to Treat Cancers

Cancer is one of the most threatening diseases and the second leading cause of death in the United States.[26] In cancer treatments, delivery strategies can be categorized as either lipid-based or polymer-based. Lipid-based nanomedicines, mainly in the form of liposomes, have been extensively studied and reviewed.[14, 27-29] Polymer-based

delivery systems includes polymer-drug conjugation[30, 31] and polymer-drug encapsulation. [32, 33]

Amphiphilic block copolymers can self-assemble in aqueous solution to form core-shell micellar nanostructures when the concentrations of the amphiphilic block copolymer are above the critical micellar concentration (CMC). Typical polymeric micelles contain a compact inner core, which serves as the “container” for hydrophobic drugs. As polymer micelles are generally more stable than hydrocarbon-based liposomes, prolonged drug release from polymeric micelles becomes possible.[34, 35] Multiple versions of synthetic copolymers have been invented to form micelles, hydrogels[36] and polymer microspheres.[37]

When applied to cancer therapies, polymeric micelles can accumulate in tumors after systemic administration.[28] Their biodistributions are largely determined by their physical and biochemical properties, such as particle size, hydrophobicity and surface biochemical properties.[38] A major issue that limits the systemic application of micellar nanocarriers is the nonspecific uptake by the reticular-endothelial system (RES). It is critical to have delivery systems that can circulate for a long time without significant accumulation in the liver or the spleen. The sizes and the surface features of micelles must be controlled for favorable biodistribution and intracellular trafficking. [39] The hydrophilic shells of micelles usually consist of poly(ethylene glycol) (PEG) which prevent the interaction between the hydrophobic micelle cores and biological membranes,

reduce uptake by the RES, and prevent the adsorption of plasma proteins onto nanoparticle surfaces.[11]

The effect of size on polymer micelle biodistribution was found to be organ-specific and non-linear.[34] Therefore, controlling micelle sizes can be critical for some applications. Parameters controlling the size of micelles include relative length of polymer blocks, polymer composition, as well as the solvent and drug used for encapsulation. Micellar nanoparticles are typically in a range of 20–100 nm. The sizes of polymeric micelles resemble that of natural transporting systems (e.g., virus and lipoprotein), which allow efficient cellular uptake through endocytosis.[38] Scheme 1-2 outlines current drug delivery systems based on nano-sized polymer materials.

## 1.2 Treatment for Atherosclerosis

### 1.2.1 Major Causes of Atherosclerosis

Atherosclerosis is a cardiovascular disease believed to be initiated by the subedothelial retention of atherogenic apolipoprotein B-containing lipoproteins.[40, 41] Low-density lipoproteins (LDL) are the major carriers of cholesterol in the bloodstream and have a single apoprotein B-100 molecule (Apo B-100) on their surface.[42] On Apo B-100, regions can interact with extracellular matrix molecules within vascular intima, as shown in Scheme 1-3. These extracellular matrix molecules are proteoglycans (PGs).[42] The interactions between LDL and PGs are believed to be electrostatic, based on the anionic glycosaminoglycan chains and the cationic amino acids on the Apo B-100 surface.[43, 44] Negative charge density on the PGs is one of the major parameters that determine the

association of PGs with lipoproteins.[40] Model studies demonstrated that binding occurs between the sulfate and carboxylate groups (both negatively charged) of PGs and arginine and the lysine-rich parts (positively charged) on LDL.[45]

After LDL combines with PGs, its structure undergoes serial changes and is eventually oxidized in the vascular intima.[43] The oxidation of LDL converts the positive charges on its surface into negative charges, leading to a reduced affinity of LDL with PGs. The dissociated highly oxidized LDL, which is now negatively charged, will be recognized by the scavenger receptors on macrophages or smooth muscle cells in the intima. These events may trigger the uncontrolled, unregulated uptake and accumulation of the modified LDL within macrophages and smooth muscle cells, which further initiates a cascade of atherogenic processes including foam cell formation.[43, 46, 47]

In summary, LDL oxidation and uptake by macrophages and smooth muscle cells in the intima is the major cause of atherosclerosis. Therefore, active agents that inhibit the binding of modified LDLs to scavenger receptors should be effective in the treatment of atherosclerosis.

### 1.2.2 Nanoparticles as Therapies

Suzuki et al. reported that class A scavenger receptor inhibitors would prevent the progress of atherosclerosis.[48] Brown and Goldstein later observed that negatively charged macromolecules, such as poly(vinyl sulfate), polyG and maleyl-LDL, inhibited the binding of radioactive LDL to the surface of macrophages.[49] Within the last five years,

Yushiizumi et al. successfully made a series of small molecular weight compounds bearing carboxylate and sulfate functional groups.[50, 51] The compounds proved active in scavenger receptor inhibition. The intriguing research of others highlights our hypothesis that negatively charged nanoparticles will prevent highly oxidized LDL uptake.

## 1.3 References


1. Drews, J., Drug discovery: A historical perspective. *Science,* **2000**. *287*: p. 1960-1964.
2. Weiss, R.and Chrostian, M., New cisplatin analogues in development: A review. *Drugs,* **1993**. *46*: p. 360-377.
3. Lipinski, C.A., Lombardo, F., Dominy, B. and Feeney, P., Experimental and computational approaches to estimate solubility and permeability in drug discovery. *Adv. Drug Delivery Rev.,* **2001**. *46*: p. 3-26.
4. Langer, R., Prolonged regional nerve blockade. Injectable biodegradable bupivacaine/polyester microspheres. *Pharmc. Ther.,* **1983**. *21*: p. 35-51.
5. Pillai, O., Dhnikula, A. and Panchagnula, R., Polymers in drug delivery. *Curr. Opin. Chem. Biol,* **2001**. *5*: p. 439-446.
6. Tian, L., in PhD Dissertation. **2004**, Rutgers University: New Brunswick.
7. Kwon, G., Natio, M., Kataoka, K., Yokoyama, M., Sakurai, Y. and Okano, T., Block copolymer micelles as vehicles for hydrophobic drugs. *Colloids and Surfaces B: Biointerfaces,* **1994**. *2*: p. 429-434.
8. Langer, R., New methods of drug delivery. *Science,* **1990**. *11*: 249-250.
9. Deen, W., Bridges, C. and Brenner, B., Lateral diffusion in planar lipid bilayers: a fluorescence recovery after photobleaching. *J. Membr. Biol.,* **1983**. *71*: p. 1-10.
10. Arshady, R., Molecular compounds having complementary surfaces to targets. *J. Mol. Recog.,* **1996**. *9*: p. 536-542.
11. Kaparissides, C., Alexandridou, S., Kotti, K. and Chaitidou, S., Recent advances in novel drug delivery systems. *Recent Adv. Novel Drug Delivery Systems,* **2006**. *2*: p. 1-11.
12. Charman, W., Chan, H., Finnin, B. and Charman, S., Drug delivery: A key factor in realising the full therapeutic potential of drugs. *Drug Develop. Res.,* **1999**. *46*: p. 316-327.
13. Bangham, A., Standish, M. and Watkins, J., Diffusion of univalent ions across the lamellae of swollen phospholipids. *J. Mol. Biol.,* **1965**. *13*: p. 238-252.
14. Barenholz, Y., Liposome application: problems and prospects. *Curr. Opin. Colloid Interface Sci.,* **2001**. *6*: p. 66-77.
15. Duncan, R., Polymer conjugates as anticancer nanomedicines. *Nat. Rev. Cancer,* **2006**. *6*: p. 688-701.
16. Marty, J., Oppenheim, R. and Speiser, P., Nanoparticles: new colloidal drug delivery system. *Pharm. Acta Helv.,* **1978**. *53*: p. 17-23.
17. Torchilin, V., Structure and design of polymeric surfactant-based drug delivery systems. *J. of Control. Rel.,* **2001**. *73*: p. 137-172.
18. Muller-Goymann, C., Physicochemical characterization of colloidal drug delivery systems such as reverse micelles, vesicles, liquid crystals and nanoparticles for topical administration. *Eur. J. Pharm. Biopharm.,* **2004**. *58*: p. 343-356.
19. Santini Jr, J., Richards A., Scheidt, R., Cima, M. and Langer, R., Microchips as controlled drug-delivery devices. *Angew. Chem. Int. Ed.,* **2000**. *39*: p. 2396-2407.

20. Kopecek, J., Smart and genetically engineered biomaterials and drug delivery systems. *Eur. J Pharm. Sci.,* **2003**. *20*(1-6): p. 1-16.
21. Schmitt, A. and Lesniak, M., Overcoming the barriers of the central nervous system: novel methods of drug delivery to brain cancer. *Horizons in Cancer Research,* **2006**. *27*: p. 1-23.
22. Batrakova, E and Kabanov, A., Polymers for CNS drug delivery. *Pharm. Tech. Eur.,* **2007**. *19*(5): p. 23-24.
23. Gelperina, S., Brain delivery by nanoparticles. *Drugs Pharm. Sci.,* **2006**. *159*: p. 273-318.
24. Agnihotri, S., Mallikarjuna, N. and Aminabhavi, T., Recent advances on chitosan-based micro- and nanoparticles in drug delivery. *J. Control. Rel.,* **2004**. *100*: p. 5-18.
25. Sood, A. and Panchagnula, R., Peroral route: An opportunity for protein and peptide drug delivery. *Chem.l Rev.,* **2000**. *101*: p. 3275-3303.
26. Jemal, A., Siegel, R., Ward, E., Murray, T., Xu, J., Smigal, C. and Thun, M., Cancer statistics, 2006. CA. *Cancer J. Clin.,* **2006**. *56*: p. 106-130.
27. Park, J., Benz, C. and Martin, F., Future directions of liposome- and immunoliposomebased cancer therapeutics. *Semin. Oncol.,* **2004**. *31*: p. 196-205.
28. Cattel, L., Ceruti, M. and Dosio, F., *From conventional to stealth liposomes a new frontier in cancer chemotherapy. Tumori,* **2003**. *89*: p. 237-249.
29. Patel, G. and Sprott, G., Archaeobacterial ether lipid liposomes (archaeosomes) as novel vaccine and drug delivery systems. *Crit. Rev. Biotechnol.,* **1999**. *19*: p. 317-357.
30. Haag, R., Supramolecular drug-delivery systems based on polymeric core-shell architectures. *Angew. Chem. Int. Ed.,* **2004**. *43*: p. 278-282.
31. Haag, R. Polymer therapeutics: Concepts and applications. *Angew. Chem. Int. Ed.,* **2006**. *45*: p. 1198-215.
32. Lavasanifar, A., Samuel, J. and Kwon, G., Poly(ethylene oxide)-block-poly(L-amino acid) micelles for drug delivery. *Adv. Drug Deliv. Rev.,* **2002**. *54*: p. 169-190.
33. Jones, M. Polymeric micelles: a new generation of colloidal drug carriers. *Eur. J. Pharm. Biopharm.,* **1999**. *48*(101-103).
34. Torchilin, V., Block copolymer micelles as a solution for drug delivery problems. *Expert Opin. Therapeutic Pat.,* **2005**. *15*: p. 63-75.
35. Kwon, G. and Kataoka, K., Block-copolymer micelles as long-circulating drug vehicles. *Adv. Drug Deliv. Rev.,* **1995**. *16*: p. 295-309.
36. Kabanov, A., Batrakova, E. and Alakhov, V., Pluronic (R) block copolymers as novel polymer therapeutics for drug and gene delivery. *J. Control. Rel.,* **2002**. *82*: p. 189-212.
37. Galindo-Rodriguez, S., Allemann, E., Fessi, H. and Doelker, E., Physicochemical parameters associated with nanoparticle formation in the salting-out, emulsification-diffusion, and nanoprecipitation methods. *Pharm. Res.,* **2004**. *21*: p. 1428-439.
38. Kabanov, A., Slepnev, V, Kuznetsova, L., Batrakova, E., Alakhov, V. and Nubarov, P., Pluronic micelles as a tool for low-molecular compound vector delivery into a cell. *Biochem Int.* **1992** *26(6)*: p. 1035-42.
39. Gref, R., Minamitake, Y., Peracchia, M., Trubetskoy, V., Torchilin, V. and Langer, R., Biodegradable long-circulating polymeric nanospheres. *Science,* **1994**. *263*: p. 1600-1603.

40. Williams, K. and Tabas, I., The response-to-retention hypothesis of early atherogenesis. *Arterioscler., Thromb. Vasc. Bio.,* **1995**. *15*: p. 551-561.
41. Olsson, U., Ostergren-Lunden, G. and Moses, J., Glycosaminoglycan-lipoprotein interaction. *Glycoconjugate J.,* **2001**. *18*: p. 789-797.
42. Camejo, G., Hurt-Camejo, E., Wiklund, O. and Bondjers, G., Association of apo B lipoproteins with arterial proteoglycans: pathological significance and molecular basis. *Atherosclerosis,* **1998**. *139*: p. 205-222.
43. Camejo, G. The extracellular matrix on atherogenesis and diabetes-associated vascular disease. *Atherosclerosis Supplements,* **2002**. *3*(1): p. 3-9.
44. Guyton, J., Phospholipid hydrolytic enzymes in a cesspool of arterial intimal lipoproteins : A mechanism for atherogenic lipid accumulation. *Arterioscler. Thromb. Vasc. Biol.,* **2001**. *21*: p. 884-886.
45. Jackson, R. and Cardin, A., Glycosaminoglycans: molecular properties, protein interactions, and role in physiological processes. *Physiol Rev,* **1991**. *71*: p. 481-539.
46. Rosengren, B., Camejo, G. and Hurt-Camejo, E., Lipoprotein oxidation and measurements of thiobarbituric acid reacting substances formation in a single microtiter plate: its use for evaluation of antioxidants. *Anal. Biochem.,* **1993**. *208*: p. 10-15.
47. Brown, M. and Goldstein, J., low-density lipoprotein pathway and its relation to atherosclerosis. *Ann. Rev. Biochem.,* **1983**. *52*: p. 223-261.
48. Suzuki, H., Kurihara, Y., Takeya, M., Kumada, N., Kataoka, M., Jishage, K., Ueda, O., Sakaguchi, H., Higashi, T., Suzuki, T., Takashima, Y, Kawabe, Y., Cynshi, O., Wada, Y., Honda, M., Kurihara, H., Aburatani, H., Doi, T., Matsumoto, A., Azuma, S., Noda, T., Toyoda, Y., Itakura, H., Yazaki, Y., Horiuchi, S., Takahashi, K., Kruijt, J., van Berkel, T., Steinbrecher, U., Ishibashi, S., Maeda, N., Gordon, S. and Kodama, T., A role for macrophage scavenger receptors in atherosclerosis and susceptibility to infection. *Nature*, **1997**. *386*: p. 292-296.
49. Brown, M. and Goldstein, J., low-density lipoprotein pathway and its relation to atherosclerosis. *Ann. Rev. Biochem.,* **1983**. *52*: p. 223-261.
50. Yoshiizumi, K., Nakajima, F., Dobashi, R., Nishimura, N. and Ikeda, S., Studies on scavenger receptor inhibitors. Part 1: synthesis and structure-activity relationships of novel derivatives of sulfatides. *Bioorg. Med. Chem.,* **2002**. *10*(8): p. 2445-2460.
51. Yoshiizumi, K., Nakajima, F., Dobashi, R., Nishimura, N. and Ikeda, S., 2,4-Bis(octadecanoylamino)benzenesulfonic acid sodium salt as a novel scavenger receptor inhibitor with low molecular weight. *Bioorg. Med. Chem., Lett.,* **2004**. *14*(11): p. 2791-2795.

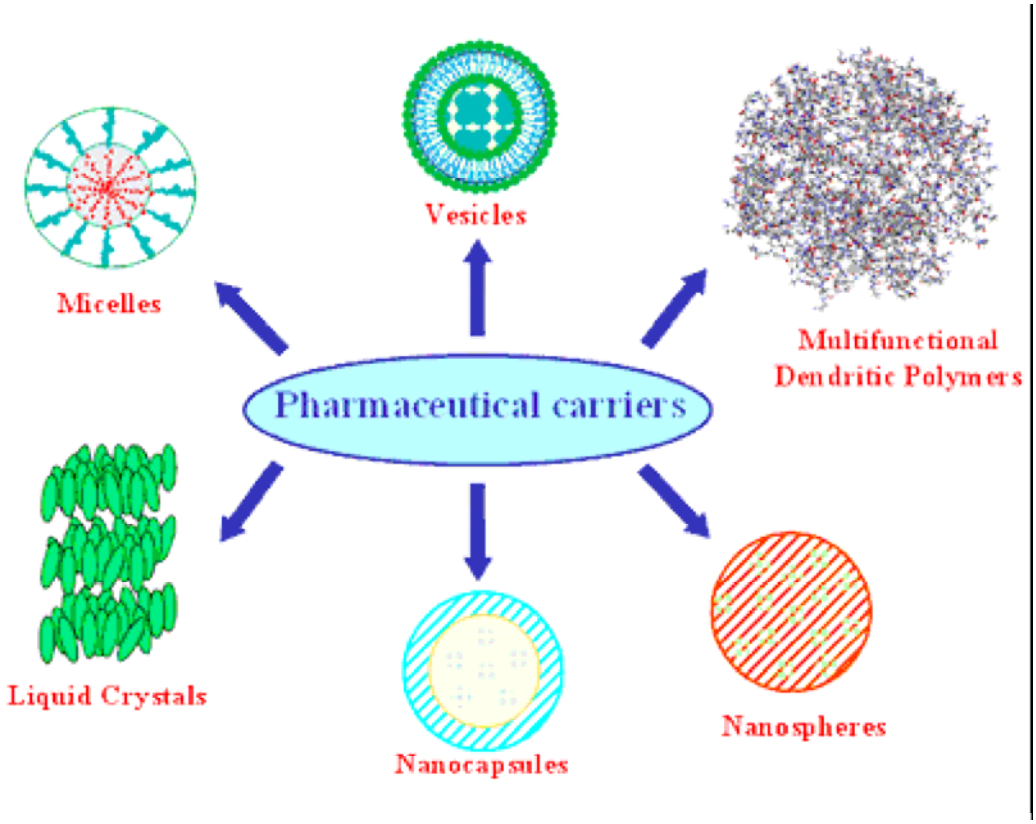


Scheme 1-1 Current pharmaceutical carriers for enhanced drug delivery [11]

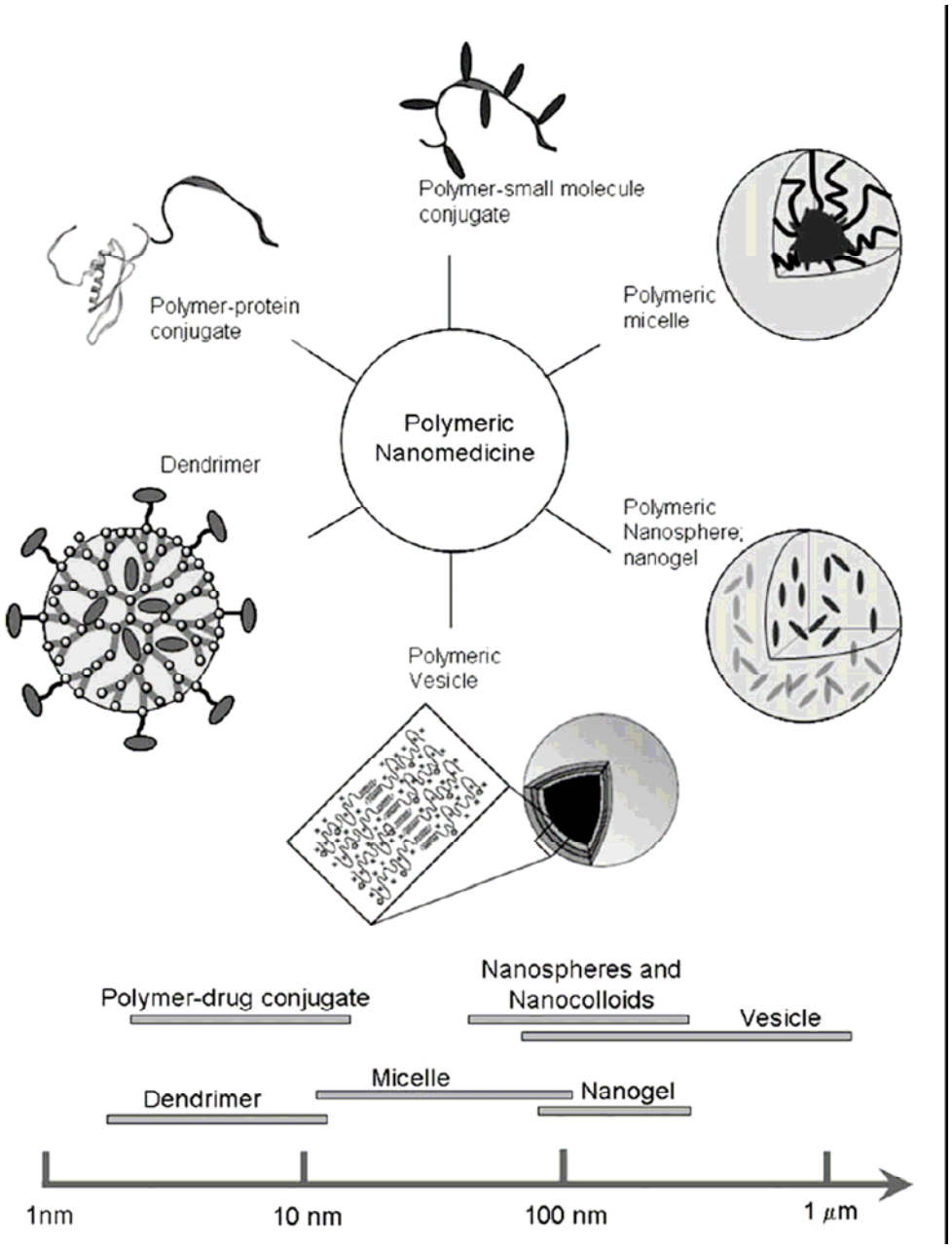


Scheme 1-2 Schematic illustration of polymeric drug delivery systems (from Rong Tong's review article: Anticancer Polymeric Nanomedicines published in Polymer Reviews, 2007, 47:345–381,

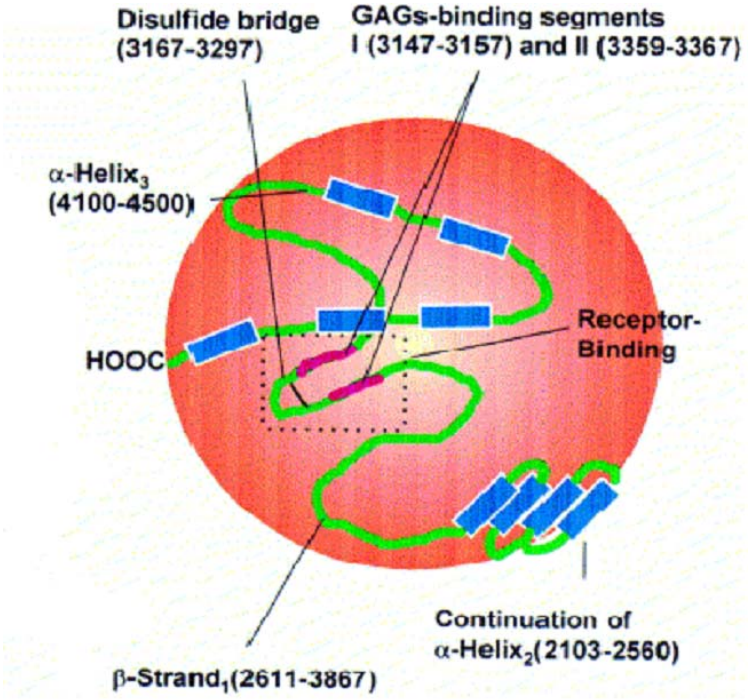


Scheme 1-3 Proteoglycans (PGs) form complex with low density lipoprotein (LDL) [42]

# CHAPTER TWO. AMPHIPHILIC STAR-LIKE MACROMOLECULES CHAIN-END FUNCTIONALIZATION

## 2.1 Introduction

Many research groups are currently focusing on the development of novel polymer architectures such dendrimers and hyperbranched polymers to generate micelles that are covalently bound as single molecules ("unimolecular micelles") to avoid undesirable dissociation while maintaining nanosized systems.[1-6] Similar to the dendrimers and hyperbranched polymers, amphiphilic star-like macromolecules (ASMs) are nanoscale, covalently bound polymeric micelles in which the hydrophobic and hydrophilic polymer segments are covalently connected such that one macromolecule behaves as a single micellar entity. [7]

Initial studies on cytotoxicity, drug encapsulation, drug release and polymer degradation demonstrated the effectiveness of the first generation ASMs as nanoscale drug delivery systems.[8, 9] With respect to drug encapsulation or solubilization, the aqueous solubility of various drug molecules displayed enhanced solubilization upon encapsulation within the ASMs: indomethacin by 2-fold,[10] suloctidil by 70- to 80- fold, and triclosan by 120 to 150-fold.[11, 12] We hypothesized that their drug loading ability can be enhanced by increasing the lipophilicity and size of the core.

In this chapter, the next generation ASMs (Scheme 2-1) were designed with four arms or branches, each connected through a tetra-functional core and spacer molecules to increase

the lipophilic environment and better encapsulate hydrophobic drug molecules. In addition to evaluating the ASMs for drug encapsulation, we utilize the amphiphilic character and nanosize to promote interactions with cell membranes and related biological systems. For example, a negatively charged, carboxylic acid on the chain ends of the ASMs preferentially interacts with low-density lipoproteins (LDL) via charge-charge interactions to prevent prolonged retention and aggregation of LDL.[13] As another example, a nucleophilic amino group on the chain ends of the ASMs can be readily conjugated with a cancer cell targeting group, such as folic acid, to promote interactions with cancer cells rather than normal cells.[14]

Based on the interesting results from selected end-functionalized ASMs, six ASMs were synthesized with neutral (methoxy), basic (amine) and acidic (carboxylic acid) groups for hydrophobic (C6 alkyl chains) and more hydrophobic (C12 alkyl chains) ASM core molecules.

## 2.2 Experimental Procedures

### 2.2.1 Materials

Heterobifunctional poly(ethylene glycol) ($HCl{\cdot}NH_2$-PEG-COOH) with molecular weights of 5000 Da and poly(ethylene glycol) bis-amine ($NH_2$-PEG-$NH_2$) with molecular weights of 3400 Da was obtained from Nektar (San Carlos, CA). 4-(Dimethylamino)pyridinium *p*-toluenesulfonate (DPTS) was prepared as previously described.[15] Monomethoxy-poly(ethylene glycol) (mPEG) with molecular weights of 5000 Da was purchased from Sigma-Aldrich. All PEG reagents were dried by azeotropic

distillation with toluene. 4-Aminothiolphenol, pentaerythritol tetraacrylate, N-hydroxyl succinimide (NHS) (99+%), triethylamine (99.7%) and 1,3-dicyclohexylcarbodiimide (DCC) in 1 M methylene chloride solution were purchased from Aldrich and used as received. All other reagents and solvents were reagent grade and used as received.

### 2.2.2 Methods

Chemical structures and compositions were confirmed by $^{1}H$ and $^{13}C$ NMR spectroscopy with samples (~ 5-10 mg/ml) dissolved in $CDCl_3$ solvent on Varian 200 MHz and 400 MHz spectrometers, using tetramethylsilane as the reference signal. IR spectra were recorded on a Mattson Series spectrophotometer (Madison Instruments, Madison, WI) by solvent (methylene chloride) casting on a KBr pellet. Negative ion-mass spectra were recorded with ThermoQuest Finnigan $LCQ^{TM}_{DUO}$ System (San Jose, CA) that includes a syringe pump, an optional divert/inject valve, an atmospheric pressure ionization (API) source, a mass spectrometer (MS) detector, and the Xcalibur data system.

Gel permeation chromatography (GPC) was used to obtain molecular weight and the polydispersity index (PDI). Gel permeation chromatography was performed on Perkin-Elmer Series 200 LC system equipped with Pl gel column (5 μm, mixed bed, ID 7.8 mm, length 300 mm) and with a Water 410 refractive index detector, Series 200 LC pump and ISS 200 Autosampler. A Digital Celebris 466 computer was used to automate the analysis via PE Nelson 900 interface and PE Nelson 600 Link box. Perkin-Elmer Turbochrom 4 software was used for data collection as well as data processing. Tetrahydrofuran (THF) was the eluent for analysis and solvent for sample preparation.

Sample was dissolved into THF (~ 5 mg/ml) and filtered through a 0.45 μm PTFE syringe filter (Whatman, Clifton, NJ) before injection into the column at a flow rate of 1.0 ml/min. The average molecular weight of the sample was calibrated against narrow molecular weight polystyrene standards (Polysciences, Warrington, PA).

### 2.2.3. Synthesis of 5 (Methoxy-terminated ASM)

Synthetic pathway for neutral macromolecules are elucidated in Scheme 2-2

#### 2.2.3.1 Synthesis of 3 (Pre-core)

Pentaerythritol tetraacrylate (**2**) (1.0 g, 3.0 mmol) dissolved in acetonitrile (5 ml) was added dropwise to a solution of triethylamine (2.5 ml, 18 mmol) and 4-aminothiolphenol (1.9 g, 15 mmol) in acetonitrile (20 ml) in an ice-water bath. After 12 h, the reaction mixture was evaporated to dryness under vacuum. The residue was dissolved into methylene chloride (50 ml), washed with 0.1 N HCl (25 ml) and brine (3x25 ml). The organic portion was then dried over $MgSO_4$, filtered and rotary-evaporated to dryness. The crude product was purified by silica gel chromatography using methylene chloride:ethyl ether:isopropanol (78:20:2) as eluent. The sample was collected and the solvent removed by evaporation to dryness.

Yield: 91% (white solid). $^{1}$H NMR ($CDCl_3$): δ 7.21 (d, 8H, ArH), 6.95 (d, 8H, ArH), 4.09 (s, 8H, $CH_2$), 3.75 (s, 8H, $NH_2$), 2.94 (t, 8H, $CH_2$), 2.53 (t, 8H, $CH_2$). $^{13}$C NMR ($CDCl_3$): δ 171.49 (C=O), 146.70 (ArC-N), 134.95 (ArC), 115.68 (ArC), 121.336 (ArC-$CH_2$), 62.49 ($CH_2$-O), 41.83 (*t*-C), 34.37 ($CH_2$), 31.48 ($CH_2$). IR (KBr, $cm^{-1}$): 3459, 3371, 1597,

733 (N-H), 3026, 825( Ar-H), 1732(C=O), 1278 (C-N), 1237, 1176 (C-O), 1027 (C-S). $T_m$=94-94.5 ˚C. FW: 853.1; MS: 853.6.

The $^{13}C$ NMR spectrum of compound **3** (pre-core) is shown in Scheme 2-3.

**2.2.3.2 Synthesis of 4 (New Core)**

Mucic acid derivatives **1**, referred to as MA(6) **1a** and MA(12) **1b**, were synthesized following previously described methods.[16, 17] Using MA(6) as an example, **1a** (3.1 g, 5.1 mmol), compound **3** (1.0 g, 1.2 mmol) and DPTS (0.38 g, 1.3 mmol) were added into a solution of $CH_2Cl_2$ (30 ml) and DMF (6 ml). DCC in $CH_2Cl_2$ solution (5.2 ml, 1.0 M) was added dropwise under argon**.** After 12 h reaction at room temperature, the DCC side product was removed by filtration, and the filtrate washed with 0.1 N HCl (20 ml) and brine (20 ml). After solvent removal by rotary evaporation, the crude product was purified by precipitation into hexane (30 ml) from $CH_2Cl_2$ (3 ml). Unreacted **1a** was removed by silica gel chromatography using $CH_2Cl_2$:$CH_3OH$ (95:5) as eluent. The sample was collected and the solvent removed by evaporation to dryness.

**4a**: Yield: 70% (yellow solid). $^1H$ NMR ($CDCl_3$): δ 7.42 (d, 8H, ArH), 7.30 (d, 8H, ArH), 5.83 (d, 4H, CH), 5.68 (d, 4H, CH), 5.45 (t, 4H, CH). 5.16 (t, 4H, CH), 4.13 (s, 8H, $CH_2$), 3.08 (t, 8H, $CH_2$), 2.60 (t, 8H, $CH_2$), 0.89 (t, 48H, $CH_3$). IR (KBr, $cm^{-1}$): 3336 (N-H), 1754, 1716, 1687, 1656 (C=O), 1401 (C-N), 1241, 1154 (C-O), 1032 (C-S). $T_m$=82-83˚C.

**4b**: Yield: 68% (yellow solid). $^1H$-NMR ($CDCl_3$): δ 7.24 (d, 8H, ArH), 5.84 (d, 4H, CH). 5.70 (d, 4H, CH), 5.40 (t, 4H, CH), 5.14 (t, 4H, CH), 4.12 (s, 8h, $CH_2$), 3.08 (t, 8H, $CH_2$),

2.60 (t, 8H, $CH_2$), 2.45 (m, 16H, $CH_2$), 2.26 (m, 16H, $CH_2$), 1.62 (m, 32H, $CH_2$), 1.24 (m, 256H, $CH_2$), 0.89 (t, 48H, $CH_3$). IR (KBr, $cm^{-1}$): 3332 (N-H), 1749, 1716, 1687, 1651 (C=O), 1399 (C-N), 1238, 1145 (C-O), 1031 (C-S). $T_m$=102-103˚C.

The $^1$H NMR spectrum of compound **4b** (New core) is shown in Scheme 2-3.

**2.2.3.3 Synthesis of 5 (ASM)**

Monomethoxy-poly(ethylene glycol) (mPEG) ($M_w$=5.0 kDa) (2.0 g, 0.4 mmol) was dehydrated by azeotropic distillation in toluene (20 ml). Using **5a** as an example, molecules **4a** (0.28 g, 0.10 mmol) and DPTS (0.026 g, 0.084 mmol) were dissolved in methylene chloride (30 ml) and added dropwise to the mPEG solution in toluene at room temperature. DCC solution in methylene chloride (1.0 ml, 1.0 M) was added dropwise under argon gas. After 12 h at room temperature**,** the DCC side product was removed by vacuum filtration. The filtrate was washed with brine (3x10 ml), dried over anhydrous sodium sulfate and evaporated to dryness. Crude product was precipitated by recrystallization in diethyl ether (30 ml) from methylene chloride (3 ml). To remove the unreacted mPEG, the polymer solution was dialyzed against water using a Spectra/pro regenerated cellulose membrane (Spectrum Laboratories, Rancho Dominguez, CA) with 100,000 Mw cut-off. Polymer (100 mg) dissolved in PBS (50 ml) was placed into the dialysis bag and dialyzed against 4 L deionized water. After 8 h, the contents of the dialysis bag were lyophilized (FreeZone© Benchtop and Console Freeze Dry System, Labconco, Kansas City, Missouri) overnight.

**5a:** Yield: 76% (white solid). $^{1}$H-NMR ($CDCl_3$): δ 7.42 (d, 8H, ArH), 7.31 (d, 8H, ArH), 5.72 (m, 8H, CH), 5.39 (t, 4H, CH), 5.25 (t, 4H, CH), 4.13 (s, 8H, $CH_2$), 3.68 (m, ~1.8kH, $CH_2$), 3.60 (s, 12H, $CH_3$), 3.08 (t, 8H, $CH_2$), 2.48 (m, 16H, $CH_2$), 2.26 (m, 16H, $CH_2$), 1.62 (m, 32H, $CH_2$), 1.33 (m, 64H, $CH_2$), 0.90 (t, 48H, $CH_3$). IR (KBr, $cm^{-1}$): 3333 (N-H), 2884 (C-H), 1749, 1650 (C=O), 1410 (C-N), 1242, 1149, 1111 (C-O). $T_m$=57.2 ˚C; $T_c$=33.3 ˚C. $M_w$: 25,800; PDI: 1.2.

**5b**: Yield 69% (white solid). $^{1}$H-NMR ($CDCl_3$): δ 7.40 (d, 8H, ArH), 7.30 (d, 8H, ArH), 5.71 (m, 8H, CH), 5.37 (t, 4H, CH), 5.25 (t, 4H, CH), 4.14 (s, 8H, $CH_2$) 3.68 (m, ~1.8kH, $CH_2$), 3.58 (s, 12H, $CH_3$), 3.06 (t, 8H, $CH_2$), 2.60 (t, 8H, $CH_2$), 2.46 (m, 16H, $CH_2$), 1.63 (m, 32H, $CH_2$), 1.26 (m, 256H, $CH_2$), 0.88 (t, 48H, $CH_3$). IR (KBr, $cm^{-1}$): 3338 (N-H), 2887 (C-H), 1749, 1651 (C=O), 1410 (C-N), 1242, 1149, 1113 (C-O). $T_m$=56.4 ˚C $T_c$=30.2 ˚C . $M_w$: 27,500; PDI: 1.1.

### 2.2.4 Synthesis of 7 (the carboxyl-terminated ASM)

The synthetic pathway is outlined in Scheme 2-4. Using **7a** as an example, molecule **4a** (0.28 g, 0.10 mmol) and N-hydroxyl succinimide (NHS) (1.38 g, 1.2 mmol) were dissolved in 20 ml methylene chloride. DCC in methylene chloride (1.0 ml, 1.0 M) was added dropwise under argon. After 12 h, the DCC side product was removed by vacuum filtration. The organic portion was washed with brine (3x10 ml), dried over anhydrous sodium sulfate, and evaporated to dryness. TLC (ethyl acetate: hexane/2:1) was used to monitor the NHS activation reaction to yield **6a**.

**6a:** Yield 90% (pale yellow solid). $^{1}$H-NMR ($CDCl_3$): δ 7.38 (d, 8H, ArH), 7.31 (d, 8H, ArH), 5.80 (d, 4H, CH), 5.71 (d, 4H, CH), 5.55 (t, 4H, CH), 5.22 (t, 4H, CH), 4.13 (s, 8H, $CH_2$) 3.07 (t, 8H, $CH_2$), 2.81 (t, 16H, $CH_2$), 2.58 (t, 8H, $CH_2$), 2.46 (m, 16H, $CH_2$), 2.44 (m, 16H, $CH_2$), 1.63 (m, 32H, $CH_2$), 1.30 (m, 64H, $CH_2$), 0.88 (t, 48H, $CH_3$). IR (KBr, $cm^{-1}$): 3341 (N-H), 2931, 2857 (C-H), 1747 (C=O), 1389 (C-N), 1203, 1146, 1103 (C-O). $T_m$= 73-76 ºC.

**6b:** Yield 85% (pale yellow solid). $^{1}$H-NMR ($CDCl_3$): δ 7.36 (d, 8H, ArH), 7.25 (d, 8H, ArH), 5.89 (d, 4H, CH), 5.68 (d, 4H, CH), 5.52 (t, 4H, CH), 5.20 (t, 4H, CH), 4.10 (s, 8H, $CH_2$), 3.03 (t, 8H, $CH_2$), 2.76 (t, 16H, $CH_2$), 2.60 (t, 8H, $CH_2$), 2.48 (m, 16H, $CH_2$), 2.43 (m, 16H, $CH_2$), 1.66 (m, 32H, $CH_2$), 1.22 (m, 256H, $CH_2$), 0.85 (t, 48H, $CH_3$). IR (KBr, $cm^{-1}$): 3330 (N-H), 2924, 2853 (C-H), 1749 (C=O), 1380 (C-N), 1233, 1146, 1112 (C-O). $T_m$= 96-98 ºC.

Heterobifunctional poly (ethylene glycol) ($HCl{\cdot}NH_2$-PEG-COOH) was dehydrated by azeotropic distillation in toluene (20 ml). The NHS-activated core molecule **6a** and heterobifunctional poly(ethylene glycol) ($HCl{\cdot}NH_2$-PEG-COOH) were dissolved in 10 ml methylene chloride, then triethylamine (1.0 g, 9.7 mmol) added and the reaction mixture stirred at room temperature. After 30 h, the reaction mixture was washed by 0.1 N HCl (10 ml) and brine (3x10 ml). The organic portion was dried over anhydrous sodium sulfate, filtered and evaporated to dryness. Crude product was precipitated by recrystallization in diethyl ether (30 ml) from methylene chloride (3 ml). Further purification was carried out using dialysis, as described for compound **5** above.

**7a:** Yield: 71% (white solid). $^1$H-NMR ($CDCl_3$): δ 7.37 (d, 8H, ArH), 7.26 (d, 8H, ArH), 5.71 (m, 8H, CH), 5.36 (t, 4H, CH), 5.22 (t, 4H, CH), 4.09 (s, 8H, $CH_2$) 3.66 (m, ~1.8kH, $CH_2$), 3.56 (s, 12H, $CH_3$), 3.03 (t, 8H, $CH_2$), 2.45 (m, 16H, $CH_2$), 2.24 (m, 16H, $CH_2$), 1.56 (m, 32H, $CH_2$), 1.30 (m, 64H, $CH_2$), 0.82 (t, 48H, $CH_3$). IR (KBr, $cm^{-1}$): 3333 (N-H), 2887 (C-H), 1749, 1760, 1650 (C=O), 1410 (C-N), 1242, 1149, 1110 (C-O). $T_m$=51.8 ˚C; $T_c$=24.2 ˚C . $M_w$: 23,400; PDI: 1.2.

**7b:** Yield: 65% (white solid). $^1$H-NMR ($CDCl_3$): δ 7.35 (d, 8H, ArH), 7.26 (d, 8H, ArH), 5.73 (m, 8H, CH), 5.33 (t, 4H, CH), 5.20 (t, 4H, CH), 4.10 (s, 8H, $CH_2$) 3.68 (m, ~1.8kH, $CH_2$), 3.56 (s, 12H, $CH_3$), 3.00 (t, 8H, $CH_2$), 2.44 (m, 16H, $CH_2$), 2.29 (m, 16H, $CH_2$), 1.54 (m, 32H, $CH_2$), 1.34 (m, 256H, $CH_2$), 0.83 (t, 48H, $CH_3$). IR (KBr, $cm^{-1}$): 3329 (N-H), 2878 (C-H), 1740, 1755, 1651 (C=O), 1412 (C-N), 1241, 1145, 1105 (C-O). $T_m$=49.0 ˚C; $T_m$=22.8 ˚C. $M_w$: 26,800; PDI: 1.3.

### 2.2.5 Synthesis of 8 (the amine-terminated ASM)

The synthetic pathway is outlined in Scheme 2-4. Poly(ethylene glycol) bis-amine (Mw=3.4 kDa) (13.6 g, 0.4 mmol) was dehydrated by azeotropic distillation in toluene (20 ml). Using **8a** as an example, molecule **4a** (0.28 g, 0.10 mmol) and DPTS (0.026 g, 0.084 mmol) in methylene chloride (30 ml) were added to the *bis*-amine PEG at room temperature. DCC in methylene chloride (1.0 ml, 1.0 M) was added dropwise under argon. After 12 h, the DCC side product was removed by vacuum filtration. The filtrate was washed with brine (3x10 ml), dried over anhydrous sodium sulfate and evaporated to

dryness. Crude product was purified by recrystallization in diethyl ether (30 ml) from methylene chloride (3 ml). Further purification was carried out using dialysis, as described for compound **5** above.

**8a:** Yield: 66% (white solid). $^{1}$H-NMR ($CDCl_3$): δ 7.35 (d, 8H, ArH), 7.26 (d, 8H, ArH), 5.73 (m, 8H, CH), 5.33 (t, 4H, CH), 5.20 (t, 4H, CH), 4.10 (s, 8H, $CH_2$) 3.68 (m, ~1.8kH, $CH_2$), 3.56 (s, 12H, $CH_3$), 3.00 (t, 8H, $CH_2$), 2.44 (m, 16H, $CH_2$), 2.29 (m, 16H, $CH_2$), 1.54 (m, 32H, $CH_2$), 1.34 (m, 256H, $CH_2$), 0.83 (t, 48H, $CH_3$). IR (KBr, $cm^{-1}$): 3329 (N-H), 2878 (C-H), 1740, 1755, 1651 (C=O), 1412 (C-N), 1241, 1145, 1105 (C-O). $T_m$=50.0 ˚C; $T_c$=25.4 ˚C. $M_w$: 18,100; PDI: 1.2.

**8b:** Yield: 62% (white solid). $^{1}$H-NMR ($CDCl_3$): γ 7.22 (d, 8H, ArH), 7.21 (d, 8H, ArH), 5.63 (m, 8H, CH), 5.30 (t, 4H, CH), 5.10 (t, 4H, CH), 4.03 (s, 8H, $CH_2$) 3.62 (m, ~1.8kH, $CH_2$), 3.50 (s, 12H, $CH_3$), 3.01 (t, 8H, $CH_2$), 2.38 (m, 16H, $CH_2$), 2.22 (m, 16H, $CH_2$), 1.51 (m, 32H, $CH_2$), 1.34 (m, 256H, $CH_2$), 0.81 (t, 48H, $CH_3$). IR (KBr, $cm^{-1}$): 3329 (N-H), 2878 (C-H), 1741, 1755, 1641 (C=O), 1415 (C-N), 1243, 1135, 1112 (C-O). $T_m$=48.8 ˚C; $T_c$=24.1 ˚C. $M_w$: 20,500; PDI: 1.1.

### 2.2.6 Determination of Melting Temperatures

A Meltemp (Cambridge, Mass) apparatus was used to determine the melting temperatures ($T_m$) of all the intermediates. For the final polymers, melting temperature ($T_m$) and crystallization temperatures ($T_c$) were determined by differential scanning calorimeter (DSC). Thermal analyses were performed on a Perkin-Elmer system consisting of a Pyris

1 DSC analyzer with TAC 7/DX instrument controllers. Perkin-Elmer Pyris software was used for data collection on a Dell OptiPlex GX110 computer. For DSC, samples (5 mg) were heated under dry nitrogen gas. Data were collected at heating and cooling rates of 10 ºC/min with a two-cycle minimum.

### 2.2.7 Dynamic Light Scattering Measurements

Dynamic light scattering (DLS) analyses were performed in aqueous buffer solution by photon correlation spectroscopy using a PSS Nicomp 380 submicron particle sizer instrument (Particle Sizing Systems, Santa Barbara, CA). A 20 mW, 523 nm diode-pumped solid-state laser module and an avalanche photodiode detector were used. Polymer solutions (1 wt%) in three different buffered aqueous solutions were prepared: pH 2.0 (0.01 N HCl), 7.4 (PBS) and 9.0 (sodium carbonate). Measurements were performed at a 90° scattering angle at 25°C. Nicomp number-weight analysis and multimodal Laplace transform analysis were used to process data.

## 2.3 Results and Discussion

### 2.3.1 Synthesis and Characterization

In contrast to previous examples,[7] the star-like amphiphilic macromolecules (ASMs) described herein were generated from an alkyl-based core to increase the number of poly(ethylene glycol) arms to four, and to potentially increase the loading capabilities of the hydrophobic interior. As shown in Scheme 2-2, core molecule **4** was prepared by Michael addition of pentaerythritol tetraacrylate **2** with 4-aminothiolphenol to form the extended core molecule **3**, which is then coupled to the acylated mucic acid **1** using

DCC/DPTS. Methoxy-terminated polymer **5** was prepared by coupling the hydrophobic core **4** to monomethoxy-poly(ethylene glycol) (mPEG) with DCC/DPTS.

Representative NMR spectra are presented in Scheme 2-3. The top graph is the $^{13}$C NMR spectrum of compound **3**, which clearly shows that the Michael addition was complete on all four alkenes of compound **2**. The bottom graph is the $^{1}$H-NMR (Scheme 2-3) spectrum of compound **4b**; the ratio of protons associated with the alkyl chains of the mucic acid derivative **1** to aromatic protons corresponds with the structure **4b**. For the final products (**5**, **7** and **8**), the ethylene oxide of PEG comprises a significant component and dominates the $^{1}$H-NMR and IR spectra.

The carboxy-terminated polymer **7** was prepared by first activating the expanded core **4** with N-hydroxysuccinimide to yield the intermediate **6** before coupling with the amine groups of heterobifunctional poly(ethylene glycol) to generate the carboxylic acid chain ends of **7** as outlined in Scheme 2-4. Amine-terminated polymer **8** was prepared by coupling the hydrophobic core **4** to PEG-*bis* amine again using DCC/DPTS. All coupling reactions were reasonably high yield, even with the difunctional PEGs. For example, the amine-terminated ASMs **8** reacted with two molecules of **4** to generate a product that was difficult to separate from our desired product, **8**, yet the final product was isolated in yields > 60% even with more extensive purification.

The NMR and IR spectral data was very similar for all polymers, as a major component is PEG. Several trends in the polymer characteristics were observed as a function of

chain ends and alkyl chains in the core. First, the melting transition temperatures of the methoxy-terminated polymers **5** were approximately 7 and 8 degrees higher than for the carboxy- and amine-terminated polymers **7** and **8**, respectively. With the ability of the amine- and carboxy-terminated polymers to hydrogen-bond, we had anticipated that these polymers would actually have higher melting transitions relative to the neutral polymer. Second, polymers with core structures comprised of the longer alkyl chains **5b**, **7b** and **8b** had slightly lower melting transition temperature and crystallization temperatures. This effect is most likely due to the increased mobility of the polymer with longer alkyl chains as compared with the poly(ethylene glycol) arms. Third, alkyl chain lengths in the core influenced the overall polymer size in solution, as measured by GPC. For example, final polymers with core structures comprised of the longer alkyl chains **5b**, **7b** and **8b** had slightly higher molecular weights, according to GPC results taken in THF, relative to polymers containing the shorter alkyl chains in the hydrophobic core **5a**, **7a** and **8a**. Although a shorter PEG chain (~3400 Da) was used for the amine-terminated polymers **8**, the methoxy- and carboxy-terminated polymers contain longer PEG chains (~5000 Da). Thus, the observed size change in the GPC data is strictly a function of the four carboxylic acids of the chain ends.

### 2.3.2 Influence of Solution pH Values

The size and potential aggregation of all six ASMs were also evaluated in DLS studies, in aqueous solutions at three different pH values, as shown in Table 2-1. As with the GPC data in THF, polymers with core structures comprised of the longer C12 chains **5b**, **7b** and **8b** were slighter larger in size (Table 2-1) in aqueous solutions. The shorter C6 chain

polymers displayed sizes that were independent of pH, whereas the longer chain polymers displayed a more pronounced response to pH changes. At neutral pH, the carboxy-terminated polymer **7b** was approximately 5 nm larger than the methoxy-terminated polymer **5b**, which in turn, was approximately 4 nm larger than the amine-terminated polymer **8b**. In acidic (pH 2.0), neutral (pH 7.4) and basic (pH 9.0) aqueous solutions, the micellar sizes change less than 10 nm for both the shorter C6 and longer C12 ASM series. Some secondary aggregation is observed, likely as higher aggregation micelles.

## 2.4 Conclusions

This study highlights the synthesis and physical properties of the second generation nanoscale ASMs, in which two design features were incorporated: (i) expansion to four arms via a tetrafunctional aliphatic molecule and (ii) controlled functionality of the four chain ends. The ASMs presented herein are easily synthesized from pentaerythritol tetraacrylate, mucic acid, oligomeric alkyl chains (C6 and C12) to generate the hydrophobic core and PEG with methoxy-, carboxy- and amine-terminated chain ends to generate the hydrophilic shell. In aqueous solution, the ASMs maintain their nanosize, ranging from 20 nm to 40 nm, even with pH changes. The variation of alkyl chain length (from 6 to 12 carbons) controls the solution and hemolytic stability,[18] drug loading capacity and release rate,[11] whereas the carboxylate or amine functional groups of the PEG chain ends are utilized to conjugate targeting molecules. As described in the introduction, the carboxylic acid groups on the four chain ends of the

ASMs preferentially and distinctly interact with low-density lipoproteins (LDL) to prevent prolonged retention and aggregation of LDL.[13]

**2.5 Future Works**

For targeting purposes, the nucleophilic amine on the four PEG chain ends of the ASMs may be conjugated with folic acid that target cancer cells.[14]

In addition to applications in nanoscale drug delivery, carboxylic acid-terminated ASMs demonstrate an unanticipated ability to promote interactions with biological entities, such as LDL receptor-mediated uptake.[19] Inhibition of hoxLDL uptake by macrophages will be assessed using carboxylate-functionalized ASM.

## 2.6 References


1. Chen, G., and Guan, Z., Transition metal-catalyzed one-pot synthesis of water-soluble dendritic molecular nanocarriers. *J. Amer. Chem. Soc.,* **2004**. *126*: p. 2662-2663.
2. Van Alstine, J., and Malmsten, M., Poly(ethylene glycol) amphiphiles: Surface behavior of biotechnical significance. *Langmuir,* **1997**. *13*: p. 4044-4053.
3. Ghosh, S., Kawaguchi, S., Jinbo, Y., Izumi, Y., Yamaguchi, K., Taniguchi, T., Nagai, K. and Koyama, K., Nanoscale solution structure and transfer capacity of amphiphilic poly(amidoamine) dendrimers having water and polar guest molecules inside. *Macromolecules*, **2003**. *36*: p. 9162-9169.
4. Esfand, R. and Tomalia, D., Poly(amidoamine) (PAMAM) dendrimers: From biomimicry to drug delivery and biomedical applications. *Drug Delivery Today*, **2001**. *6*(8): p. 427.
5. Newkome, G., Kotta, K. and Moorefield, C., Convenient synthesis of 1,3 c-branched dendrons. *J. Org. Chem.*, **2005**. *70*: p. 4893-4896.
6. Wang, F., Bronich, T., Kabanov, A., Rauh, R. and Roovers, J., Synthesis and evaluation of a star amphiphilic block copolymer from poly(caprolactone) and poly(ethylene glycol) as a potential drug delivery carrier. *Bioconj. Chem.,* **2005**. *16*: p. 397-405.
7. Liu, H., Jiang, A., Guo, J. and Uhrich, K., Unimolecular micelles: Synthesis and characterization of amphiphilic polymer systems. *J. Poly. Sci: Part A: Polym Chem*, **1999**. *37*(6): p. 703-712.
8. Liu, H., Farrell, S. and Uhrich, K., Drug release characteristics of unimolecular polymeric micelles. *J. Control. Re.l*, **2000**. *68*: p. 167-174.
9. Schmalenberg, K., Frauchiger, L., Nikkhouy-Albers, L. and Uhrich, K., Cytotoxicity of a unimolecular polymeric micelle and its degradation products. *Biomacromolecules*, **2001**. *2*: p. 851-855.
10. Djordjevic, J., Michniak, B and Uhrich, K., Amphiphilic star-like macromolecules as novel carriers for topical delivery of nonsteroidal anti-inflammatory drugs. *Pharm. Sci.*, **2003**. *5*(4): p. 256-267.
11. Tao, L. and Uhrich, K., Stabilized polymeric micelles formed by novel amphiphilic macromolecules: amphiphilic scorpion like macromolecules (AScM) and amphiphilic star like macromolecules (ASM)) as drug delivery dystems for hydrophobic compounds. *AAPS National Meeting*, Nashville, TN, Nov. **2005**.
12. Tao, L. and Uhrich, K., Novel amphiphilic macromolecules and their in vitro characterization as stabilized micellar drug delivery systems. *J. Colloid Interf. Sci.,* **2006**. *298*(1): p. 102-110.
13. Chnari, E., Lari, HB., Tian, L., Uhrich, K. and Moghe, P, Nanoscale anionic macromolecules for selective retention of low density lipoproteins. *Biomaterials*, **2005**. *26*: p. 3749-3758.

14. Djordjevic, J., Tian, L., Gutierrez, J. and Uhrich, K., Folic acid-conjugated amphiphilic starlike macromolecules (FA-ASMs) as a targeted anti-cancer drug delivery system. *CRS Trans. #167* **2004**.
15. Moore, J. and Stupp, S., Room temperature polyesterification. *Macromolecules*, **1990**. *23*: p. 65-70.
16. Tian, L., Yam, L., Zhou, N., Tat, H. and Uhrich, K., Amphiphilic scorpion-like macromolecules (AScMs): Design, synthesis and characterization. *Macromolecules*, **2004**. *37*(2): p. 538-543.
17. Kisliuk, R. Folates. *Encyclopedia of Life Sciences.* Vol. DOI: 10.1038/npg.els.0003924. 2006, Chichester, UK: John Wiley & Sons, Ltd.
18. Tao, L., Novel amphiphilic scorpion-like macromolecules (AScM) and amphiphilic star-like macromolecule (ASM): physico-chemical characterization and application in stabilized colloidal drug delivery systems, in P*HD Dissertation.* **2006**, Rutgers University: New Brunswick.
19. Chnari, E., Nikitczuk, J., Uhrich, K. and Moghe, P., Nanoscale anionic macromolecules can inhibit cellular uptake of differentially oxidized low density lipoproteins. *Biomacromolecules*, **2005**. *26*: p. 3749-3758.

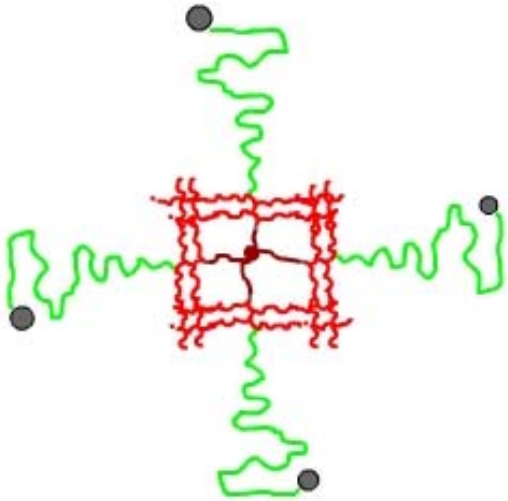

Scheme 2-1 Graphic description of PEG chain-end functionalized ASM.

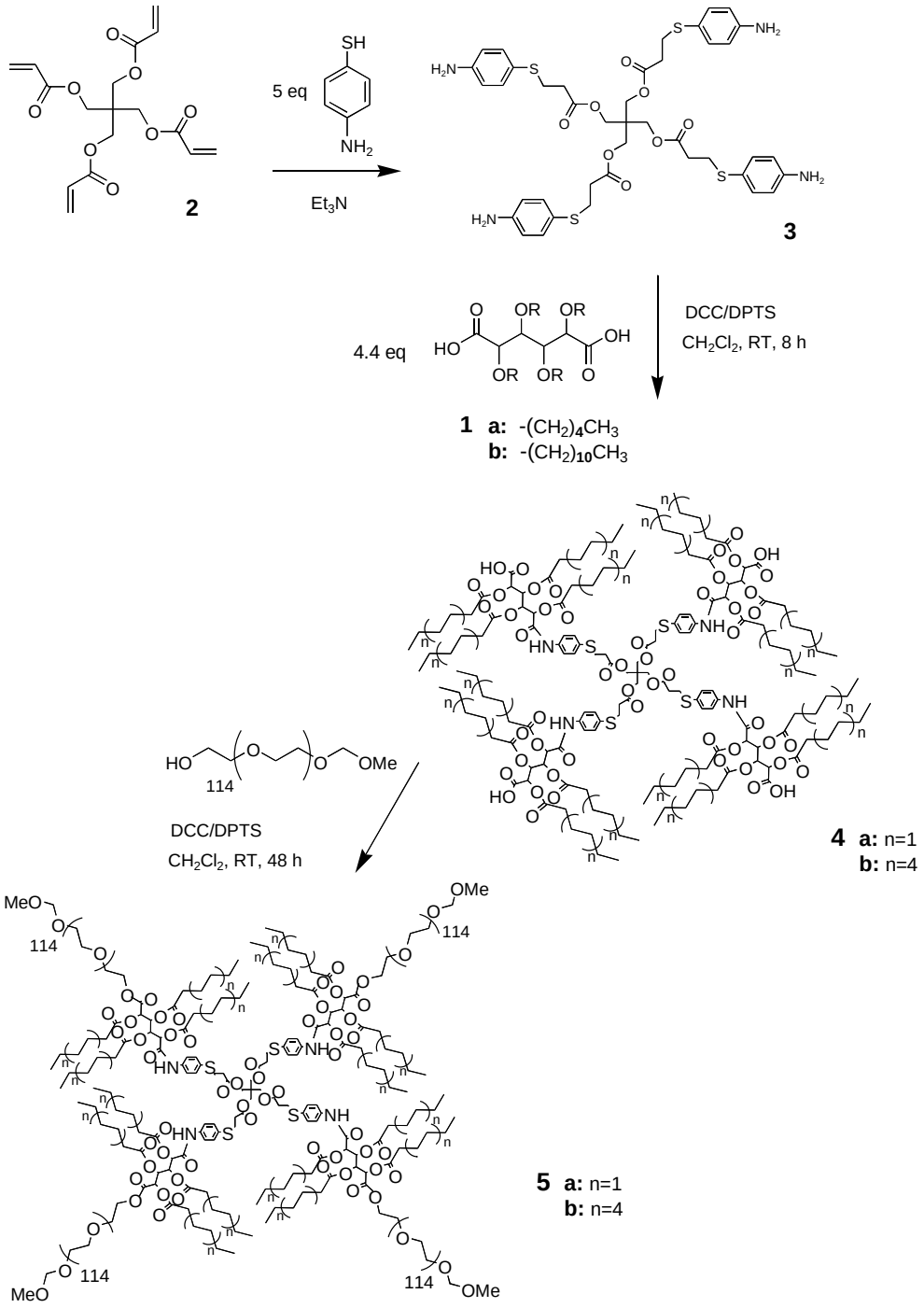


Scheme 2-2 Synthetic pathway of ASM with methoxy-termination PEGs

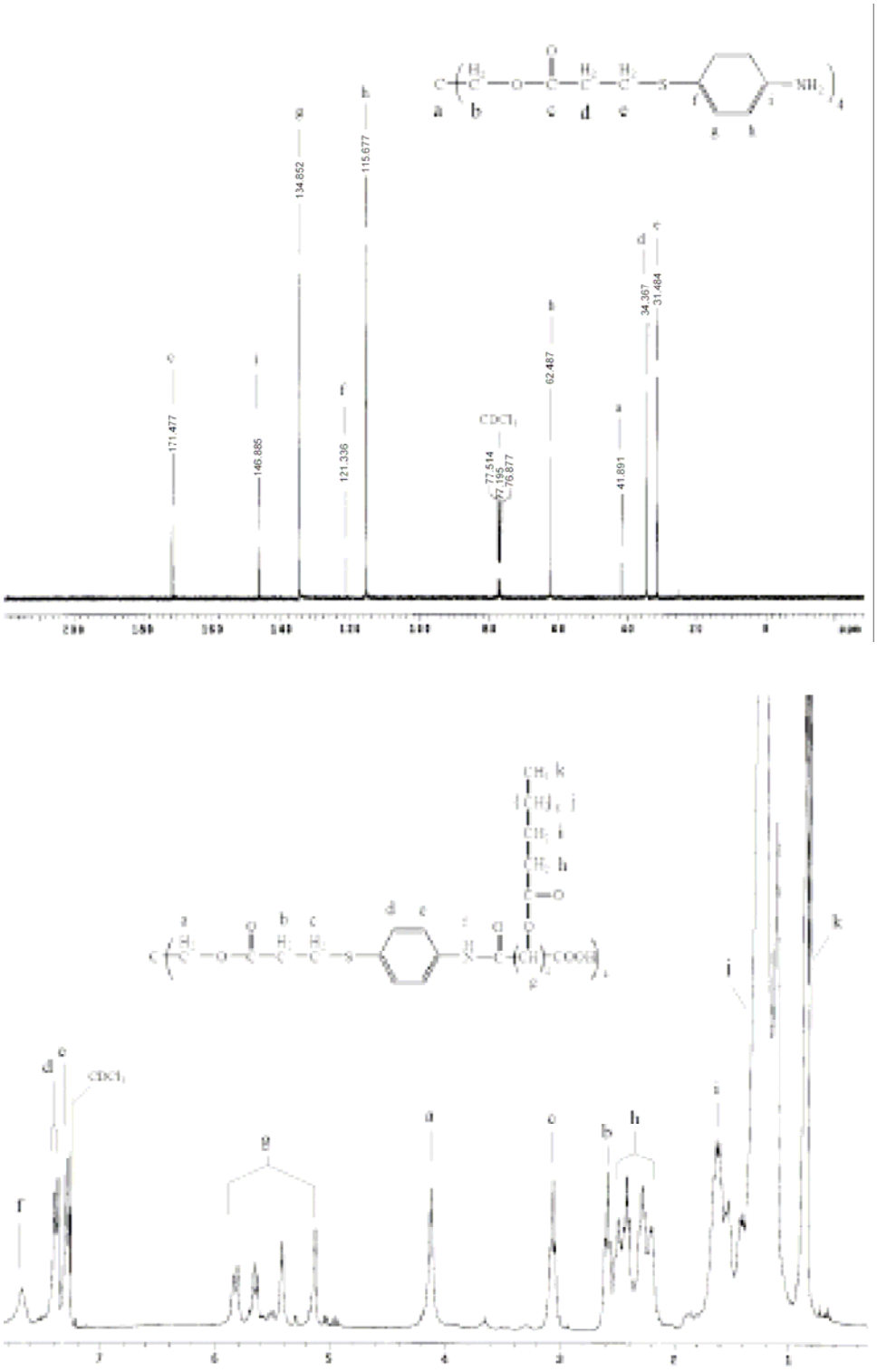


Scheme 2-3 $^{13}$C NMR data for **3** (top) and $^{1}$H-NMR data for **4b** (bottom).

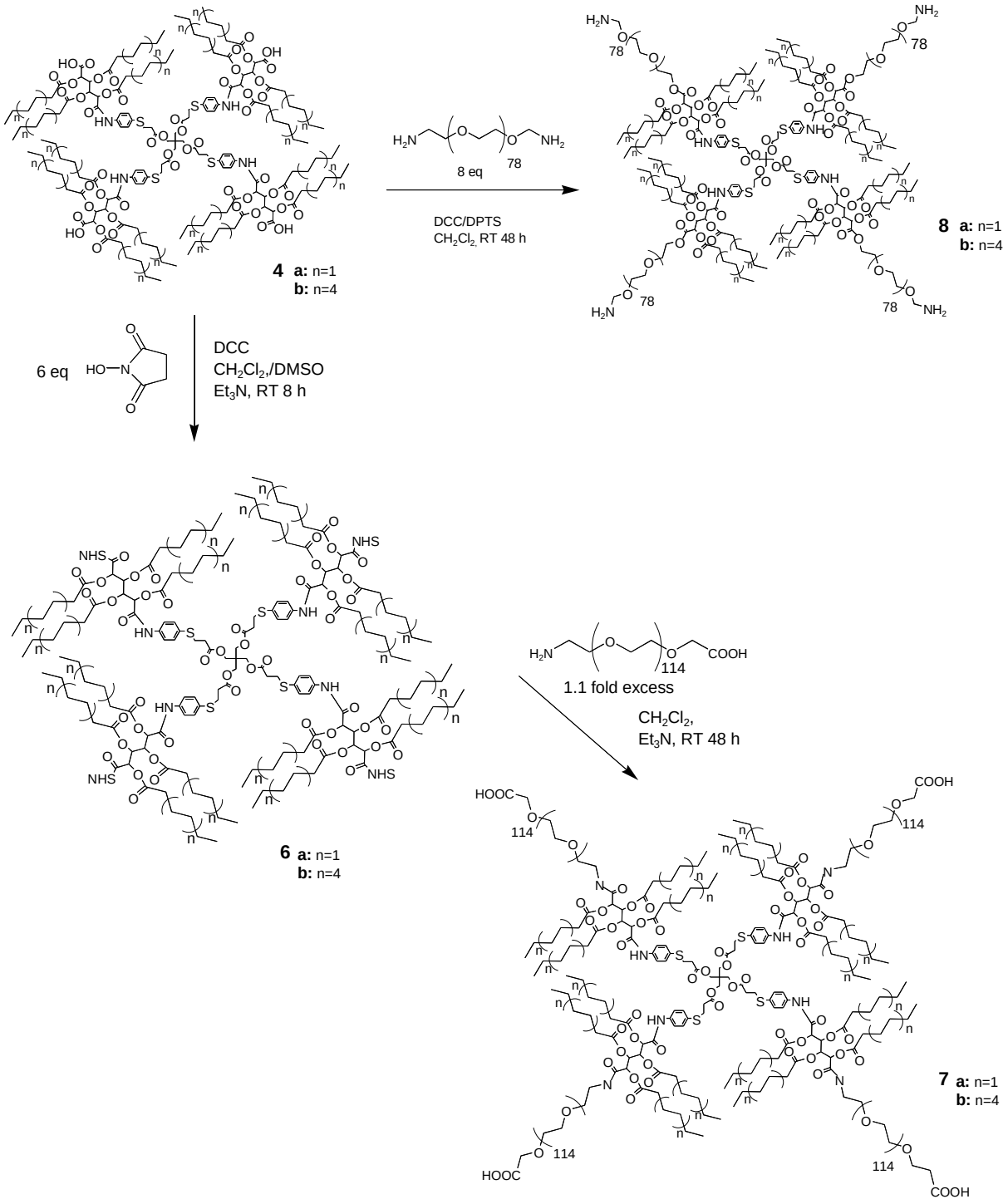


Scheme 2-4 Synthetic pathway of ASM with carboxylate-terminated PEGs and amine-termination PEGs

| pH | 5a | 5b | 7a | 7b | 8a | 8b |
|---|---|---|---|---|---|---|
| 2.0 | 26.3±2.2 | 33.6±4.1 | 24.2±3.2 | 36.7±4.4 | 24.6±2.2 | 27.9±3.7 |
| 7.4 | 26.0±2.5 | 31.1±3.8 | 26.7±3.0 | 35.2±4.0 | 26.1±2.4 | 29.0±3.8 |
| 9.0 | 25.0±2.0 | 33.0±3.8 | 25.0±2.6 | 32.4±4.0 | 24.8±1.9 | 29.5±3.8 |

Table 2-1 Particle size of the various ASMs as a function of pH.

# CHAPTER THREE. AMPHIPHILIC SCORPION-LIKE MACROMOLECULES: NOVEL TREATMENT FOR ATHEROSCLEROSIS

## 3.1 Introduction

Atherosclerosis is a process characterized by the buildup of low-density lipoproteins (LDL) within the vascular intima and ensuing interactions between macrophages and their extracellular matrix molecules; it is the single leading cause of death in America.[1-3] Recent advances in nanotechnology for cardiovascular health are abundant and include the application of nanosensors to monitor nitro-oxidative species produced in the failing heart,[4] microarrays or microchips for the study of cardiovascular disease,[5] electrospun nanofibers as tissue engineered vascular grafts,[6, 7] and carbon nanotubes implanted for anticoagulant and antithrombotic properties.[8, 9] In contrast to the implantable devices described above, an avenue of particular interest in nanotechnology is the use of a "nano-blocker" to prevent highly oxidized LDL (hoxLDL) uptake via scavenger receptors. Native LDL uptake is mediated by feedback inhibition, whereas binding of hoxLDL to macrophage scavenger receptors leads to unregulated cholesterol accumulation and foam cell formation. Thus, controlling binding to hoxLDL is an important focus for new atherosclerotic treatments.[10, 11]

Previous work on LDL uptake has focused on synthetic compounds that target and bind scavenger receptors, such as SR-A and CD36, that appear to be of primary importance in atherogenesis.[12, 13] For example, phosphocholine as a ligand for CD36 has been shown to inhibit the binding of hoxLDL in CD36 expressing cells.[12] In addition, sulfatide derivatives for targeting SR-A have been shown to reduce acetylated LDL

binding and uptake.[13] Although previous efforts to develop scavenger receptor blockers are encouraging, increased efficiency may be reached through the use of an organized 3D presentation of the targeting groups or a multifunctional particle to simultaneously target several scavenger receptors.[14] To create a multifunctional nano-blocker, one could exploit the fact that all scavenger receptors share an affinity for anionic ligands.[15]

We previously reported a unique series of polymers, amphiphilic scorpion-like macromolecules (AScM),[16] that self-organize into micelles and not only act as a drug delivery system but also decrease LDL uptake. Previous results show promise for AScMs as a hydrophobic drug carrier in terms of low CMC (critical micelle concentration), low cytotoxicity, high drug loading efficiency, and sustained release.[17, 18]

These prior studies have focused on anionic AScMs that spontaneously form micelles at concentrations above the CMC ($10^{-7}$ M).[16] Each AScM is functionalized with a carboxylic acid, such that the micellar nanoparticle presents anionic charges in an organized and clustered configuration. The anionic AScMs reduced hoxLDL uptake by up to 80%, and both SR-A and CD36 receptors were involved in the uptake of the polymers and hoxLDL. [14, 19]

In this chapter, we present a series of macromolecules that maintain two structural elements as previously described: mucic acid derivatives as the hydrophobic component and PEG as the hydrophilic component. First, the location and number of carboxylic acid groups were varied with our synthetic design; carboxylate groups can be precisely located

in either the hydrophobic or hydrophilic domains or in both domains. (Scheme 3-1) Second, sulfuric acid monomethyl ester, a negatively charged functional group, was introduced onto the hydrophobic domains. The inhibition ability of these novel macromolecules with carboxylic acid groups were evaluated by our collaborator for highly oxidized LDL binding with macrophages. The name and chemical structures of the macromolecules we made are shown in Scheme 3-2.

The AScMs may also function as drug delivery systems to promote the encapsulation and controlled release of hydrophobic drugs. Drug-loaded AScMs may control the inflammatory responses accompanying atherosclerosis as described herein. A number of liver X receptor (LXR) target genes in macrophages have been linked to the regulation of reverse cholesterol transport, where excess cholesterol is transported to the liver via HDL particles.[20] LXRs belong to a family of nuclear membrane proteins that are transcriptionally activated through ligand binding.[21] In addition, LXRs block NF-kB signaling, where nuclear factor-kappa B (NF-kB) is required for the induction of inflammatory cytokines.[20, 22] Treatment with a LXR agonist reduces foam cell formation in macrophages by increasing cellular cholesterol efflux.[20, 22, 23] In this chapter, we also incorporated GW3965, a hydrophobic LXR agonist, within the macromolecules.

When protonated, the tertiary amine group on GW3965 is positively charged; this charge may allow the binding of GW3965 with the anionic AScMs. An example of GW3965 encapsulation is shown in Scheme 3-3. Encapsulation in the small-sized micelles could

potentially increase delivery of GW3965 into the nucleus.[24] The aim of GW3965 loading is to further reduce oxLDL uptake caused by scavenger receptor binding. The chemical structure of GW3965 is shown in Scheme 3-4.

## 3.2 Experimental Procedures

### 3.2.1 Materials

Heterobifunctional poly(ethylene glycol) ($HCl{\cdot}NH_2$-PEG-COOH) with molecular weight of 5000 Da was obtained from Nektar (San Carlos, CA). 4-(Dimethylamino)pyridinium *p*-toluenesulfonate (DPTS) was prepared as previously described.[25] Monomethoxy-poly(ethylene glycol) (mPEG) with molecular weights of 5000 Da was purchased from Sigma-Aldrich. All PEG reagents were dried by azeotropic distillation with toluene. β-Glutamic acid, 5-aminoisophthalic acid, 4-hydroxybenzoic acid, N-hydroxyl succinimide (NHS), triethylamine (99.7%) and 1,3-dicyclohexylcarbodiimide (DCC) in 1 M methylene chloride solution were purchased from Aldrich and used as received. All other reagents and solvents were reagent grade and used as received.

### 3.2.2 Methods

The macromolecules **1CM**, **0CM** and **1CP** were prepared as previously described.[14] Chemical structures and compositions were confirmed by $^1H$ and $^{13}C$ NMR spectroscopy with samples (~ 5-10 mg/ml) dissolved in $CDCl_3$ solvent on Varian 400 MHz spectrometers, using tetramethylsilane as the reference signal. IR spectra were recorded on a Mattson Series spectrophotometer (Madison Instruments, Madison, WI) by solvent (methylene chloride) casting on a KBr pellet. Negative ion-mass spectra were recorded

with a ThermoQuest Finnigan LCQ$^{TM}_{DUO}$ System (San Jose, CA) that includes a syringe pump, an optional divert/inject valve, an atmospheric pressure ionization (API) source, a mass spectrometer (MS) detector, and the Xcalibur data system. Meltemp (Cambridge, Mass) was used to determine the melting temperatures ($T_m$) of all the intermediates.

Gel permeation chromatography (GPC) was used to obtain molecular weight and polydispersity index (PDI). It was performed on Perkin-Elmer Series 200 LC system equipped with Pl gel column (5 μm, mixed bed, ID 7.8 mm, and length 300 mm) and with a Water 410 refractive index detector, Series 200 LC pump and ISS 200 Autosampler. Tetrahydrofuran (THF) was the eluent for analysis and solvent for sample preparation. Sample was dissolved into THF (~ 5 mg/ml) and filtered through a 0.45 μm PTFE syringe filter (Whatman, Clifton, NJ) before injection into the column at a flow rate of 1.0 ml/min. The average molecular weight of the sample was calibrated against narrow molecular weight polystyrene standards (Polysciences, Warrington, PA).

### 3.2.3 Synthesis of 1CM1CP

Compound **1** (0.47 g, 0.50 mmol) was mixed with thionyl chloride (20 ml, 270 mmol) and heated to reflux at 60 °C for 4 hours. After cooling to room temperature, the excess thionyl chloride was removed by rotary evaporation. The acyl chloride intermediate was dissolved in 5.0 ml anhydrous methylene chloride solution with 2.0 ml pyridine. Heterobifunctional poly(ethylene glycol) (HCl·$NH_2$-PEG-COOH) ($M_w$ = 5.0 kDa) (0.50 g, 0.10 mmol) in 5.0 ml methylene chloride solution was added dropwise over 2 min. After 24 hours stirring under room temperature, the reaction mixture was acidified by 0.1 N

HCl aqueous solution (10 ml x 2) and washed by brine (10 ml). The organic portion was dried over sodium sulfate, concentrated to 1 ml and added into diethyl ether (60 ml) was to precipitate out the product.

**1CM1CP** was obtained as white waxy solid: 0.52 g, 86% yield. $^1$H NMR ($CDCl_3$) ($\delta$): 5.59 (d, 1H, C*H*), 5.62 (d, 1H, C*H*) 5.21 (m, 1H, C*H*), 5.02 (m, 1H, C*H*), 3.64 (m, ~0.4kH, C$H_2$ on PEG), 2.38 (t, 4H, C$H_2$), 2.21 (t, 4H, C$H_2$), 2.57 (t, 2H, C$H_2$-COOH of PEG), 1.61 (m, 4H, C$H_2$), 1.51 (m, 4H, C$H_2$), 1.25 (m, 48H, C$H_2$), 0.88 (t, 12H, C$H_3$). IR (KBr, $cm^{-1}$): 2911 (C-H), 1754 (C=O), 1250, 1105(C-O). $T_m$: 58.0-59.5 °C; GPC: Mw: 5,500; PDI: 1.1.

### 3.2.4 Synthesis of 1BM

Molecule **1** (0.94 g, 1.0 mmol) was mixed with thionyl chloride (20 ml, 270 mmol) and heated to reflux at 60 °C for 4 hours. After cooling to room temperature, the excess thionyl chloride was removed by rotary evaporation. A solution of anhydrous THF (10 ml) and pyridine (5.0 ml) was added to the reaction mixture. 4-Hydroxybenzoic acid (0.55 g, 4.0 mmol) dissolved in THF (5.0 ml) was added dropwise over 2 min at 0°C. The reaction was warmed up to room temperature and stirred for 6 hours. The reaction was quenched by adding 1 N HCl (400 ml) to the reaction mixture. White solid was collected and dried as intermediate product, **2.**

Intermediate **2** was obtained as white solid: 0.89 g, 75% yield. $^1$H NMR ($CDCl_3$) ($\delta$): 8.02 (d, 4H, Ar*H*), 6.95 (d, 4H, Ar*H*), 5.59 (m, 2H, C*H*), 4.94 (m, 2H, C*H*), 2.32 (m, 8H, C$H_2$),

1.49 (m, 8H, C$\underline{H}_2$), 1.25 (m, 48H, C$\underline{H}_2$), 0.86 (t, 12H, C$\underline{H}_3$). IR (KBr, $cm^{-1}$): 2930 (C-H), 1752 (C=O), 1250, 1148 (C-O), 742 (Aromatic C-C). FW: 1167; MS: 1165.5. $T_m$: 154.5-156.5°C.

Intermediate **2** (0.59 g, 0.50 mmol), mPEG ($M_w$ = 5.0 kDa, after azeotropic distillation) (0.50 g, 0.10 mmol) and DPTS (0.16 g, 0.50 mmol) were dissolved in methylene chloride (10 ml) and DMF (1.5 ml). DCC (1.0 M in methylene chloride solution) (1.0 ml, 1.0 mmol) was slowly added. After 24 hours stirring at room temperature, the side product was removed by filtration. The organic solution was washed by 0.1 N HCl aqueous solution (10 ml x 2) and brine (10 ml). The organic portion was dried over sodium sulfate and concentrated by rotary evaporator. Diethyl ether (15 ml) was added to precipitate the product **1BM**. Additional ethyl ether (15 ml x 2) was used to wash the product.

**1BM** was obtained as white waxy solid: 0.54 g, 88% yield. $^1$H NMR ($CDCl_3$) ($\delta$): 8.00 (d, 4H, Ar$\underline{H}$), 6.93 (d, 4H, Ar$\underline{H}$), 5.60 (m, 2H, C$\underline{H}$), 4.94 (m, 2H, C$\underline{H}$), 2.31 (m, 8H, C$\underline{H}_2$), 1.47 (m, 8H, C$\underline{H}_2$), 1.25 (m, 48H, C$\underline{H}_2$), 0.88 (t, 12H, C$\underline{H}_3$). IR (KBr, $cm^{-1}$): 2956 (C-H), 1755 (C=O), 1258, 1106 (C-O), 733 (Aromatic C-C). $T_m$: 55.4 -56.5°C. GPC: *M*w: 5,500; PDI: 1.2.

### 3.2.5 Synthesis of 2CM

Compound **1CM** (0.60 g, 0.10 mmol) was azeotropically distilled with toluene, then mixed with NHS (0.50 g, 0.43 mmol) in a solution of methylene chloride (20 ml) and DMF (0.8 ml). DCC (1.0 M in methylene chloride) (0.50 ml, 0.50 mol) was added

dropwise under argon. The reaction mixture was stirred for 12 hours at room temperature and then DCU removed by vacuum filtration. The isolated solution was directly reacted with β-glutamic acid (63 mg, 0.43 mmol) in the present of triethylamine (1.0 ml, 7.0 mmol) under stirring at room temperature. After 8 hours, the reaction mixture was washed by 0.1 N HCl aqueous solution (10 ml x 2) and brine (10 ml), dried over sodium sulfate and concentrated by rotary evaporator. Diethyl ether (15 ml) was added to precipitate the product **2CM**.

**2CM** was obtained as white waxy solid: 0.43 g, 71% yield. $^{1}$H NMR ($CDCl_3$) ($\delta$): 5.62 (m, 2H, C<u>*H*</u>), 5.08 (m, H, C<u>*H*</u>), 3.66 (m, ~0.4kH, C<u>$H_2$</u> on PEG), 2.38 (t, 4H, C<u>$H_2$</u>), 2.21 (t, 4H, C<u>$H_2$</u>), 1.61 (m, 4H, C<u>$H_2$</u>), 1.51 (m, 4H, C<u>$H_2$</u>), 1.25 (m, 48H, C<u>$H_2$</u>), 0.88 (t, 12H, C<u>$H_3$</u>). IR (KBr, $cm^{-1}$): 2925 (C-H), 1750 (C=O), 1229, 1146 (C-O). $T_m$: 54.6 –55.9.2°C. GPC: *M*w: 5,500; PDI: 1.2.

### 3.2.6 Synthesis of 0BM

Compound **1CM** (0.60 g, 0.10 mmol; after azeotropic distillation with toluene), DPTS (0.31 g, 1.0 mmol) and *p*-phenetidine (0.80 ml, 10 mmol) were dissolved in methylene chloride (20 ml). DCC (1.0 M in methylene chloride) (0.20 ml, 0.20 mol) was added dropwise under argon. Reaction was stirred for 12 hours at room temperature and by-product removed by vacuum filtration. The organic portion was washed by 0.1 N HCl solution (10 ml x 2), brine (10 ml), dried over sodium sulfate and concentrated under rotary evaporator. Diethyl ether (15 ml) was added to precipitate the product.

**0BM** was obtained as white waxy solid: 0.56 g, 92% yield. $^1$H NMR ($CDCl_3$) ($\delta$): 7.21 (d, 2H, Ar*H*), 6.71 (d, 2H, Ar*H*), 5.78 (d, 1H, C*H*), 5.49 (d, 1H, C*H*) 5.38 (m, 1H, C*H*), 4.95 (m, 1H, C*H*), 3.66 (m, ~0.4kH, C$H_2$ on PEG), 2.38 (t, 4H, C$H_2$), 2.21 (t, 4H, C$H_2$), 1.61 (m, 4H, C$H_2$), 1.51 (m, 4H, C$H_2$), 1.25 (m, 48H, C$H_2$), 0.88 (t, 12H, C$H_3$). IR (KBr, cm$^{-1}$): 2917 (C-H), 1737 (C=O), 1250, 1120 (C-O), 780 (Aromatic C-C). $T_m$: 55.5–57.2 °C. GPC: *M*w: 5,500; PDI: 1.2.

### 3.2.7 Synthesis of 1SM

Compound **3** (0.30 g, 0.05 mmol) was mixed with excess 2-aminoethanol (0.040 g, 0.65 mmol) in methylene chloride (50 ml) at room temperature and stirred for 4 hours. The reaction mixture was then washed with 0.1 N HCl (50 ml) and water (50 ml), then dried over $MgSO_4$ and concentrated by rotary evaporator. Ethyl ether (100 ml) was added to precipitate the product. Compound **4** was obtained as a slight yellow solid: 0.27 g, 91% yield. $^1$H NMR ($CDCl_3$) ($\delta$): 5.80 (d, 1H, C*H*), 5.54 (d, 1H, C*H*) 5.35 (m, 1H, C*H*), 5.05 (m, 1H, C*H*), 3.65 (m, ~0.4kH, C$H_2$ on PEG), 3.20 (t, C$H_2$-OH), 2.77 (t, C$H_2$-NH), 2.59 (m, C$H_2$), 2.42 (t, 4H, C$H_2$), 2.24 (t, 4H, C$H_2$), 1.62 (m, 4H, C$H_2$), 1.56 (m, 4H, C$H_2$), 1.22 (m, 48H, C$H_2$), 0.83 (t, 12H, C$H_3$). IR (KBr, cm$^{-1}$): 2900 (C-H), 1745 (C=O), 1248, 1110 (C-O).

Compound **4** (0.15 g, 0.025 mmol) was mixed with pyridine-sulfur trioxide complex (40 mg, 0.25 mmol) in DMF (5.0 ml). The reaction mixture was stirred for eight hours at room temperature. Following the addition of methylene chloride (50 ml), the reaction mixture solution was acidified with 0.5 N HCl (30 ml x 3), washed with water (30 ml),

and dried over $MgSO_4$. The product was filtered, concentrated to 5 ml by rotary evaporator. Ethyl ether (50 ml) was added to precipitate the product. **1SM** was obtained as a slight yellow solid: 0.12 g, 81% yield. $^1$H NMR ($CDCl_3$) ($\delta$): 8.15 (s, $CH_2$-N$\underline{H}$), 5.82-5.18 (m, 4H, C$\underline{H}$), 3.65 (m, ~0.4kH, C$\underline{H_2}$ on PEG), 3.22 (t, C$\underline{H_2}$-OH), 2.75 (t, C$\underline{H_2}$-NH), 2.48 (m, C$\underline{H_2}$), 2.38 (t, 4H, C$\underline{H_2}$), 2.13 (t, 4H, C$\underline{H_2}$), 1.90 (1.64 m, 4H, C$\underline{H_2}$), (m, 4H, C$\underline{H_2}$), 1.56 (m, 4H, C$\underline{H_2}$), 1.34 (m, 48H, C$\underline{H_2}$), 0.95 (t, 12H, C$\underline{H_3}$). IR (KBr, $cm^{-1}$): 2920 (C-H), 1750 (C=O), 1240, 1100 (C-O).

### 3.2.8 Synthesis of 3SM

Compound **3** (0.30 g, 0.05 mmol) was added to tris-(hydroxymethyl)-aminoethane (0.06 g, 0.25 mmol) in acetone (10 ml). The reaction mixture was stirred at room temperature for four hours. The reaction mixture was washed with 0.1 N HCl (50 ml), water (50 ml), dried over $MgSO_4$ and concentrated to 10 ml by rotary evaporator. Ethyl ether (100 ml) was added to precipitate the product. Compound **5** was obtained as a yellow solid: 0.28 g, 88% yield. $^1$H NMR ($CDCl_3$) ($\delta$): 8.05 (s, N$\underline{H}$), 5.70-5.80 (m, 1H, C$\underline{H}$), 5.62 (d, 1H, C$\underline{H}$) 5.20 (m, 1H, C$\underline{H}$), 5.11 (m, 1H, C$\underline{H}$), 3.60 (m, ~0.4kH, C$\underline{H_2}$ on PEG), 2.80 (t, C$\underline{H_2}$-OH), 2.62 (m, C$\underline{H_2}$), 2.40 (t, 4H, C$\underline{H_2}$), 2.23 (t, 4H, C$\underline{H_2}$), 1.57 (m, 4H, C$\underline{H_2}$), 1.50 (m, 4H, C$\underline{H_2}$), 1.24 (m, 48H, C$\underline{H_2}$), 0.82 (t, 12H, C$\underline{H_3}$). IR (KBr, $cm^{-1}$): 2900 (C-H), 1730 (C=O), 1230, 1122 (C-O). 820( Ar-H),

Compound **5** (0.15 g, 0.025 mmol) was added to pyridine-sulfur trioxide complex (40 mg, 0.25 mmol) in DMF (5.0 ml). The reaction mixture was stirred for eight hours at room temperature. Following the addition of methylene chloride (50 ml), the reaction mixture

solution was acidified with 0.5 N HCl (30 ml x 3), washed with water (30 ml) and dried over $MgSO_4$. The product was filtered, concentrated to 5 ml by rotary evaporator. Ethyl ether (50 ml) was added to precipitate the product. Compound **3SM** was obtained as a slight yellow solid: 0.12 g, 81% yield. $^1$H NMR ($CDCl_3$) ($\delta$): 8.03 (s, $CH_2$-N<u>*H*</u>), 5.80-5.20 (m, 4H, C<u>*H*</u>), 3.62 (m, ~0.4kH, C<u>$H_2$</u> on PEG), 3.20 (t, C<u>$H_2$</u>-O), 2.48 (m, C<u>$H_2$</u>), 2.38 (t, 4H, C<u>$H_2$</u>), 2.13 (t, 4H, C<u>$H_2$</u>), 1.90 (1.64 m, 4H, C<u>$H_2$</u>), (m, 4H, C<u>$H_2$</u>), 1.56 (m, 4H, C<u>$H_2$</u>), 1.34 (m, 48H, C<u>$H_2$</u>), 0.95 (t, 12H, C<u>$H_3$</u>). IR (KBr, $cm^{-1}$): 2920 (C-H), 1750 (C=O), 1240, 1100 (C-O).

### 3.2.9 Dynamic Light Scattering Measurement

Dynamic light scattering (DLS) analyses were performed using a Malvern Instruments Zetasizer Nano ZS-90 instrument (Southboro, MA), with reproducibility verified by collection and comparison of sequential measurements. Polymer solutions (1.0 wt %) in phosphate buffered aqueous solution (PBS) (pH 7.4) were prepared. Measurements were performed at a 90° scattering angle at 25°C.

### 3.2.10 Fluorescence Spectroscopy

Critical micelle concentration (CMC) measurements were carried out on a Spex fluoroMax (Piscataway, NJ) spectrofluorometer at 25°C. Using pyrene as the probe molecule, a stock solution of 5.00 $x10^{-7}$ M in pH 7.4 PBS buffer solution was prepared. Polymer samples were dissolved in the stock pyrene solutions then diluted to specific concentrations. Excitation was performed from 300 nm to 360 nm, using 390 nm as the emission wavelength. Pyrene maximum absorption shifted from 332 nm to 334.5 nm

upon secondary micelle formation. The ratio of absorption of polymer (334.5 nm) to pyrene only (332 nm) was plotted as the logarithm of polymer concentrations. The inflection point of the curves was taken as CMC.

### 3.2.11 Zeta Potential

Charge densities of all polymeric micelle solutions were measured by the zeta potential method using a Malvern instruments Zetasizer Nano ZS-90 instrument (Southboro, MA), with reproducibility verified by collection and comparison of sequential measurements. The zeta potential is calculated using the Henry Equation, where ε is the solvent dielectric constant, η is the solvent viscosity, κ is the inverse Debye length, a is the particle radius, and f(κa) is the model dependent Henry Function, which varies from 1 to 1.5.

Zeta potential= $3\eta u_E/(2\varepsilon f(\kappa a))$

The model independent property measured in a ELS experiment is the electrophoretic mobility. The model we used is Huchel model. It is assumed that the particle can be treated as a point charge, relative to the thickness of the double layer f(κa)=1.0. Instrument settings and calculation parameters were: temperature at 25°C, dispersant viscosity at 0.89 cP and dielectric constant at 78.5. The viscosity of the samples was estimated to be that of water. All the samples measured were prepared at $10^{-4}$ M in PBS buffer solution (pH 7.4, 0.05 mM).

### 3.2.12 GW 3965 Encapsulation by oil/water emulsion

GW encapsualtion was performed using the following protocol. A GW 3965 solution (1.0 mg/ml) in dichloromethane was prepared by adding dichloromethane (5.0 ml) into the vial containing GW 6265 (5.0 mg). One equivalent (mole) of triethylamine (1.2 µl, 0.88 mg) was added to neutralize the HCl salt.

**1CM**, **0CM**, **1CP**, **1CM1CP** polymer solutions (1.6 mg/ml) in water were prepared by dissolving the polymers (40 mg) in HPLC-grade water (25.0 ml) and gently stirred over 40 minutes at room temperature. The GW 3965 solution (0.50 ml) was then added dropwise into polymer solutions (25.0 ml, wt/wt drug:polymer 1:80) with vigorous stirring at room temperature. The mixture was capped and stirred in the dark at room temperature for 12 hours, then stirred uncapped for another 24 hours to completely evaporate dichloromethane. The aqueous mixture was filtered under vacuum using a cellulose acetate membrane (8 µm pore size) to remove free GW 3965.

### 3.2.13 GW 3965 Encapsulation efficiency assessment

GW 3965 solution (0.50 mg/ml) in 1:1 DMA: $H_2O$ was prepared by adding a solution of 1:1 DMA: $H_2O$ (10 ml) into the vial containing GW 3965 (5.0 mg). One equivalent of triethylamine (1.2 µl, 0.88 mg) was added to neutralize the HCl salt. The solutions were diluted to 0.250, 0.188, 0.125, 0.0938, 0.0625, 0.0469, 0.0313 and 0.0157 mg/ml. The UV spectra for each solution were obtained from 90 to 400 nm. Based on these experiments, 272 nm was chosen as the value for calibration. Encapsulation efficiency was calculated based on the concentration of detected drug over the initial concentration of drug.

## 3.3 Results and Discussion

### 3.3.1 Synthesis of Macromolecules

Several different amphiphilic macromolecules were synthesized in which the number and location, and type of anionic groups were modified, as is shown in Scheme 3-5 and 3-6. The **1CM, 0CM** and **1CP** were prepared as described in previous work.[14] The design rationale for each macromolecule is as follows. **1CM1CP** probes the combinatorial activity of a carboxylic acid present in both the hydrophilic and hydrophobic blocks of AScMs. It was successfully synthesized by coupling bifunctional PEG with mucic acid acyl derivatives **1** activated as acyl chloride. **1BM** was prepared to investigate differences between aliphatic and aromatic carboxylates; in this molecule, carboxylates are located in the hydrophobic domain. Our first attempt to generate an aromatic carboxylate group was not successful; we attempted to couple molecule **1CM** directly with 4-hydroxybenzoic acid. However, the low nucleophilicity of the phenol yielded unacceptably low coupling efficiencies. Instead, we prepared the symmetric intermediate **2**, which was easy to purify and then successfully coupled with hydroxy-terminated PEG to obtain **1BM**. The macromolecule **0BM** was prepared as a control for **1BM** and synthesized through direct esterification of the carboxylate on polymer **1CM**. **2CM** was designed to study how two carboxylates in the hydrophobic block may synergistically influence hoxLDL uptake. Overall, all coupling reactions were achieved in reasonably high coupling efficiency and yield. All macromolecules displayed comparable molecular weights (~5500) and melting temperatures (~56 ˚C), likely due to the predominance of the PEG chain.

### 3.3.2 Physical Properties of AScMs

Micelle formation and nanoscale size are both important in highly oxidized LDL uptake inhibition; our hypothesis is that the macrophage receptors are slightly positively charged, such that nanoscale micelles with a high density of negative charges are more accessible via electrostatic interactions.

All amphiphilic macromolecules could self-organize to form micelles in aqueous solutions. Their size distributions were assessed and are shown in Table 3-1 and Scheme 3-7. The formation of micelles by macromolecules in water is indicated by the CMC values near $10^{-6}$ to$10^{-7}$ M, as shown in Table 3-1. The critical micelle concentration (CMC) is a crucial parameter that measures the stability of amphiphiles, a critical characteristic for biological applications to prevent dilution in blood plasma. Most of the AScMs have similar CMC values, indicating that a single negative charge does not prevent self-aggregation into micelles at pH 7.4. Notably, molecule **2CM** has a relatively higher CMC value compared to the other macromolecules. The two aliphatic carboxylate groups on the hydrophobic domain appear to slightly inhibit micelle formation, possibly due to the repulsion between adjacent negative charges in a slightly basic (pH 7.4) solution.

Similar to the CMC data, molecule **2CM** displays different behavior than the other macromolecules in terms of size. The micellar sizes of all AScMs, except **2CM**, are approximately 20 nm (Table 3-1), indicating that a single negative charge does not change the micelle aggregation size. In contrast, molecule **2CM** is larger in size (35 nm)

than the other macromolecules. Compared with the other macromolecules, **2CM** is relatively less hydrophobic due to the presence of two carboxylates in the hydrophobic block, resulting in a "looser" aggregation or larger size.

Zeta potential measurements determine the overall charge densities, which is expected to be negative for the carboxylate-containing amphiphilic macromolecules. The neutral macromolecules (**0CM** and **0BM**) registered slight negative charges (-3.5 mV and -0.4 mV, respectively). **1BM** has a slightly more negative zeta potential than **1CM** as benzoic acid is more acidic than the aliphatic carboxylic acid. Notably, **1CM1CP** has the most negative value (-20 mV) likely because it contains two carboxylate groups, one in the hydrophobic block and one in the hydrophilic block. Molecule **2CM** also bears two negative charges, but both carboxylate reside within the hydrophobic core. As a result, the charge density does not increase in comparison with **1CM**.

### 3.3.3 Highly-oxidized LDL Uptake Inhibition Studies Using Our Synthetic AScMs

Professor Prabhas Moghe's research group in the Biomedical Engineering Department performed this study. Their results are shown in Scheme 3-8 and briefly outlined.

At 24 hours, hoxLDL uptake in macrophages was significantly reduced in the presence of the anionic nano-sized micelles. The degree of uptake was normalized to non-micelle controls; positive controls included the neutral micelles (**0CM** and **0BM**). Among the effective hoxLDL uptake inhibitors, **1CM1CP** micelles resulted in the highest inhibition of hoxLDL uptake.

The key finding in their study was that charge alone does not determine the extent of hoxLDL internalization reduction by macrophage cells. **1CM1CP** is the most effective macromolecule in reducing hoxLDL internalization, while the similarly charged **2CM** reduced hoxLDL uptake even less than **1CM**. We hypothesize that the size of the **2CM** might modulate the behavior of nanoparticle binding to the scavenger receptors. Scavenger receptors typically bind to particles and are then internalized through clathrin-coated pits.[26] Previous studies have shown that the increased size of PEGylated nanoparticles, nanoscale iron oxide contrast agents, and colloids can promote their scavenger receptor mediated uptake in macrophages.[27] However, consequences for scavenger receptor ligands such as hox-LDL were not evaluated. The exact mechanism for micellar nanoparticle binding in our system is not clear, but we offer two potential mechanisms. For example, the larger **2CM** micellar nanoparticles (~35 nm) may promote the internalization of scavenger receptors in relation to the smaller diameter of **1CM1CP** micelle (23.1 nm) and reduce the availability of scavenger receptors for hoxLDL binding; this mechanism is consistent with previous reports. Alternatively, the larger nanoparticles may interfere with folding and internalization of scavenger receptors. In either case, the reduction in hoxLDL internalization is not addressed from charge alone: The **1CM** decreases hoxLDL internalization more significantly than **2CM**, even though both exhibit similar values of zeta potential (~-10mv).

### 3.3.4 GW 3965 Encapsulation into AScMs

Given the low concentration of GW3965 used in this study, nearly quantitative encapsulation was observed.

According to DLS data, the size of GW3965-encapsulated micelles (12 nm) are smaller than the free micelle alone (18-20 nm). This result may be due to the decreased aggregation number of micelle assemblies after GW loading.

### 3.4 Conclusions

Several AScMs were synthesized and evaluated in which the number and location of carboxylate groups were varied. All macromolecules formed stable micelles in physiologically relevant conditions. The negative charge located on the hydrophobic component affected micelle size and CMC values more than on charges located on the hydrophilic part. Compared with two neutral control polymers, **0CM** and **0BM,** the carboxylate-terminated polymers decreased hoxLDL uptake by macrophages. Overall, **1CM1CP** resulted in the most significant inhibition of hoxLDL uptake.

### 3.5 Future Work

Solution properties of the sulfuric acid monomethyl ester-functionalized AScMs, **1SM** and **3SM** will be assessed, including their ability to inhibit hoxLDL uptake. Future investigations may also focus on identifying the mode of micelle internalization, to address the hypothesis that micelle diameter affects scavenger receptor occupancy. Mixed micelles from different polymers could also be tested to determine whether a

micelle can be created that will decrease hoxLDL internalization even more significantly than the **1CM1CP** alone.

## 3.6 References


1. Williams, K. and Tabas, I., The response-to-retention hypothesis of early atherogenesis. *Arterioscler. Thromb. Vasc. Biol.,* **1995**. *15*: p. 551-561.
2. Olsson, U., Ostergren-Lunden, G. and Moses, J., Glycosaminoglycan-lipoprotein interaction. *Glycoconj. J.,* **2001**. *18*(10): p. 789-97.
3. Camejo, G., Olsson, U., Hurt-Camejo, E., Baharamian, N. and Bondjers, G., The extracellular matrix on atherogenesis and diabetes-associated vascular disease. *Atherosclerosis Suppl.,* **2002**. *3*(1): p. 3-9.
4. Malinski, T., Understanding nitric oxide physiology in the heart: a nanomedical approach. *Am. J. Cardiol.*, **2005**. *96*(7B): p. 13i-24i.
5. Carella, M., Volinia, S. and Gasparini, P., Nanotechnologies and microchips in genetic diseases. *J. Nephrol.,* **2003**. *16*(4): p. 597-602.
6. Ma, Z., He, W., Yong, T. and Ramakrishna, S., Grafting of gelatin on electrospun poly(caprolactone) nanofibers to improve endothelial cell spreading and proliferation and to control cell Orientation. *Tissue Eng.,* **2005**. *11*(7-8): p. 1149-1158.
7. He, W., Ma, Z., Yong, T., Teo, W. and Ramakrishna, S., Fabrication and endothelialization of collagen-blended biodegradable polymer nanofibers: potential vascular graft for blood vessel tissue engineering. *Tissue Eng.,* **2005**. *11*(9-10): p. 1574-1588.
8. Endo, M., Koyama, S. and Matsuda, Y., Thrombogenicity and blood coagulation of a microcatheter prepared from carbon nanotube nylonbased composite. *Nano Lett.*, **2005**. *5*: p. 101-105.
9. Meng, J., Kong, H. and Xu, H., Improving the blood compatibility of polyurethane using carbon nanotubes as fi llers and its implications to cardiovascular surgery. *J. Biomed. Mater. Res. A*, **2005**. *74*: p. 208-214.
10. Steinberg, D., Low density lipoprotein oxidation and its pathobiological significance. *J. Biol. Chem.*, **1997**. *272*: p. 20963-20966.
11. Brown, M. and Goldsten, J., Lipoprotein metabolism in the macrophage: implications for cholesterol deposition in atherosclerosis. *Ann. Rev. Biochem.*, **1983**. *52*: p. 223-261.
12. Boullier, A., Friedman, P. and Harkewicz, R., Phosphocholine as a pattern recognition ligand for CD36. *J. Lipid. Res.,* **2005**. *46*: p. 969-976.
13. Yoshiizumi, K., Nakajima, F., Dobashi, R., Nishimura, N., Ikeda, S., 2,4-Bis(octadecanoylamino)benzenesulfonic acid sodium salt as a novel scavenger receptor inhibitor with low molecular weight. *Bioorg. Med. Chem. Lett.,* **2004**. *14*(11): p. 2791-2795.
14. Chnari, E., Nikitczuk, J., Wang, J., Uhrich, K. and Moghe, P., Engineered polymeric nanoparticles for receptor-targeted blockage of oxidized low density lipoproteins uptake and atherogenesis in macrophages. *Biomacromolecules*, **2006**. *7*: p. 1796-1805.

15. Krieger, M., Acton, S. and Ashkenas, J., Molecular flypaper, host defense, and atherosclerosis: structure, binding properties, and functions of macrophage scavenger receptors. *J. Biol. Chem.*, **1993**. *268*: p. 4569-4572.
16. Tian, L., Yam, L., Zhou, N., Tat, H. and Uhrich, K., Amphiphilic scorpion-like macromolecules: Design, synthesis, and characterization. *Macromolecules,* **2004**. *37*(2): p. 538-542.
17. Djordjevic, J., Barch, M. and Uhrich, K., Polymeric micelles based on amphiphilic scorpion-like macromolecules: Novel carriers for water-insoluble drugs. *Pharm. Res.*, **2005.** *22*(1): p. 24-32.
18. Tao, L. and Uhrich, K., Novel amphiphilic macromolecules and their in vitro characterization as stabilized micellar drug delivery systems, *J. Colloid Interfac. Sci.,* **2006**. *298*: p. 102-110.
19. Chnari, E., Lari, H., Tian, L., Uhrich, K. and Moghe, P., Nanoscale anionic macromolecules for selective retention of low density lipoproteins,. *Biomaterials*, **2005**. *26*: p. 3749-3758.
20. Joseph, S., Castrillo, A., Laffitte, B., Mangelsdorf, D. and Tontonoz, P., Reciprocal regulation of inflammation and lipid metabolism by liver X receptors. *Nat. Med.*, **2003**. *9*(2): p. 213-219.
21. Geyeregger, R., Zeyda, M. and Stulnig, T., Liver X receptors in cardiovascular and metabolic disease. *Cell Mol. Life Sci.,* **2006**. *63*: p. 524-39.
22. Joseph, S., McKilligin, E., Pei, L., Watson, M., Collins, A., Laffitte, B., Chen, M., Noh, G., Goodman, J., Hagger, G., Tran, J., Tippin, K., Wang, X., Lusis, A., Hsueh, W., Law, R., Collins, J., Willson, T. and Tontonoz, P., Synthetic LXR ligand inhibits the development of atherosclerosis in mice. *Proc. Natl. Acad. Sci. U S A,* **2002**. *99*(11): p. 7604-7609.
23. Law, R., Collins, J., Willson, T. and Tontonoz, P., Synthetic LXR ligand inhibits the development of atherosclerosis in mice. *Proc. Natl. Acad. Sci. U S A,* **2002**. *99*(11): p. 7604-7609.
24. Lai, S., Hida, K., Man, S., Chen, C., Machamer, C., Shroer, T. and Hanes, J., Privileged delivery of polymer nanoparticles to the perinuclear region of live cells via a non-clathrin, non-degradative pathway. *Biomaterials*, **2007**. *28*: p. 2876-2884.
25. Moore, J. and Stupp, S., Room temperature polyesterification. *Macromolecules,* **1990**. 23: p. 65-70.
26. Platt, N., and.Glen, S., Is the class A macrophage scavenger receptor (SR-A) multifunctional? - The mouse's tale. *J. Clin. Investigation,* **2001**. *108*: p. 649-654.
27. Moghimi, S. and Stupp, J., Stealth liposomes and long circulating nanoparticles: critical issues in pharmacokinetics, opsonization, and protein-binding properties. *Prog. Lipid Res.,* **2003**. *42*: p. 463-478.

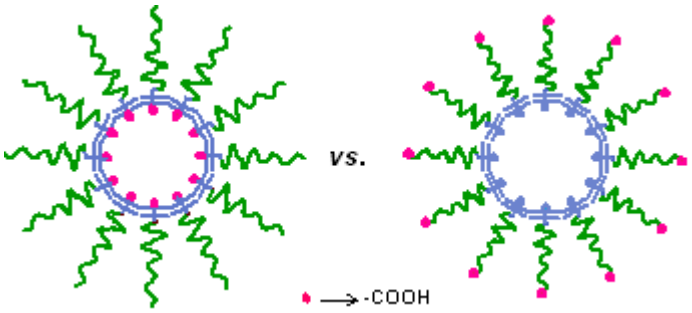


Scheme 3-1. Cartoon illustration of the potential location for carboxylate groups on AScM micelles

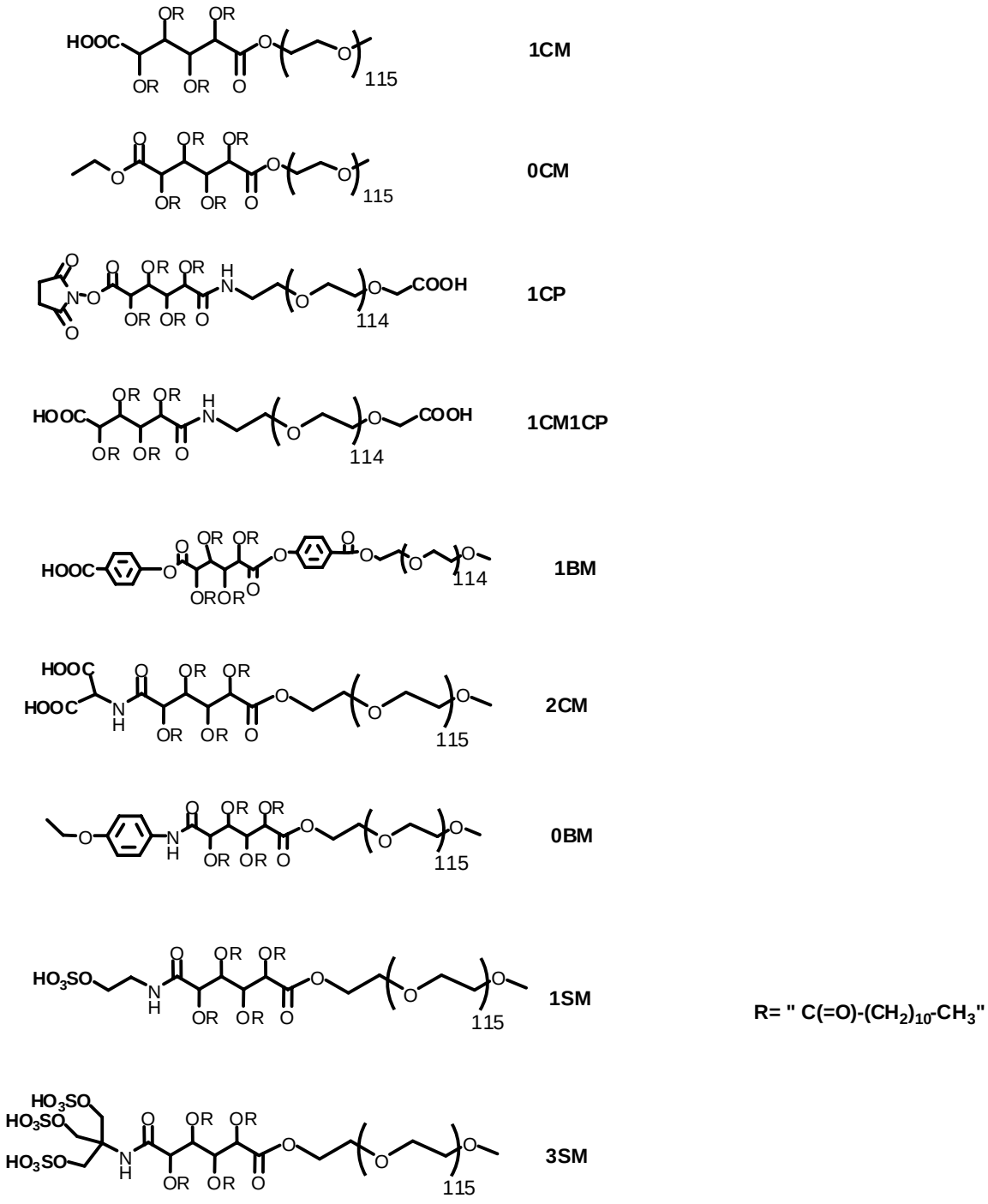


Scheme 3-2. Abbreviation and chemical structures of AScMs

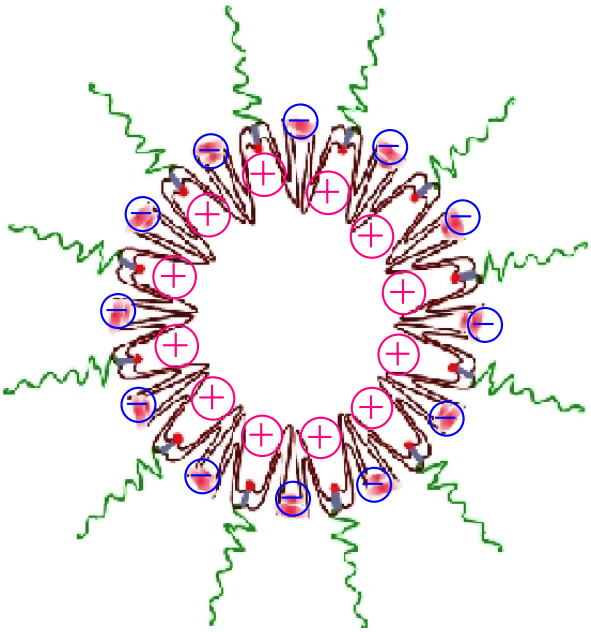

⊕: $H^+NR_3$ on GW 3965; ⊖: $R\text{-}COO^-$ on polymers

Scheme 3-3 Graphic description of GW-loaded AScM, **1CM**.

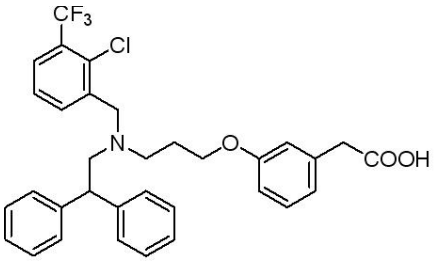

· HCl

Scheme 3-4 Chemical structure of GW 6295

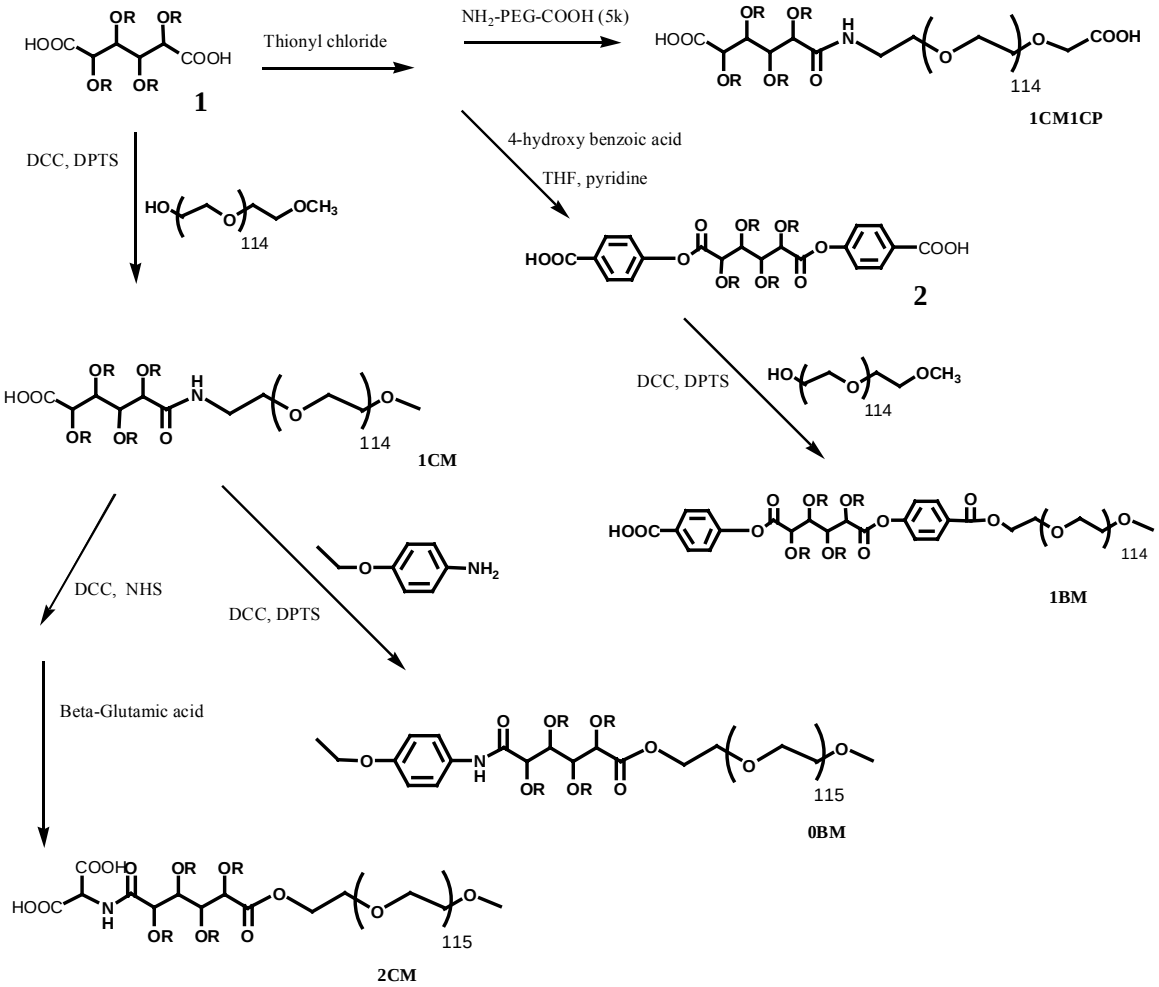


Scheme 3-5. Synthesis of macromolecules **1CM1CP**, **1BM**, **0BM** and **2CM**.

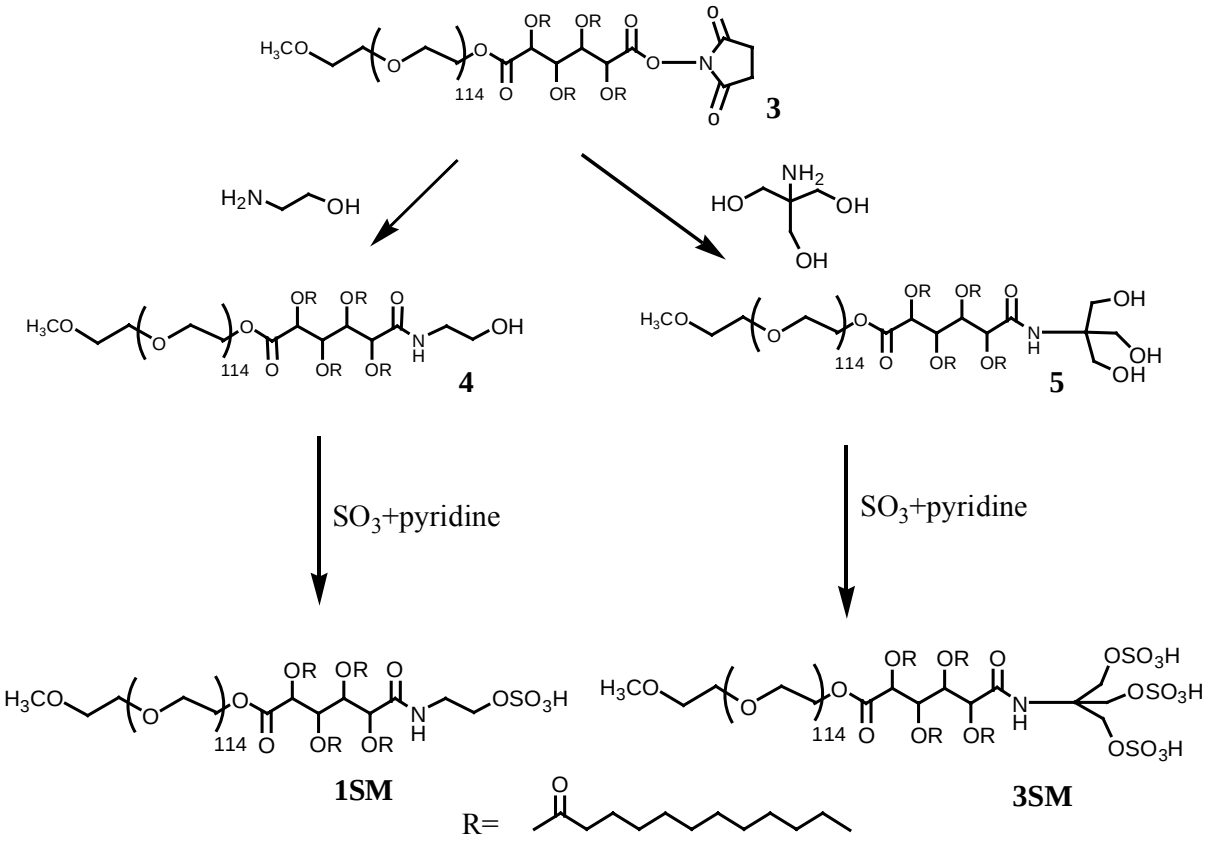


Scheme 3-6. Synthesis of macromolecules **1SM** and **3SM**.

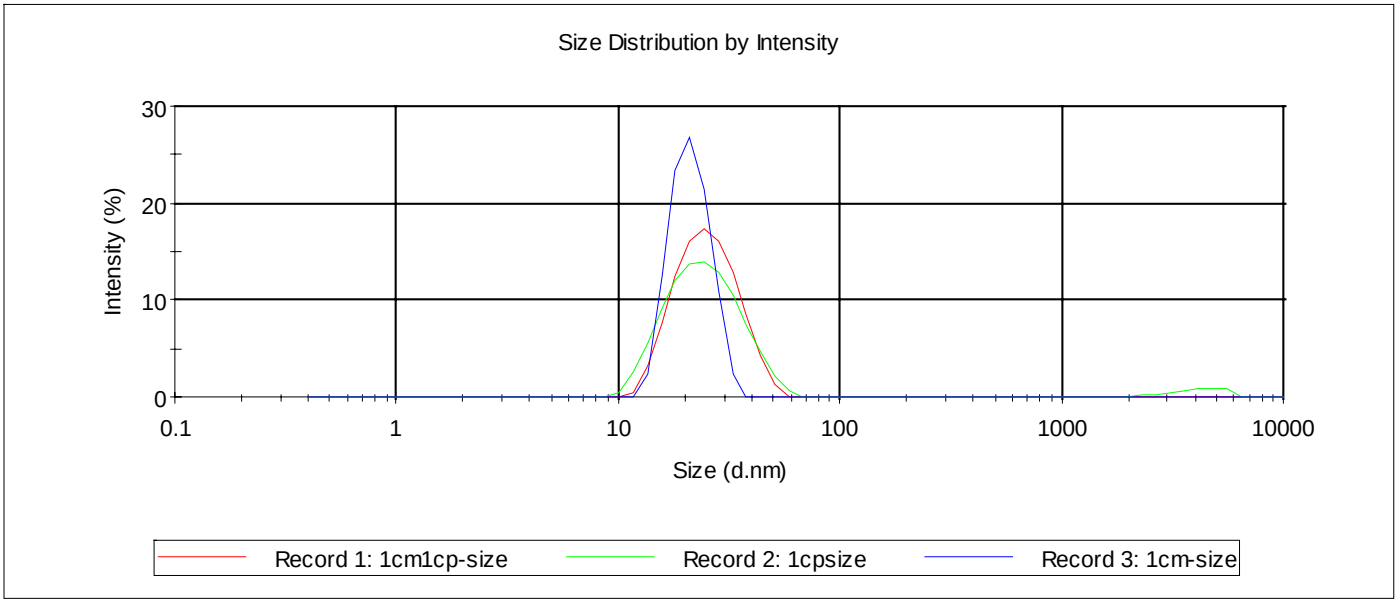


Scheme 3-7. Representative dynamic light scattering data of **1CM, 1CP and 1CM1CP** in aqueous solutions.

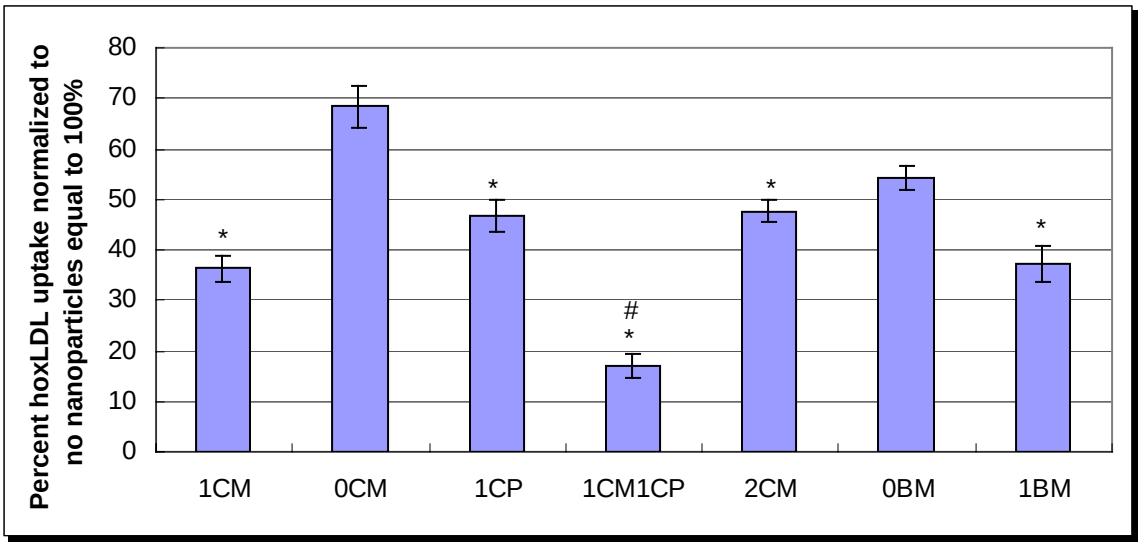


*Scheme 3-8: Percent of hoxLDL uptake by macrophage cells after 24 hours when compared to hoxLDL uptake with no AScM present. (* represents a significant decrease (P<.05) in comparison to hoxLDL alone; # represents a significant decrease (P<.05) in comparison to hoxLDL with **1BM** or **1CM**)*

*-----Result obtained from our collaborator, Prof. Moghe's research group*

| | **1CM** | **0CM** | **1CP** | **1CM1CP** | **1BM** | **2CM** | **0BM** |
|---|---|---|---|---|---|---|---|
| **Size (nm)** | 23.2±5.2 | 27.4±2.5 | 23.6±5.9 | 23.1±4.8 | 23.4±3.7 | 35.1±4.7 | 23.9±4.2 |
| **CMC (M)** | $3.2x10^{-7}$ | $5.7x10^{-7}$ | $1.0x10^{-7}$ | $8.8x10^{-7}$ | $7.0x10^{-7}$ | $1.8x10^{-7}$ | $7.8x10^{-7}$ |
| **Zeta-potential (mv)** | -10±5.0 | -0.47±0.21 | -9.6±3.8 | -20±6.6 | -15±6.0 | -9.2±2.9 | -3.5±1.0 |

Table 3-1. Particle sizes, CMC and zeta-potential values of the AScMs at pH 7.4 at $10^{-4}$ M.

# CHAPTER FOUR. AMPHIPHILIC STAR-LIKE AND SCORPION-LIKE MACROMOLECULES OPTIMIZATION TO ACHIEVE A BETTER DRUG DELIVERY SYSTEM BASED ON POLYMER MICELLES

## 4.1 Introduction

Polyethylene glycol (PEG) is widely used to modify biological macromolecules. Its applications in pharmaceutical chemistry are receiving increasing attention due to its unique properties, as related by the large number of reviews in the field.[1-3]

The synthesis of branched PEG for modifying drugs and protein therapeutics has become a major focuses.[4] Monfardini and coworkers reported that enzymes modified with branched PEG chains presented greater stability to proteolytic digestion relative to those modified with the linear PEG chains.[5] Reddy reported that branched-chain PEGylated proteins are more stable against enzyme proteolysis than linearPEg analogs, and may even display enhanced the absorption and distribution.[6] These studies indicated that branched PEG might be a better choice in protein therapeutics.

'Branched' PEG analogues are superior with respect to the linear PEG chains in creating an 'umbrella-like' surface coverage of the protein, thus protecting it from proteolysis and reducing its inactivation during conjugation,[2, 5] while branched PEG is becoming popular in drug PEGylation and protein therapeutics, the use of branched PEG in polymeric micelles is rarely studied by scientists. Yet, the advantages of branched PEG in proteins should also apply to polymeric micelles as drug delivery systems (e.g., reduced

proteolysis and enhanced drug absorption). In star-like micelles, branched PEG can provide a larger hydrophilic surface to volume number compare with its linear counterpart.[7,8] This feature may prevent higher order aggregation and maintain a smaller size, while providing the same PEG total chain length.[9-11]

In this chapter, scorpion-like and star-like macromolecules were optimized to include shorter and more branched hydrophilic PEG shells (Scheme 4-1 and Scheme 4-2). The second generation ASM and AScM polymers were prepared to explore how shorter, branched PEG chains influence the overall size of the micelles, water-solubility and drug loading capacity. A hydrophobic anti-inflammatory drug, indomethacin, was used to evaluate the encapsulation ability of the polymeric micelles.

## 4.2 Experimental Procedures

### 4.2.1 Materials

Indomethacin (IMC), phosphate buffer tablets, heparin sodium salt (grade I-A from porcine intestinal mucosa), cellulose acetate membranes (Spectra/Por MWCO 3500) and regenerated cellulose membrane (Spectra/Pro MWCO 100,000) were purchased from Sigma-Aldrich (St. Louis, MO, USA). Monomethoxy-poly(ethylene glycol) (mPEG) with molecular weights of 5000 Da and 2000 Da were purchased from Sigma-Aldrich. All PEG reagents were dried by azeotropic distillation with toluene. All other reagents and solvents were purchased from Sigma-Aldrich and used as received. Compounds were prepared as previous described: **MA12**[9], Compound **5** [10], **M12P5** [11] and **NC12P5** [10].

### 4.2.2 Synthesis and Characterization Methods

Compounds were analyzed by $^{1}H$ and $^{13}C$ NMR spectroscopy with samples (~ 5-10 mg/ml) dissolved in DMSO-*d* and $CDCl_3$-*d* solvent on Varian 300 MHz and 400 MHz spectrometers, using tetramethylsilane as the reference signal.

Gel permeation chromatography (GPC) was used to obtain molecular weight and polydispersity index (PDI). Measurements were performed on Waters Breeze GPC system equipped with Styragel® HR3 column (ID 7.8 mm, and length 300 mm) and with a Water 2414 refractive index detector, 1515 isocratic HPLC pump and Waters 717 plus Autosampler. Tetrahydrofuran (THF) was the eluent for analysis and solvent for sample preparation. Sample was dissolved into THF (~ 5 mg/ml) and filtered through a 0.45 μm PTFE syringe filter (Whatman, Clifton, NJ) before injection into the column at a flow rate of 0.8 ml/min. The average molecular weight of the sample was calibrated against narrow molecular weight polystyrene standards (Polysciences, Warrington, PA).

IR spectra were recorded on a Mattson Series spectrophotometer (Madison Instruments, Madison, WI) by solvent (methylene chloride) casting on a KBr pellet. Negative ion-mass spectra were recorded with ThermoQuest Finnigan $LCQ^{TM}_{DUO}$ System (San Jose, CA) that includes a syringe pump, an optional divert/inject valve, an atmospheric pressure ionization (API) source, a mass spectrometer (MS) detector, and the Xcalibur data system.

### 4.2.3 Synthesis of Double-chained PEG Chain with Amine Functional Group 4

Aminoisophthalic acid (1.8 g, 10 mmol) **1** was reacted with di-*t*-butyl dicarbomate (2.4 g, 11 mmol) in 1,4-dioxane (20 ml) and 1 N NaOH (20 ml) for 3 h at 0˚C. After filtration and drying, **2** was obtained as white powder: 2.6 g, 92% yield. $^1$H NMR ($CDCl_3$): δ 11.07 (s, 2H, COO*H*), 8.85 (s, 2H, Ar*H*), 8.77 (s, 1H, Ar*H*), 8.10 (s, 1H, N*H*), 1.41 (s, 9H, C*H*$_3$). IR (KBr, cm$^{-1}$): 3310 (COOH), 2940 (C-H), 1742, 1758 (C=O), 821( Ar-H). FW: 281.1; MS: 281.2. $T_m$: 278-279˚C.

Two equivalents of mPEG-OH (2,000 Da) (12 g, 6.0 mmol) were reacted with *t*-Boc-5-aminoisophthalic acid **2** (0.70 g, 2.5 mmol) by DCC (6.0 ml of 1M methylene chloride solution)/DPTS (2.6 g) for 48 h at room temperature in $CH_2Cl_2$ (20 ml) and DMF (5 ml). After filtration, the filtrate was washed with 0.1 N HCl and brine. After solvent removal, the crude product was purified by precipitation into ethyl ether (100 ml) from $CH_2Cl_2$ (5.0 ml). Unreacted mPEG-OH was removed by gel filtration chromatography using Sephadex G-75 as resin and HPLC-grade water as eluent. Product was lyophilized. Compound **3** was obtained as white solid: 7.8 g, 73% yield. $^1$H NMR ($CDCl_3$): δ 9.75 (s, 1H, N*H*), 8.28 (s, 2H, Ar*H*), 8.05 (s, 1H, Ar*H*), 3.36 (m, ~360 H, C*H*$_2$O), 1.47 (s, 9H, C*H*$_3$). IR (KBr, cm$^{-1}$): 2951 (C-H), 1744, (C=O), 1230, 1173 (C-O), 821(Ar-H). $T_m$: 51-53˚C,

The *t*-Boc protecting group was removed by stirring compound **3** in excess 50% TFA (20 ml) in $CH_2Cl_2$ (40 ml) solution at 0˚C for 4 h. After evaporation, the product was recrystallized in ethyl ether (100 ml) to obtain **4** as white powder: 7.6 g, 98% yield. $^1$H

NMR ($CDCl_3$): δ 8.05 (s, 1H, Ar*H*), 7.55 (s, 1H, N*H*), 7.32 (s, 1H, Ar*H*), 4.47 (t, 4H, C*H*$_2$), 3.36 (m, ~360 H, C*H*$_2$O). IR (KBr, $cm^{-1}$): 3300 (N-H), 2944 (C-H), 1740, (C=O), 1232, 1175 (C-O), 824 (Ar-H). $T_m$: 53-54˚C.

### 4.2.4 Synthesis of Double-chained AScM M12P2x2

Mucic acid derivative **MA12** (0.49 g, 0.50 mmol) was reacted with **4** (0.71 g, 0.17 mmol) in the presence of DCC (0.50 ml of 1 M methylene chloride solution)/DPTS (0.31 g) in $CH_2Cl_2$ (15 ml) for eighteen hours at room temperature. After filtration, the filtrate was washed with 0.1 N HCl (20 ml × 2) and brine (20 ml × 2). The solution was concentrated to 5 ml and product precipitated by adding ethyl ether (100 ml). Product **M12P2x2** was collected as white powder: 0.65 g, 93% yield. $^1$H NMR ($CDCl_3$): δ 8.42 (s, 1H, Ar*H*), 8.38 (s, 2H, Ar*H*), 5.75 (d, 2H, C*H*), 5.51 (m, 1H, C*H*), 5.14 (d, 1H, C*H*), 4.43 (t, 4H, C*H*$_2$), 3.68 (m, ~360 H, C*H*$_2$O), 2.37 (m, 4H, C*H*$_2$), 2.25 (m, 4H, C*H*$_2$), 1.59 (m, 4H, C*H*$_2$), 1.24 (m, 48H, C*H*$_2$), 0.84 (t, 12H, C*H*$_3$). IR (KBr, $cm^{-1}$): 3311 (N-H), 2985 (C-H), 1742, 1749 (C=O), 1230, 1168 (C-O), 819 (Ar-H). $T_m$=49-50˚C. GPC: Mw: 5,010; PDI: 1.2.

### 4.2.5 Synthesis of Double-chained ASM NC12P2x2

Compound **5** (0.33 g, 0.1 mmol) was dissolved in $SOCl_2$ (50 ml) and heated at 70˚C for four hours, then excess $SOCl_2$ removed by rotary evaporator. The reaction flask was dried under vacuum oven, then dissolved in THF (5 ml). To this solution was added excess 5-aminophthalic acid (0.11g, 1.0 mmol) in THF (15 ml) and pyridine (5 ml). The reaction mixture was stirred at room temperature for six hours, then the reaction mixture

poured into 1 N HCl solution (200 ml) and the precipitate collected by filtration was rinsed by deionized water. A yellow solid **6** was obtained: 0.34 g, 93% yield. NMR data is not shown here (due to larger number of COOH group on the surface, all the peaks are broad). IR (KBr, $cm^{-1}$): 2945 (C-H), 1751, 1731 (C=O), 1225, 1161 (C-O), 815, 780 (Ar-H).

Compound **6** (0.07 g, 0.2 mmol) and mPEG (2k) (4.0 g, 2.0 mmol, 10 fold) were dissolved in $CH_2Cl_2$ after azeotropic distillation in toluene (20 ml). DPTS (0.54 g, 2.0 mmol) and DCC (2.0 ml in 1 M $CH_2Cl_2$, 2.0 mmol) were then added dropwise. The reaction mixture was stirred at room temperature for 48 hours. The side product was removed by vacuum filtration; the filtrate was washed with brine (3x10 ml), dried over anhydrous sodium sulfate and evaporated to dryness. Crude product **6** was precipitated by recrystallization in diethyl ether (30 ml) from methylene chloride (3 ml). To remove the unreacted mPEG, the polymer solution was dialyzed against water using a dialysis membrane with MWCO 100,000. Polymer (100 mg) dissolved in PBS (50 ml) was placed into a dialysis bag and dialyzed against 4 L deionized water. After 8 h, the content of the dialysis bag was lyophilized (FreeZone© Benchtop and Console Freeze Dry System, Labconco, Kansas City, Missouri) overnight. Compound **NC12P2x2** was isolated as a slight yellow powder: 2.1 g, 64% yield. $^1$H NMR ($CDCl_3$): δ 8.20 (s, 2H, Ar*H*), 7.23 (d, 8H, Ar*H*), 6.95 (d, 8H, Ar*H*), 4.05 (s, 8H, C*H*$_2$), 3.71 (m, ~360 H, C*H*$_2$O), 2.99 (t, 8H, C*H*$_2$), 2.50 (t, 8H, C*H*$_2$). IR (KBr, $cm^{-1}$): 3459, 3371, 1597, 733 (N-H), 3026, 829( Ar-H), 17 45, 1732 (C=O), 1276 (C-N), 1236, 1176 (C-O), 1020 (C-S). $T_m$: 50-51˚C. GPC: Mw: 12,300; PDI: 1.4.

### 4.2.6 Melting Temperature Determination

Melting temperature ($T_m$) and crystallization temperature ($T_c$) were determined by differential scanning calorimeter (DSC). Thermal analyses were performed on a Perkin-Elmer system consisting of a Pyris 1 DSC analyzer with TAC 7/DX instrument controllers. Perkin-Elmer Pyris software was used for data collection on a Dell OptiPlex GX110 computer. For DSC, samples (5 mg) were heated under dry nitrogen gas. Data were collected at heating and cooling rates of 10 ºC/min with a two-cycle minimum. $T_m$ and $T_c$ were obtained as peak values.

### 4.2.7 Dynamic Light Scattering Measurement

Dynamic light scattering (DLS) analyses were performed using a Malvern Instruments Zetasizer Nano ZS-90 instrument (Southboro, MA), with reproducibility verified by collection and comparison of sequential measurements. Polymer solutions (1.0 wt %) were prepared in phosphate buffered aqueous solution (PBS) (pH 7.4). Measurements were performed at a 90° scattering angle at 25°C.

### 4.2.8 Fluorescence Spectroscopy

Critical micelle concentration (CMC) studies were carried out on a Spex fluoroMax (Piscataway, NJ) Spectrofluorometer at 25°C using pyrene as the probe molecule. A stock solution at 5.00 $x10^{-7}$ M in pH 7.4 PBS buffer solution was prepared. Polymer samples were first dissolved in the stock pyrene solutions, and then diluted to specific

concentrations. Excitation was performed from 300 nm to 360 nm, using 390 nm as the emission wavelength. Pyrene maximum absorption shifted from 332 nm to 334.5 nm with secondary micelle formation. The ratio of absorption of polymer (334.5 nm) to pyrene only (332 nm) was plotted as the logarithm of polymer concentration. The inflection point of the curves was defined as the CMC values.

### 4.2.9 Polymer Solubility in Water

Polymer solubility was measured by gravimetric analysis. Saturated solutions of each sample were prepared with excess polymers (>500 mg) in 6.0 ml HPLC-grade water. The solutions were stirred for five hours at room temperature. Each clear polymer solution was passed through 0.45 μm PTFE syringe filter (Whatman, Clifton, NJ) and lyophilized (FreeZone© Benchtop and Console Freeze Dry System, Labconco, Kansas City, Missouri). After 48 hours, the dry polymers were weighed and solubilities calculated as mg/ml.

### 4.2.10 Indomethacin Loading by Oil/Water Emulsion

Indomethacin (10 mg) was dissolved in dichloromethane (4.0 ml) to make a 2.5 mg/ml solution. Indomethacin aliquots (1.0 ml) were added dropwise into 50.0 ml polymer solutions (0.5 mg/ml) in HPLC-grade water (wt/wt drug:polymer 1:10) with continuous stirring at room temperature. The mixtures were capped and stirred in the dark at room temperature for 24 hours to equilibrate. The solutions were uncapped and stirred for another 24 hours. The resulting aqueous mixture was filtered under vacuum using a

cellulose acetate membrane (8 μm pore size) to remove precipitated drug. All measurements were performed in triplicate.

Indomethacin was detected by UV-Vis spectrophotometry (λ = 318 nm) after complete disruption of the drug-loaded micelles with addition of N'N-dimethylacetamide (DMA) (1:1 dilution). Indomethacin standard solutions were prepared in 1:1 DMA: $H_2O$. Calculation of weight percentage loading and encapsulation efficiency were determined as follows:[12]

Weight percent loading was calculated based on the concentration of drug detected over the concentration of polymers in the solution:[13]

$$\text{Weight \% Loading} = \frac{\text{Concentration of drug detected}}{\text{Concentration of polymer}} \times 100\%$$

Encapsulation efficiency was calculated based on the concentration of drug detected over the initial concentration of drug put in the solution:

$$\text{Encapsulation Efficiency (\%)} = \frac{\text{Concentration of drug detected}}{\text{Initial concentration of drug}} \times 100\%$$

**4.2.11 Resolubilization of Lyophilized Indomethacin-Loaded Polymers**

*This experiment was performed with the help of Leilani del Rosario. The indomethacin-loaded polymer micelle solutions were frozen at -20ºC and lyophilized at < 133 x $10^{-3}$ mBar (condenser T = -50ºC) for 48-72 h. HPLC-grade water was added to the lyophilized solids to obtain a final indomethacin concentration of 1.0 mg/ml. The rate of resolubilization was determined using a timer, from the time of addition of water to*

*complete dissolution of all particles. The samples were visually assessed, with the solutions mildly swirled by hand. Each measurement was performed in triplicate. Particle size distribution of the resolubilized indomethacin-loaded polymers was determined by dynamic light scattering using a Malvern Zetasizer Nano instrument, after incubation of the solutions at 37ºC, 2h, and filtered using 0.45 µm PVDF syringe filters.*

### 4.2.12 Indomethacin Release from Polymeric Micelles

*Leilani del Rosario and Bahar Demirdirek performed the experiment in thissection.*

*The lyophilized indomethacin-loaded polymers were resolubilized in phosphate buffered saline (PBS) pH 7.4 to obtain a final polymer concentration of ~1 x $10^{-4}$ M. The release protocol consisted of pre-soaked (PBS pH 7.4, for ~18 h) regenerated cellulose membrane (MWCO 3.5 kDa) placed between the donor cell and receptor cell of equilibrium dialysis cells (Bel-Art Products, NJ), and the apparatus incubated in a 37ºC water bath. The indomethacin-polymer solutions were added into 5-mL donor cells and fresh PBS solutions into the 5-mL receptor cells. Receptor solutions were retrieved (5 mL) at specific time intervals and replaced with the same amount of fresh buffer. Indomethacin concentration was determined by UV-vis spectrophotometry (λ=318 nm) using PBS solution (pH 7.4) as blank.*

### 4.2.13 Polymer Interaction with Bovine Serium Albumin Proteins

Polymer: BSA solutions were prepared at ratios of 1:1, 1:10 and 10:1. Three samples were prepared (10 mg polymer + 10 mg BSA, 10 mg polymer + 1 mg BSA, and 1 mg

polymer + 10 mg BSA) by dissolution in 5.0 ml PBS (pH 7.4). Pure BSA (10 mg) and pure polymer (10 mg) were also prepared in 5.0 ml PBS solution as controls. Solutions were prepared with the help of Leilani del Rosario. All the samples were incubated at 37˚C for eight hours then evaluated using dynamic light scattering.

### 4.2.14 Critical Micelle Temperature Study

Polymer solutions (**M12P5**, **M12P2x2**, **NC12P5**, **NC12P2x2**, Cremophor EL and Pluronic P85) were prepared at 0.5 mg/ml, which is the lowest concentration of all polymers detectable by the Zetasizer Nano ZS-90 instrument (Southboro, MA). Particle size measurements were performed from 2˚C (lowest temperature of instrument control) to 70˚C (highest temperature for plastic cuvette resistance). The sizes of individual monomers before aggregation are beyond the instrument sensitivity limit and could not be detected. Samples were equilibrated for ten minutes at each temperature point before the measurement.

## 4.3 Results and Discussion

### 4.3.1 Synthesis and Characterization

Two novel double-chained amphiphilic polymers and two single-chained controls were designed to evaluate the influence of multiple and shorter PEG chains. Chemical structures are shown in Scheme 4-1: **M12P5** is single-chained AScM, **M12P2x2** is double-chained AScM, **NC12P5** is single-chained ASM and **NC12P2x2** is double-chained ASM.

The double-chained PEG, component **3** was prepared from a tri-functional linker 5-aminoisophthalic acid. **M12P2x2** was then prepared by coupling **4** onto derivatized mucic acid (Scheme 4-3). **NC12P2x2** was prepared by coupling four 5-aminoisophthalic acid molecules (**1**) onto the hydrophobic core **5** to generate an intermediate with eight carboxylate groups **6**, as shown in Scheme 4-4. The final product **NC12P2x2** was prepared by coupling eight PEG (2k) chains to the intermediate.

Polymer solubility in aqueous solution was measured by gravimetric analysis of lyophilized, saturated solutions. The results are shown in Table 4-1. Maximum water solubilities of the double-chained polymers (**M12P2x2** and **NC12P2x2** l) are higher than single-chained polymers (**M12P5** and **NC12P5**). This effect is notable because the total PEG content of the double-chained polymers (Mw ~4000) are less than the single-chained polymers (Mw ~5000). As PEG is the only water-soluble component in the polymer, we anticipated that **M12P2x2** and **NC12P2x2** might be *less* soluble in water than their higher Mw PEG chain analogs.

### 4.3.2 Size Distribution of Micelles

The sizes of the polymers in saturated and low concentration (0.05-0.1 mg/ml) aqueous solutions were evaluated by dynamic light scattering. (Scheme 4-6 and Table 4-1). At high concentrations (>20 mg/ml), the micelle sizes formed by double-chained polymers, **M12P2x2** (15.1 nm) and **NC12P2x2** (22.2 nm), are slightly smaller than the single-chained **M12P5** (21.3 nm) and **NC12P2x2** (51.6 nm). Higher order aggregations were not observed for the ASMs (NC12P5 and NC12P2x2), at high or low concentrations,

indicating that they form stable unimolecular micelles in water. From previous work, the CMC values are 2.74 x $10^{-6}$ M for **M12P2x2** and 1.25 x $10^{-7}$ M for **M12P5** from fluorescence studies.[11] The double-chained AScM do not aggregate as effectively as single-chained AScM, an effect likely influenced by steric hindrance.

### 4.3.3 Indomethacin Loading and Entrapment Efficiency

The loading and encapsulation efficiency of indomethacin (IMC) in **M12P5**, **M12P2x2**, **NC12P5** and **NC12P2x2** polymeric micelles were also evaluated. The IMC-loaded systems were prepared by oil/water emulsion method using 1:10 (IMC: polymer) feed ratio by weight. Pluronic P85 and Cremophor EL were used as control polymers; the results are summarized in Table 4-2.

Encapsulation efficiencies for the polymers (28-46%) were larger than for the controls, Pluronic (6%) and Cremophor (31%). Similarly, drug loading ranged from 2.8 to 4.6 wt% for the polymers, compared to 1% for Pluronic P85 and 3% for Cremophor EL. Based on this data, drug loading capacity is primarily affected by hydrophobic interaction, or drug-hydrophobic core binding affinity.[14]

### 4.3.4 Resolubilization of Lyophilized Indomethacin-Loaded Polymers

A major concern for the application of polymeric micelles as drug delivery system is storage stability and quick solubilization upon dissolution. Preferably, drug formulations are stored as dry powers that can be resolubilized prior to use. Table 4-3 shows solubilization times of the polymers after IMC loading and lyophilization. Overall,

resolubilization times were faster for ASM and AScMs than the controls, Pluronic P85 and Cremophor EL. Notably, the unimolecular micelle (**NC12P2x2** and **NC12P5**), displayed less resolubilization times, 15 and 12 seconds, respectively.

### 4.3.5 Indomethacin Release

IMC release from the polymers were conducted using a 1:10 drug:polymer ratio. As shown in Scheme 4-7, IMC release from the amphiphilic macomolecules displayed sustained release behavior over 48 hours relative to the free indomethacin control. Notably, IMC release from the amphiphilic macromolecules was slower relative to the control polymers, Pluronic P85 and Cremophor EL, within the first 48 hours. The observation may be explained by stronger interactions of IMC with the hydrophobic fatty-acid based core of the ASMs and AScMs.

In general, IMC release from the double-chained polymers (**M12P2x2** and **NC12P2x2**) is slower than from single-chained polymers (**M12P5** and **NC12P5**). This effect is likely due to the slower diffusion of IMC from the hydrophobic core through the compact PEG shells of the double-chained polymers. Furthermore, IMC release from the unimolecular micelles (ASMs) is slower relative to the AScMs.

### 4.3.6 Interaction with Bovine Serum Albumin Proteins

PEG-based systems are known to minimize their interaction with proteins due to the repelling nature of ethylene glycol chains with protein peptide chains.[2, 15-17] For these new polymers, protein interactions were evaluated by dynamic light scattering methods

using bovine serum albumin (BSA), a common protein.[18] No higher order aggregations or complexes were observed for the amphiphilic macromolecules including the control polymers. (Scheme 4-8) These experiments confirm the stability of PEG shielded micelles in serum plasma, which is consistent with related research.[7] The micelle sizes for all polymer micelle:BSA mixtures are reduced by 10-30% relative to the original micelle sizes.

### 4.3.7 Critical Micelle Concentration and Temperature Study

As outlined in previous chapters, critical micelle concentration (CMC) of micelles is a crucial parameter that measures the stability of polymeric amphiphiles.[19] Critical micelle temperature (CMT) is another measurement of micellar stability in aqueous solution. [20] CMT is the lowest temperature at which micelles can form at a given concentration; the more stable the micelle, the lower the CMT. Using dynamic light scattering, micellar sizes were measured from 2 to 70˚C. The results are shown in Scheme 4-9. For the ASMs, micellar sizes are stable over the temperature range, **NC12P5** remains at 50 nm and **NC12P2x2** at 24 nm. The same phenomenon was unexpectedly observed for the AScMs: **M12P5** was remained 26 nm and **M12P2x2** at 12 nm over the temperature range. In contrast, Cremophor EL aggregates at 15˚C and Pluronic undergoes a transition at 45 ˚C. Overall, the amphiphilic macromolecular micelles are very stable over a wide temperature range.

## 4.4 Conclusions

Novel double-chained polymers **M12P2x2** and **NC12P2x2** were successfully synthesized. The physicochemical properties were compared to their single-chained analogs, **M12P5** and **NC12P5**. Overall, double-chained polymers are more soluble than single-chained polymers, yet all four compositions form stable unimodal micelles in aqueous solutions. Double-chained polymers have competitive loading efficiencies with single-chained polymers, and displayed even slower release profiles. Loading and release studies with IMC demonstrated that all four polymers display slower IMC release profile compared to the control polymer, Cremophor CE and Pluronics P85.

## 4.5 References


1. Veronese, F., Peptide and protein PEGylation: A review of problems and solutions. *Biomaterials*, **2001**. *22*: p. 405-417.
2. Greenwald, R., Conover, C. and Choe, Y., Poly(ethylene glycol) conjugated drugs and prodrugs: A comprehensive review. *Crit. Rev. Ther. Drug,* **2000**. *17*: p. 101-161.
3. Greenwald, R., PEG drugs: an overview. *J. Control. Rel*., **2001**. *74*(1-3): p. 159-171.
4. Ren, Y., Zhang, H. and Huang, J., Synthesis and cytotoxic activity of platinum complex immobilized by branched polyethylene glycol. *Bioorg. & Med. Chem. Lett.,* **2005**. *15*(20): p. 4479-4483.
5. Monfardini, C., Schiavon, O., Caliceti, P., Morpurgo, M., Harris, J and Veronese, F., *A* branched monomethoxypoly(ethylene glycol) for protein modification. *Bioconj. Chem.*, **1995**. *61*: p. 62-69.
6. Reddy, K., Modi, M. and Peddr, S., Use of peginterferon alfa-2a (40 KD) for the treatment of hepatitis C. *Adv. Drug Delivery Rev.*, **2002.** *517*(54) p. 617-622.
7. Fee, C., Size Comparison between proteins PEGylated with branched and linear poly(Ethylene Glycol) molecules. *Biocat., Protein Eng., Nanobiotechnol*., **2007**.*15:* p. 241-243
8. Sheng, Y., Nung, C. and Tsao, H. Morphologies of star-block copolymers in dilute solutions. *J. Phys. Chem. B*, **2006**. *110*: p. 21643-21650.
9. Yurkovetskiy, A., Choi, S., Hiller, A., Yin, M., McCusker, C., Syed, S., Fischman, A. and Papisov, M. Fully degradable hydrophilic polyals for protein modification. *Biomacromolecules,* **2005**. *6*(5): p. 2648-2658.
10. Yamaoka, T., Tabata, Y and Ikada, Y. Comparison of body distribution of poly(vinyl alcohol) with other water-soluble polymers after intravenous administration. *J. Pharm. Pharmacol.,* **1995**. *47*(6): p. 479-486.
11. Conover, C., Lejeune, L., Shum, K., Gilbert, C. and Shorr, R. Physiological effect of poly(ethylene glycol) conjugation on stroma-free bovine hemoglobin in the conscious dog after partial exchange transfusion. *Artificial Organs,* **1997**. *21*(5): p. 369-378.
12. Liu, H., Joshi, N and Uhrich, K., Unimolecular micelles as controlled release systems. *Trans. Soc. Biomater.,* **1997**. *20*: p. 363.
13. Wang, J., Tian, L., Argenti, A and Uhrich, K. Nanoscale amphiphilic star-like macromolecules with carboxy-, methoxy- and amine-terminated chain ends. *Journal of Bioactive and Biocompatible polymers,* **2006**. *21*: p. 297-313.
14. Tian, L., Yam, L., Zhou, N., Tat, H and Uhrich, K. Amphiphilic scorpion-like macromolecules (AScMs): Design, synthesis and characterization. *Macromolecules,* **2004**. *37*(2): p. 538-543.

15. Zhang, Z. and Feng, S. The drug encapsulation efficiency, in vitro drug release, cellular uptake and cytotoxicity of paclitaxel-loaded poly(lactide) ocopheryl polyethylene glycol succinate nanoparticles. *Biomaterials*, **2006.** *27*: p. 4025-4033.
16. Hu, Y., Jiang, X., Ding, Y., Ge, H., Yuan, Y and Yang, C., Synthesis and characterization of chitosan-poly(acrylic acid) nanoparticles. *Biomaterials,* **2002.** *23:*p. 3193-3201
17. Khoee, S., Hassanzadeh, S. and Goliaie, B. Effects of hydrophobic drug polyesteric core interactions on drug loading and release profiles of poly(ethylene glycol) polyester poly (ethlene glycol) triblock core shell nanoparticles. *Nanotechnology.* **2005.** *18* p. 1-9.
18. Bergstrom, K., Holmberg, K., Safranj, A., Hoffman, A and Edgell, M. Reduction of fibrinogen adsorption on PEG-coated polystyrene surfaces. *J. Biomed. Mater. Res.,***2004.** *26*: p. 779-790
19. Tang, G., Zheng, J., Gao, S., Ma, Y., Shi, L., Li, Y. and Too, S. Poly(ethylene glycol) modified poly(ethylenimine) for improved CNS gene transfer: Effects of PEGylation extent. *Biomaterials*, **2003**. *24*: p. 2351-2362.
20. Chern, C., Lee, C., Kuan, C. and Liu, K. Adsorption of BSA on the amphiphilic PEG graft copolymer-coated particles. *Colloid Polym. Sci.,* **2005**. *238*: p. 917-924.
21. Hiemenz, P., Principles of colloid and surface chemistry. *1997*, New York: Marcel Dekker. Chapter 1.
22. Zhang, Y., Lam, Y. and Tan, W. Poly(ethylene oxide)-poly(propylene oxide)-poly(ethylene oxide)-g-poly(vinylpyrrolidone)*:* Association behavior in aqueous solution and interaction with anionic surfactants. *J. Colloid. Interf. Sci.,* **2005**. *285*: p. 74-79.

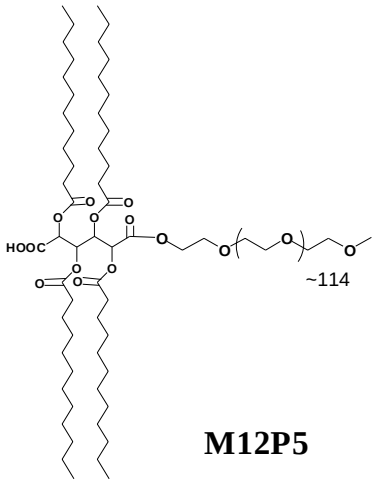


**M12P5**

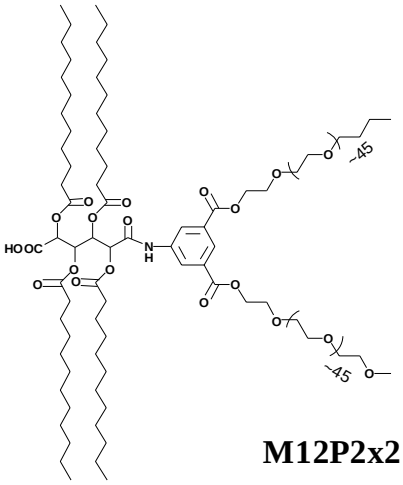


**M12P2x2**

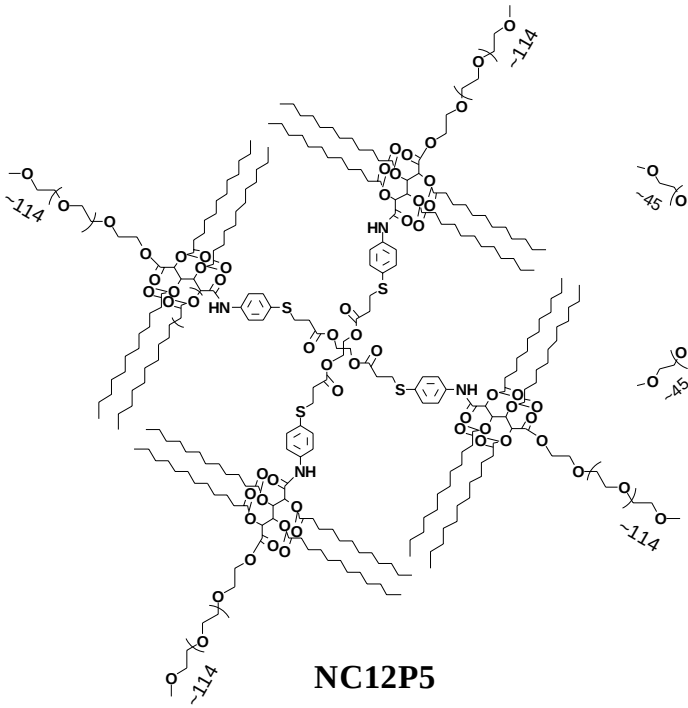


**NC12P5**

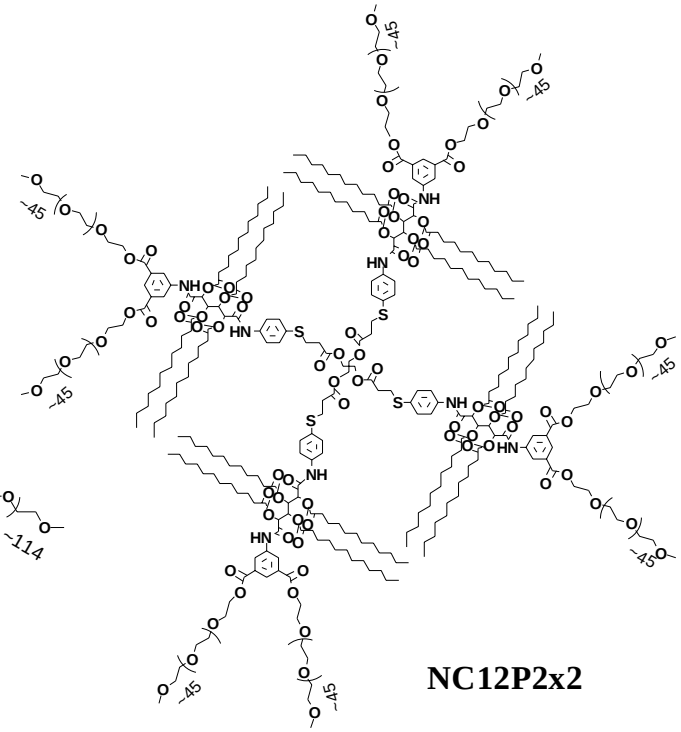


**NC12P2x2**

Scheme 4-1 Chemical structures of amphiphilic macromolecules.

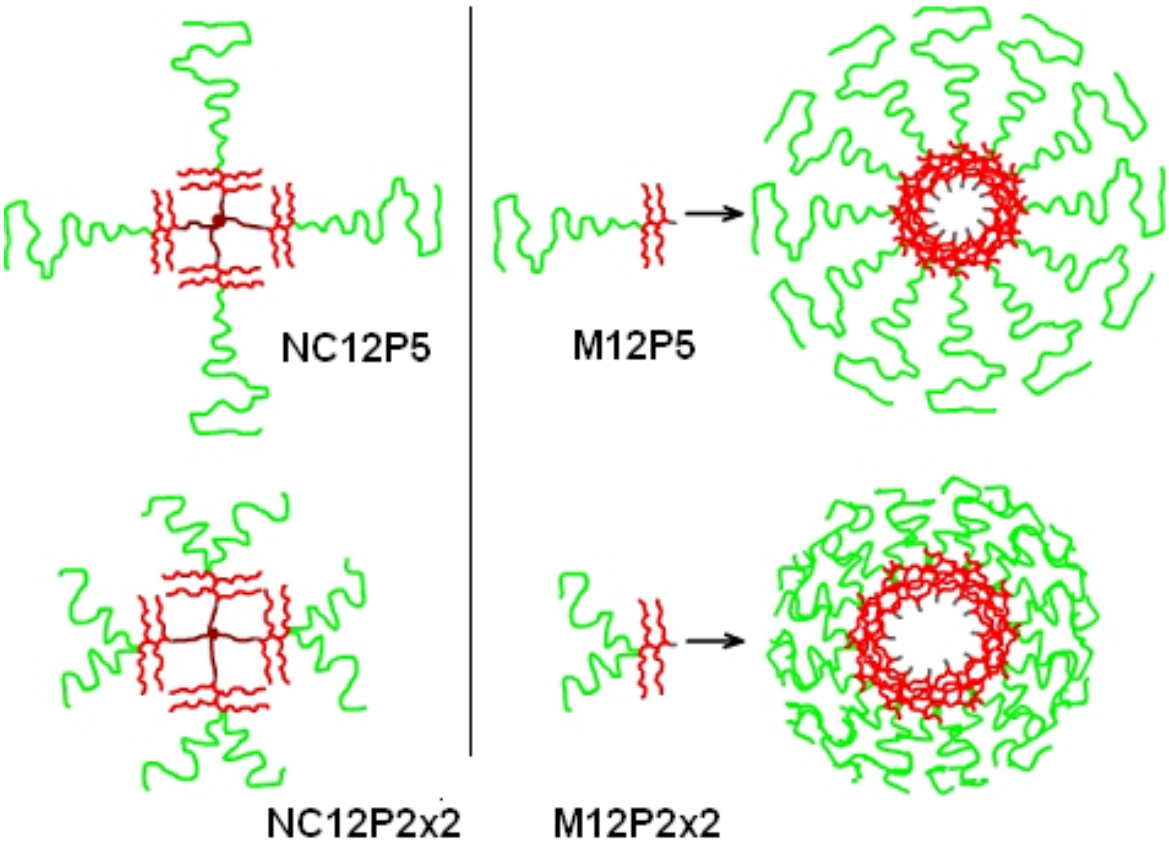


Scheme 4-2 Graphical compares of amphiphilic macromolecules.

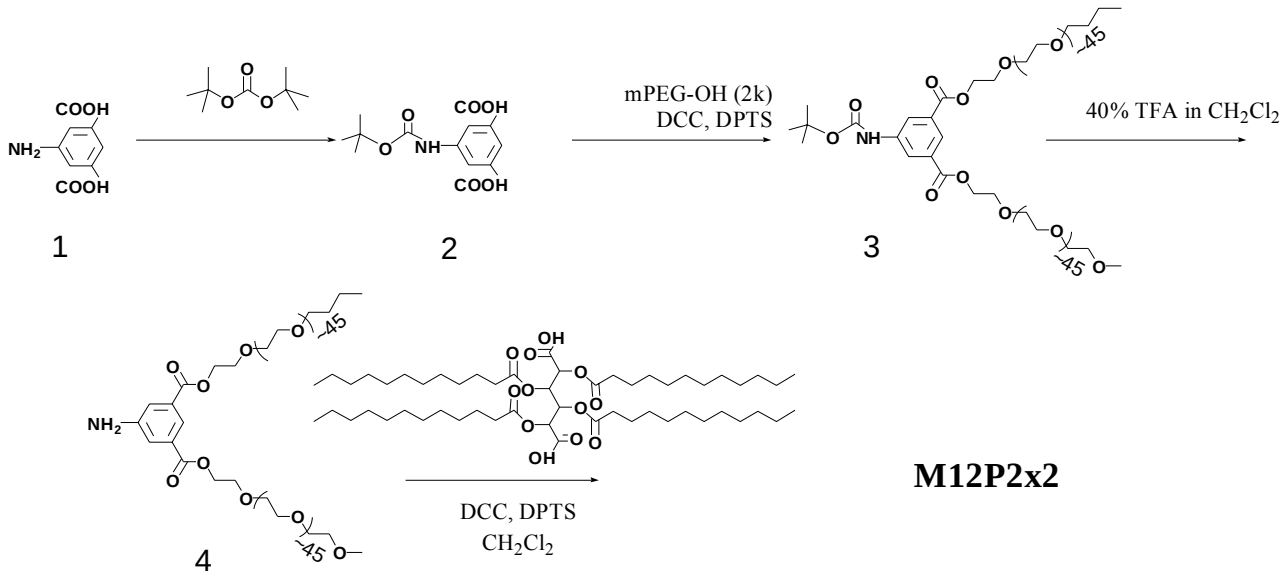


Scheme 4-3 Synthesis of **M12P2x2**

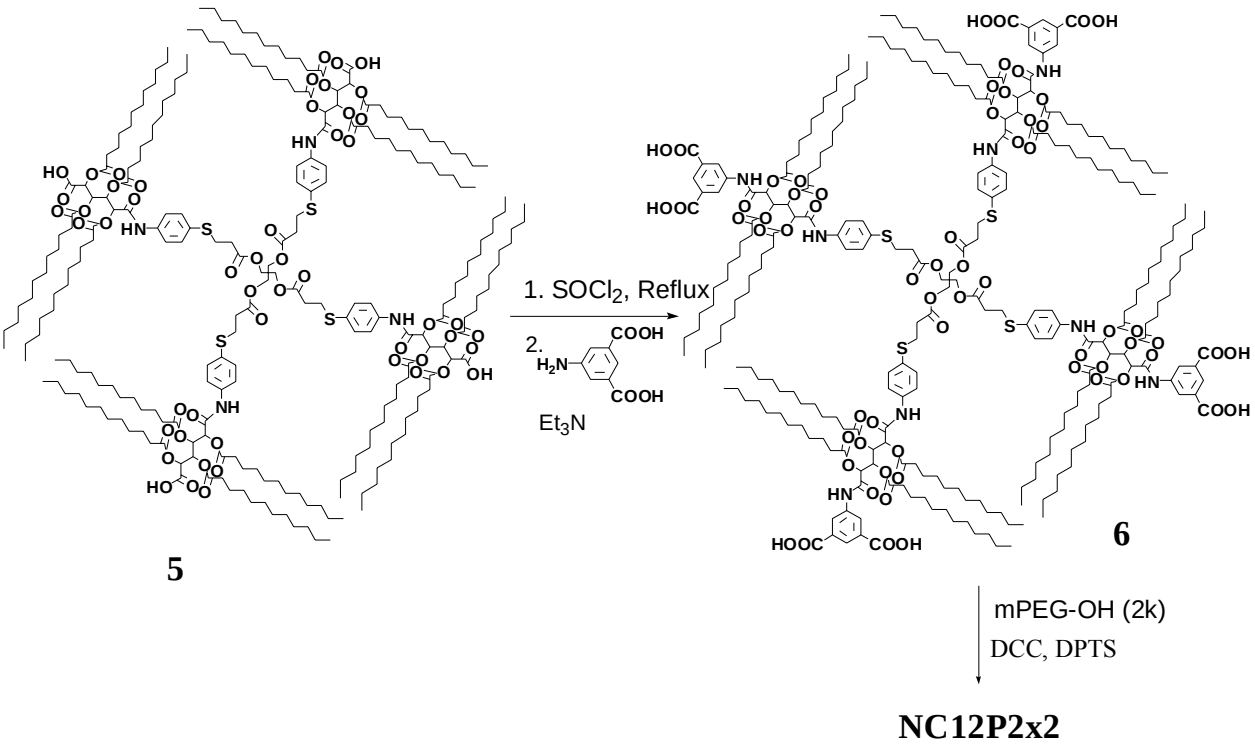


Scheme 4-4 Synthesis of **NC12P2x2**

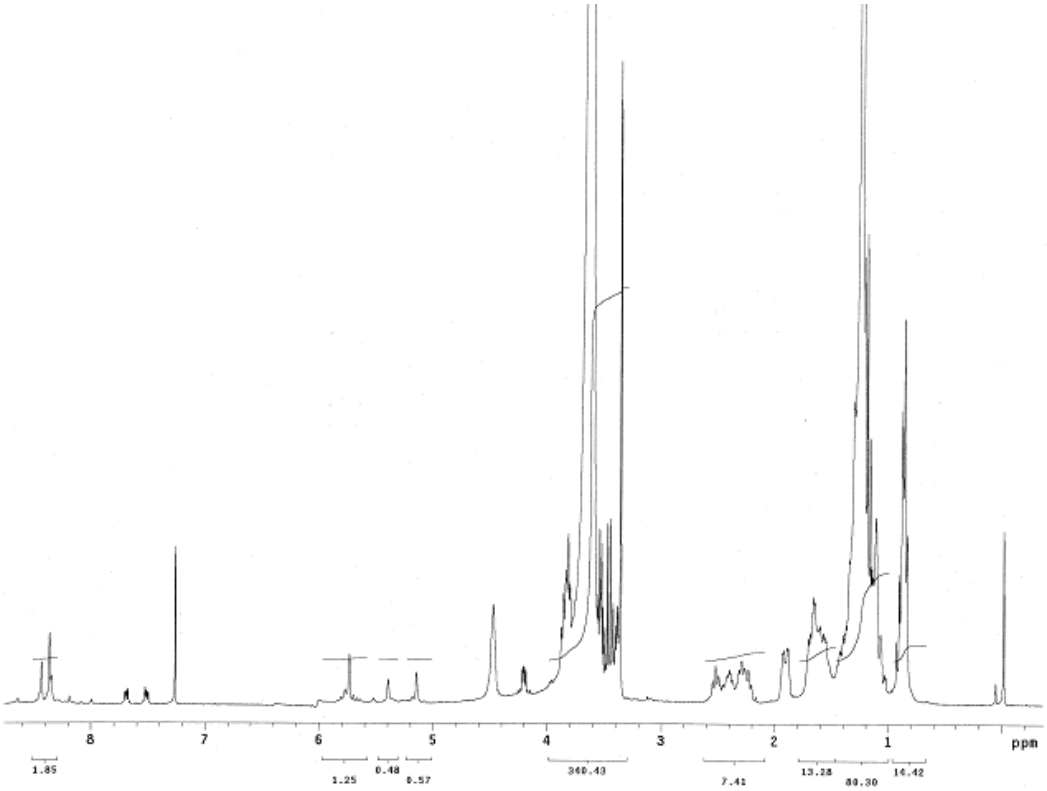


$^{1}$H NMR spectrum of **M12P2x2**

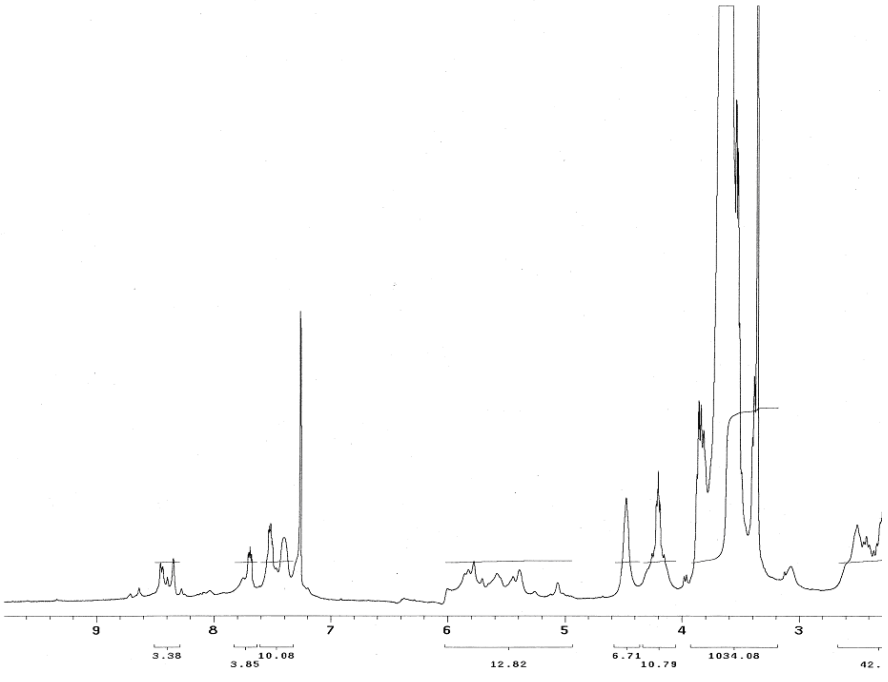


$^{1}$H NMR spectrum of **NC12P2x2**

Scheme 4-5 Representative NMR spectra of ASMs

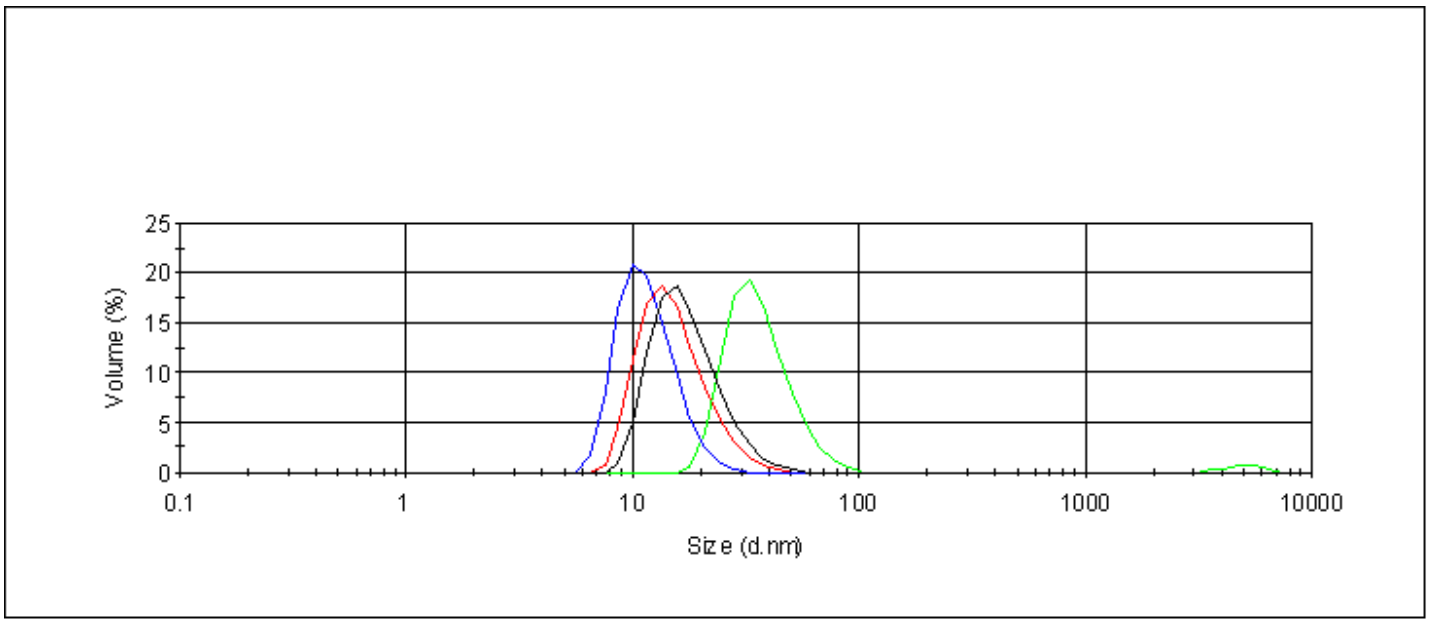


Scheme 4-6 Dynamic light scattering measurements of amphiphilic macromolecules: **M12P2x2** (Blue), **M12P5** (Black), **NC12P2x2** (Red), **NC12P5** (Green).

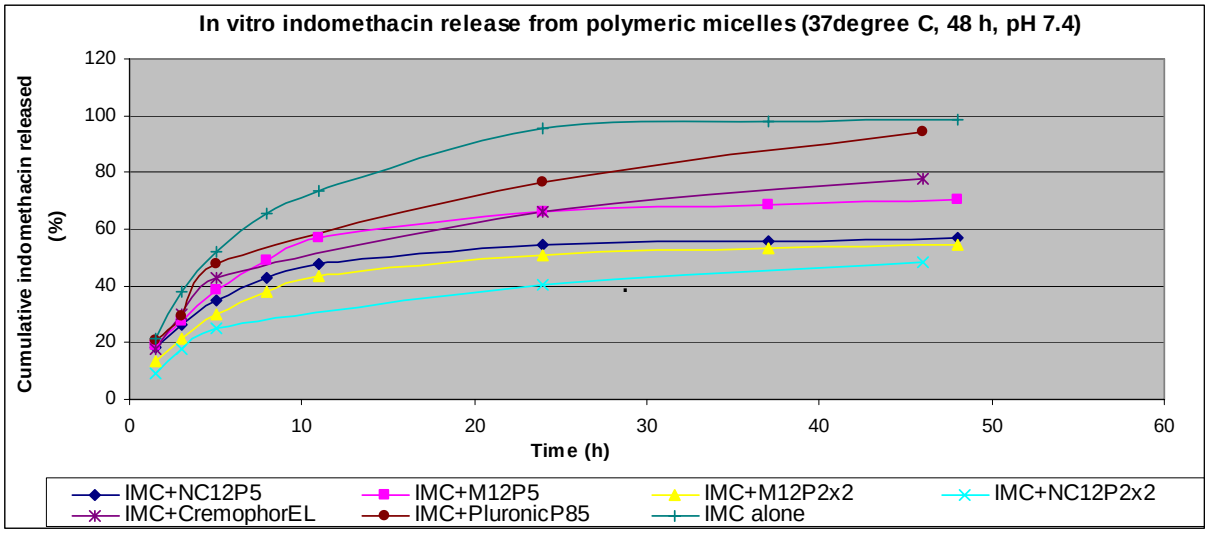


Scheme 4-7 Release profile of IMC from polymer samples

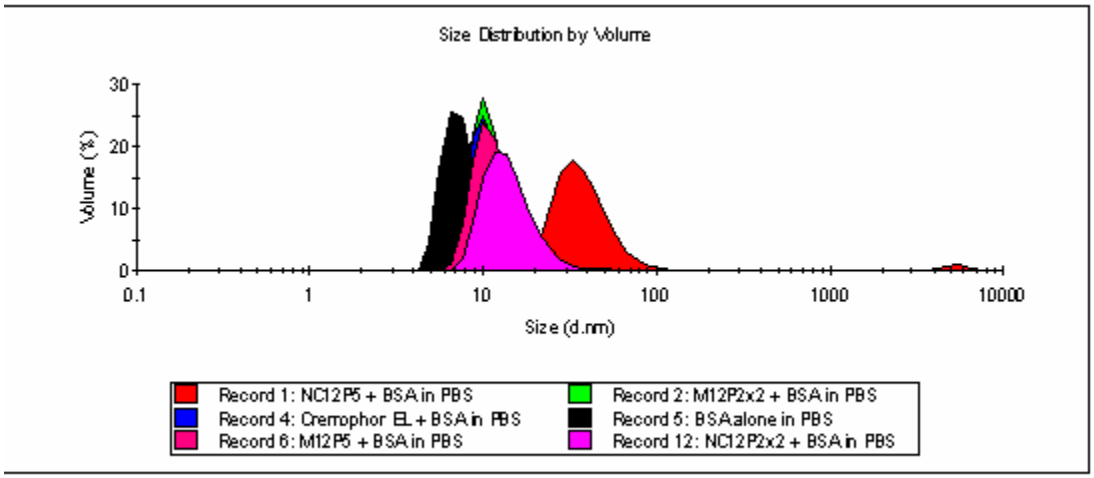


Scheme 4-8 Particle size distribution of samples at polymer:BSA ratio of 1:1

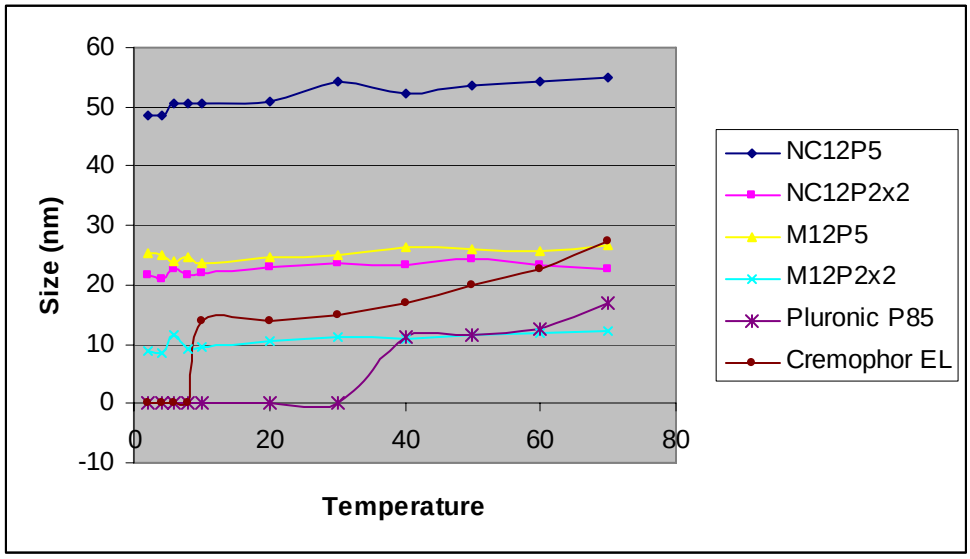


Scheme 4-9 Comparison of critical micelle temperatures for polymer samples at 0.5 M.

| | **Z-ave (nm) (for 0.1 mg/ml solution)** | **Z-ave (nm) (for saturated solution)** | **Solubility (mg/ml)** |
|---|---|---|---|
| **M12P5** | 19.0 ± 1.9 | 21.3 ± 2.3 | 35.5 |
| **M12P2x2** | 15.1 ± 2.9 | 15.1 ± 3.3 | 54.4 |
| **NC12P5** | 47.3 ± 3.8 | 51.6 ± 4.1 | 21.6 |
| **NC12P2x2** | 19.6 ± 1.1 | 22.2 ± 1.2 | 66.5 |

Table 4-1 Particle size distributions of synthetic amphiphilic macromolecules in water at high and low concentrations. Solubility of each macromolecules

| **Solution (0.1:1 wt/wt drug:polymer)** | **Encapsulation Efficiency (%)** | **Wt % Loading** | **Solubility Enhancement** |
|---|---|---|---|
| IMC + **M12P5** | 46.2±5.2 | 4.62±0.52 | 2.1 x |
| IMC + **M12P2x2** | 27.7±3.8 | 2.77±0.38 | 1.7 x |
| IMC + **NC12P5** | 39.8±4.0 | 3.98±0.40 | 1.9 x |
| IMC + **NC12P2x2** | 40.1±3.5 | 4.01±0.35 | 2.0 x |
| IMC + Pluronic P85 | 6.32±0.81 | 0.63±0.08 | 1.2 x |
| IMC + Cremophor EL | 30.6±3.3 | 3.06±0.33 | 1.7 x |

Table 4-2 Results for physical encapsulation of IMC loading using oil/water emulsion.

| Lyophilized sample | Time (sec) |
|---|---|
| IMC + **M12P5** | 50 |
| IMC + **M12P2x2** | 40 |
| IMC + **NC12P5** | 12 |
| IMC + **NC12P2x2** | 15 |
| IMC + Pluronic P85 | 56 |
| IMC + Cremophor EL | 73 |
| IMC alone | *ND |

Table 4-3 Resolubilization time of lyophilized, IMC-loaded samples

* Not detectable.

| | **Polymer micelle size (Z-ave) (nm)** | **Mixture micelle size (Z-ave) (nm)** |
|---|---|---|
| **M12P5** | 19.0±1.7 | 13.6±1.2 |
| **M12P2x2** | 17.1±1.5 | 11.7±1.1 |
| **NC12P5** | 47.3±3.8 | 44.2±3.7 |
| **NC12P2x2** | 19.6±1.9 | 19.2±2.0 |
| Pluronic P85 | 12.4±1.2 | 10.7±0.9 |
| Cremophor EL | 14.0±1.6 | 12.3±1.5 |
| BSA alone | 7.43±0.7 | - |

Table 4-4. Particle size distribution of polymer:BSA samples at 1:1 ratio.

# CHAPTER FIVE APPENDICES

## 5.1 Amphiphilic Scorpion-Like Macromolecules Folate Coupling For Targeting Drug Delivery

### 5.1.1 Introduction

Folic acid (folate) is a vitamin required by eukaryotic cells.[1, 2] Folic acid cellular internalization is normally achieved through a low affinity reduced folate transporter located on all cells in the body.[3] However, on cancer cell surfaces, an over-expression of high affinity folate receptors is observed. This receptor not only regulates the transportation of free folate, but also regulates folate-conjugated molecules.[4] Therefore, folate has been used as targeting ligand to direct delivery systems to specific cancer cells and minimize the diffusion of toxic anti-cancer drugs to healthy cells.[3, 5] Our strategy here is to conjugate folic acid with our scorpion-like micelles (AScMs) to achieve targeting delivery of anti-cancer drugs. [6]

### 5.1.2 Experimental procedures

#### 5.1.2.1 Materials

Folic acid (99% reagent), DCC, N-hydroxysuccinimide and ethylenediamine were purchased from Sigma-Aldrich (St. Louis, MO, USA). PEG-bis-amine ($NH_2$-PEG-$NH_2$) with molecular weights of 3400 Da was purchased from Nektar (San Carlos, CA). All PEG reagents were dried by azeotropic distillation with toluene. All other reagents and

solvents were purchased from Sigma-Aldrich and used as received. Compounds were prepared as previous described: **3** [7] and **6** [8].

### 5.1.2.2 Synthesis and Characterization Methods

Compounds were analyzed by $^{1}H$ and $^{13}C$ NMR spectroscopy with samples (~ 5-10 mg/ml) dissolved in DMSO-$d_6$ and $CDCl_3$ solvent on Varian 300 MHz and 400 MHz spectrometers, using tetramethylsilane as the reference signal. IR spectra were recorded on a Mattson Series spectrophotometer (Madison Instruments, Madison, WI) by solvent (methylene chloride) casting on a KBr pellet. A Meltemp (Electrothermal Systems, Cambridge, MA) apparatus was used to determine the melting temperatures ($T_m$) of all the intermediates and products.

Gel permeation chromatography (GPC) was used to obtain molecular weight and polydispersity index (PDI). Measurements were performed on Waters Breeze GPC system equipped with Styragel® HR3 column (ID 7.8 mm, and length 300 mm) and with a Water 2414 refractive index detector, 1515 isocratic HPLC pump and Waters 717 plus Autosampler. Tetrahydrofuran (THF) was the eluent for analysis and solvent for sample preparation. Sample was dissolved into THF (~ 5 mg/ml) and filtered through a 0.45 μm PTFE syringe filter (Whatman, Clifton, NJ) before injection into the column at a flow rate of 0.8 ml/min. The average molecular weight of the sample was calibrated against narrow molecular weight polystyrene standards (Polysciences, Warrington, PA).

### 5.1.2.3 Synthesis of M12P5-folate (on the hydrophilic end)

The synthesis is shown in Scheme 5-1. Folic acid (**1**) (4.4 g, 0.01 mol) was heated to 95˚C in oven for six hours, then dissolved in anhydrous DMSO (10.0 ml) together with N-hydroxysuccinimide (1.2 g, 0.01 mol). To this solution, DCC (12 ml, 1.0 M methylene chloride solution) was slowly added with stirring. The reaction mixture was stirred for six hours in the dark at room temperature. The by-product was removed by filtration. The reaction intermediate **2** in DMSO solution was used in *situ*.

Compound **3** (9.4 g, 0.01 mol) and N-hydroxysuccinimide (1.2 g, 0.01 mol) were dissolved in methylene chloride (20 ml) and DMF (1.2 ml). To this solution, DCC (10 ml, 1.0 M methylene chloride solution) was slowly added. The reaction was stirred for six hours at room temprature, then the by-product removed by filtration. A white solid was obtained following the solvent removal. Purification was performed by silica gel chromatography using ethyl acetate/hexanes (2:1) as eluent. Product **4** was obtained as white powder: 7.8 g, 74% yield. $^{1}$H NMR ($CDCl_3$) ($\delta$): 5.70 (s, 2H, C$\underline{H}$), 5.15 (s, 2H, C$\underline{H}$), 2.78 (t, 4H, C$\underline{H_2}$), 2.42 (t, 4H, C$\underline{H_2}$), 2.28 (t, 4H, C$\underline{H_2}$), 1.63 (m, 4H, C$\underline{H_2}$), 1.57 (m, 4H, C$\underline{H_2}$), 1.29 (m, 64H, C$\underline{H_2}$), 0.92 (t, 12H, C$\underline{H_3}$). IR (KBr, cm-1): 1754 (COOR), 1738 (COOH), 1245, 1170 (C-O). $T_m$: 144-145 °C.

Poly(ethylene glycol)-bis-amine (3.4 k Da) (0.34 g) was dissolved in methylene chloride (10 ml). Compound **4** (0.10 g, 1.0 equivalent) was also dissolved in methylene chloride (4.0 ml) and added dropwise. The reaction was stirred at room temperature for four hours. Product **5** was isolated by concentration and precipitation with ethyl ether (100 ml).

Product **5** was obtained as a slight yellow solid: 0.42 g, 95% yield. $^1$H NMR ($CDCl_3$) ($\delta$): 8.10 (s, N*H*), 5.77 (m, 2H, C*H*), 5.49 (m, 2H, C*H*), 3.65 (m, ~0.4kH, C$H_2$ on PEG), 2.44 (m, C$H_2$), 2.10 (t, 4H, C$H_2$), 1.55 (m, 4H, C$H_2$), 1.50 (m, 4H, C$H_2$), 1.27 (m, 48H, C$H_2$), 0.85 (t, 12H, C$H_3$). IR (KBr, $cm^{-1}$): 2990 (C-H), 1751 (COOR), 1736 (COOH). $T_m$: 57-58 °C. GPC: Mw: 4020; PDI: 1.3, crosslinked by-product: Mw: 11,000, PDI: 1.6.

Compound **5** (0.22 g) was dissolved in methylene chloride (10 ml) and added dropwise to the solution of **2** (0.054 g, 0.01 mmol). The reaction was stirred at room temperature for four hours in the dark. Excess methylene chloride (100 ml) was added, the reaction mixture washed with water (50 ml x 3) and evaporated to dryness. The resulting reaction mixture was dissolved in acetone (10.0 ml), placed in Spectra/Por dialysis bag (MWCO 3500) and extensively dialyzed against deionized water for twenty-four hours. The purified product was lyophilized (-50ºC, 65 x $10^{-3}$ mbar, Labconco Freezone 4.5) **M12P3.4-Folate** was obtained as a yellow solid: 0.21 g, 80% yield. $^1$H NMR ($CDCl_3$) ($\delta$): 8.65 (s, Ar*H*), 7.60 (s, N*H*), 6.88 (ArN*H*), 5.85-5.20 (m, 4H, C*H*), 3.63 (m, ~0.3kH, C$H_2$ on PEG), 4.54 (m, 4H, C$H_2$), 2.77 (t, 4H, C$H_2$), 1.85 (d, 2H, C$H_2$), 0.85 (s, 12H, C$H_2$). IR (KBr, $cm^{-1}$): 2988 (C-H), 1744 (COOR), 1729 (COOH), 1230, 1119 (C-O). $T_m$: 61-62 °C.

### 5.1.2.4 Synthesis of Folate-M12P5 (on the hydrophobic end)

The synthesis is shown in Scheme 5-2. **6** (0.603 g, 0.100 mmol) was dissolved in dichloromethane (5.0 ml) to which ethylenediamine (55 µl, 0.800 mmol) was added dropwise. The reaction was performed at room temperature for five hours. The precipitate was removed by gravity filtration, and then washed with brine (3 x 10 mL).

Solvent and unreacted ethylenediamine were removed under vacuum. The product was purified by recrystallization (2 mL dichloromethane: 20 mL diethyl ether), then centrifuged at 3000 rpm 5 min (Hettich Zentrigugen, Monroe CT). Product was washed again by diethyl ether (3 x 50 mL) and placed in vacuum oven at 60˚C for twenty-four hours to remove unreacted ethylenediamine. Polymer **7** was obtained as light yellow solid: 0.38 g, yield: 62%. Polymer **7** was used without further characterization except to confirm the presence of the primary amine. Kaiser reagent was prepared and used to confirm the presence of a primary amine on **7** [9]

To Polymer **7** (0.30 g, 0.050 mmol) dissolved in methylene chloride (10 ml) folic acid (0.044 g, 0.10 mmol) dissolved in DMSO (0.5 ml) was added. To this stirring solution DCC (0.05 ml, 1 M in methylene chloride) was added dropwise. The reaction solution was stirred at room temperature twenty-four hours in the dark. The reaction mixture was filtered and evaporated to dryness. The reaction mixture was dissolved in water (10 ml), placed in Spectra/Pro dialysis bag (MWCO 3500) and extensively dialyzed against deionized water for twenty-four hours. **Folate-M12P5** was obtained as yellow powder: 0.28 g, 82% yield. $^{1}$H NMR ($CDCl_3$) ($\delta$): 8.86 (s, Ar*H*), 7.88 (s, N*H*), 6.80 (ArN*H*), 5.80-5.10 (m, 4H, C*H*), 3.60 (m, ~0.4kH, C$H_2$ on PEG), 4.34 (m, 4H, C$H_2$), 2.75 (t, 4H, C$H_2$), 1.88 (d, 2H, C$H_2$), 0.80 (s, 12H, C$H_2$). IR (KBr, $cm^{-1}$): 2990 (C-H), 1740 (COOR), 1230, 1111 (C-O). $T_m$: 63-64 °C. GPC: Mw: 4,380; PDI: 1.4.

### 5.1.3 Future Work

Solution properties of the folic acid-conjugated polymeric micelles will be evaluated, such as micelle size and stability. An anti-cancer drug (e.g. ellipticine or doxorubicin) will be evaluated for loading and release using the **Folate-M12P5** and **M12P3.4-Folate**. Improvements in targeting between cancer and normal cells will be performed in *vitro*.

## 5.2 Amphiphilic Scorpion-Like Macromolecules Florescence Labeling And Multi-Functional Group Introducing

### 5.2.1 Introduction

AScMs are water-soluble nanocarriers with promising potential for delivering hydrophobic drugs.[7] Modern drug delivery systems aim to transport the drugs to the specific cell compartments, such as their site of action may be within a range of organelles.[10] The drug may need to escape the endosomes or lysosomes prior to reaching its desired cellular target.[11, 12] Thus, it may be optimal for drug delivery systems to promote early escape from endosomes as well as to delay drug exportation from the cell following its entry into recycling or secretion pathways. [13]

Thus, an understanding of AScMs intracellular fate is essential for selective delivery of drugs at the sub-cellular level.[11, 13] To accomplish this goal, a good imaging reagent is used to fluorescently label the polymer micelles. Specifically, we labeled the AScMs with fluorescein isothiocyanate (FITC) at two different locations of the macromolecules: the hydrophilic part (Scheme 5-3) and hydrophobic part (Scheme 5-4).[10] FITC-conjugation

to the hydrophobic part of the macromolecules could potentially enhance aggregation as FITC itself is relatively hydrophobic (LogP=3.77 from Chemdraw calculation). In contrast, FITC conjugated onto the hydrophilic part could enable the macromolecule to retain its established physiochemical properties useful for therapeutical application.

### 5.2.2 Experimental procedures

#### 5.2.2.1 Materials

FITC, DCC (1.0 M methylene chloride solution), N-hydroxysuccinimide and ethylenediamine were purchased from Sigma-Aldrich (St. Louis, MO, USA). PEG-bis-amine ($NH_2$-PEG-$NH_2$) with molecular weights of 3400 Da was purchased from Nektar (San Carlos, CA). All PEG reagents were dried by azeotropic distillation with toluene. All other reagents and solvents were purchased from Sigma-Aldrich and used as received. Acyl chloride activated MA12 was prepared as previous described in Chapter 3.

#### 5.2.2.2 Synthesis and Characterization Methods

Compounds were analyzed by $^{1}H$ and $^{13}C$ NMR spectroscopy with samples (~ 5-10 mg/ml) dissolved in DMSO-$d_6$ and $CDCl_3$ solvent on Varian 300 MHz and 400 MHz spectrometers, using tetramethylsilane as the reference signal. IR spectra were recorded on a Mattson Series spectrophotometer (Madison Instruments, Madison, WI) by solvent (methylene chloride) casting on a KBr pellet. A Meltemp (Electrothermal Systems, Cambridge, MA) apparatus was used to determine the melting temperatures ($T_m$) of all the intermediates and products.

### 5.2.2.3 Synthesis of M12P5-FITC (on the hydrophilic end)

The synthesis is shown in Scheme 5-3. Compound **8** (0.60 g, 0.10 mmol) was dissolved in methylene chloride (10 ml) and triethylamine (0.50 ml, 5.0 mmol), followed by the addition of ethylene diamine (0.20 ml, 0.80 mmol). The reaction mixture stirred for four hours at room temperature. The reaction intermediate was purified by recrystallization with ethyl ether (100 ml) and used immediately without further characterization. **$NH_2$-PEG(5k)-FITC** (0.50 g, 0.83 mmol) was dissolved in methylene chloride (10 ml) and mixed with acyl chloride activated **MA12** (0.30 g, 0.30 mmol) and pyridine (1.0 ml, 13 mmol). The reaction mixture was stirred for four hours at room temperature. The final product was purified by recrystallization with ethyl ether (100 ml). **M12P5-FITC** was obtained as yellow solid: 0.41 g, 81% yield. $^1$H NMR ($CDCl_3$) ($\delta$): 8.1 (t, N*H*), 8.0 (t, N*H*), 7.50 (Ar*H*), 7.20 (Ar*H*), 7.10 (Ar*H*), 6.85 (Ar*H*), 6.70 (Ar*H*), 6.60 (Ar*H*), 5.60-5.80 (m, 2H, C*H*), 5.10-5.25 (m, 2H, C*H*), 3.62 (m, ~0.4kH, C$H_2$ on PEG), 2.40 (m, C$H_2$), 2.28 (t, 4H, C$H_2$), 1.61 (m, 4H, C$H_2$), 1.58 (m, 4H, C$H_2$), 1.25 (m, 48H, C$H_2$), 0.83 (t, 12H, C$H_3$). IR (KBr, $cm^{-1}$): 2902 (C-H), 1754 (COOR), 1730 (COOH), 1230, 1122 (C-O), 820 (Ar-H). $T_m$: 61-62 °C.

### 5.2.2.4 Synthesis of FITC-M12P5 (on the hydrophobic end)

The synthesis is shown in Scheme 5-4. Compound **7** (0.30 g, 0.050 mmol) was dissolved in phosphate buffer (PBS) (50 ml). The corresponding amount of FITC (polymer:FITC molar ratio 1:20) (4.0 mg) was dissolved in acetone (1.0 ml) and added dropwise to the polymer solution at room temperature and incubated for twenty-four hours in the dark. The reaction mixture was placed in a Spectro/Pro dialysis bag (MWCO 3500) and

extensively dialyzed against deionized water for twenty-four hours. The solution was further purified by gel filtration chromatography (Sephadex G-25M) using HPLC grade water as eluent, then lyophilized (Labconco Kansas City, Missouri) **FITC-M12P5** was obtained as yellow solid: 0.30 g, 88% yield. $^{1}$H NMR ($CDCl_3$) ($\delta$): 9.2 (t, N*H*), 8.5 (t, N*H*), 7.70 (Ar*H*), 7.24 (Ar*H*), 7.12 (Ar*H*), 7.00 (Ar*H*), 6.70 (Ar*H*), 5.60-5.80 (m, 2H, C*H*), 5.12-5.30 (m, 2H, C*H*), 3.66 (m, ~0.4kH, C$H_2$ on PEG), 2.43 (m, C$H_2$), 2.16 (t, 4H, C$H_2$), 1.60 (m, 4H, C$H_2$), 1.55 (m, 4H, C$H_2$), 1.24 (m, 48H, C$H_2$), 0.85 (t, 12H, C$H_3$). IR (KBr, $cm^{-1}$): 2985 (C-H), 1742 (COOR), 1231, 1125 (C-O). 820-825 ( Ar-H). $T_m$: 62-63 °C.

### 5.2.3 Future Work

Mixed micelles will be prepared by adding FITC-labeled AScMs (5-10 wt %) and unlabeled AScMs (90-95 %) to retain and preserve the original physico-chemical micelle properties. Micelle bio-distribution and micelle cellular internalization could be further investigated using confocal laser scanning microscopy. If physically encapsulating other dye reagents or fluorescence active therapeutic molecules (e.g. ellipticine), the mechanism of drug controlled release from polymeric micelles in the plasma and inside the cells could be achieved.

## 5.3 Functional Polymer Preparation For Drug Conjugation Through "Click" Chemistry

### 5.3.1 Introduction

Coupling therapeutic molecules with synthetic polymers through covalent bonds is a viable strategy to improve drug delivery.[14] As previous outlined, many problems are related with the administration of chemotherapeutics. For example, camptothecin has poor water-solubility and *in vivo* stability, accompanied by the possible ring-opening of the lactone that contributes to drug deactivation.[15] Encapsulation of physiologically sensitive drugs within polymeric micelles is one approach to improve their water solubility and stability. Alternately, drug solubility and stability may be improved by conjugation of the drug directly to the delivery system. [16] The high molecular weight of polymer-drug conjugates may target tumors as a result of the enhanced permeability and retention effect that localizes drugs in the leaky vasculature of tumor tissue.[17]

We have demonstrated that our AScMs are good candidates as drug delivery system due to amphiphilicity.[7] However, the small amount of the hydrophobic block (17 wt %) in the polymer may limit total drug loading capacity. In addition, no functional groups are accessible for further polymer modification except for the single carboxylic acid group on mucic acid end. In this study, we functionalized the chain ends on the aliphatic hydrocarbon branches of AScM with azide groups. We use this azide modified AScM to react with alkyne-linked drug molecules via 1,2,3-triazole ring bonds; a method known as

"click" chemistry that is tolerant to a wide variety of physiochemical environments. [18-20]

### 5.3.2 Experimental procedures

#### 5.3.2.1 Materials

6-bromo-hexanoyl chloride (97% reagent grade), 12-bromo-docecanoic acid, zinc chloride and sodium azide were purchased from Sigma-Aldrich (St. Louis, MO, USA). Monomethoxy-poly(ethylene glycol) (mPEG) with molecular weights of 5000 Da was purchased from Sigma-Aldrich. PEG was dried by azeotropic distillation with toluene. All other reagents and solvents were purchased from Sigma-Aldrich and used as received.

#### 5.3.2.2 Synthesis and Characterization Methods

Compounds were analyzed by $^{1}H$ and $^{13}C$ NMR spectroscopy with samples (~ 5-10 mg/ml) dissolved in DMSO-$d_6$ and $CDCl_3$ solvent on Varian 300 MHz and 400 MHz spectrometers, using tetramethylsilane as the reference signal. IR spectra were recorded on a Mattson Series spectrophotometer (Madison Instruments, Madison, WI) by solvent (methylene chloride) casting on a KBr pellet. A Meltemp (Electrothermal Systems, Cambridge, MA) apparatus was used to determine the melting temperatures ($T_m$) of all the intermediates and products.

Gel permeation chromatography (GPC) was used to obtain final product molecular weight and polydispersity index (PDI). Measurements were performed on Waters Breeze GPC system equipped with Styragel® HR3 column (ID 7.8 mm, and length 300 mm) and

with a Water 2414 refractive index detector, 1515 isocratic HPLC pump and Waters 717 plus Autosampler. Tetrahydrofuran (THF) was the eluent for analysis and solvent for sample preparation. Sample was dissolved into THF (~ 5 mg/ml) and filtered through a 0.45 μm PTFE syringe filter (Whatman, Clifton, NJ) before injection into the column at a flow rate of 0.8 ml/min. The average molecular weight of the sample was calibrated against narrow molecular weight polystyrene standards (Polysciences, Warrington, PA).

#### 5.3.2.3 Synthesis of Azide Functionalized AScMs

The synthesis is shown in Scheme 5-5. Mucic acid (**9**) (4.20 g, 18.6 mmol) and zinc chloride (0.3 g, 2.0 mmol) were added into 6-bromo-hexanoyl chloride (18.0 ml, 150 mmol). The reaction mixture was heated to 85 °C for 10-12 h. After cooling to room temperature, diethyl ether (20 ml) was added to the reaction mixture, and the solution was poured into ice water (150 ml) with stirring. Additional diethyl ether (80 ml) was added to the mixture and stirring continued for another 30 min. The ether portion was separated, washed with brine to neutral, dried over anhydrous magnesium sulfate, and evaporated to dryness. The crude product was purified by precipitation into hexane (200 ml) from diethyl ether (20 ml), then dried under vacuum oven. Product **10a** was obtained as white solid: 9.4 g, 55% yield. $^{1}$H NMR ($CDCl_3$) ($\delta$): 8.68 (s, 2H, COO*H*), 5.67 (s, 2H, C*H*), 5.14 (s, 2H, C*H*), 3.38 (t, 8H, C$H_2$), 2.45 (t, 4H, C$H_2$), 2.32 (t, 4H, C$H_2$), 1.84 (t, 8H, C$H_2$), 1.64 (m, 4H, C$H_2$), 1.55 (m, 4H, C$H_2$), 1.48 (m, 4H, C$H_2$), 1.40 (m, 4H, C$H_2$). IR (KBr, cm-1): 1730 (COOH), 1752 (COOR), 1240, 1160 (C-O). $T_m$: 162-164 °C.

The synthesis of **10b** followed the same method as **10a** above. **10b** was obtained as a white solid: 2.0 g, 51% yield. $^{1}$H NMR ($CDCl_3$) ($\delta$): 8.70 (s, 2H, COO*H*), 5.68 (s, 2H, C*H*), 5.16 (s, 2H, C*H*), 3.41 (t, 8H, C$H_2$), 2.44 (t, 4H, C$H_2$), 2.32 (t, 4H, C$H_2$), 1.84 (t, 8H, C$H_2$), 1.60 (m, 4H, C$H_2$), 1.55 (m, 4H, C$H_2$), 1.40 (m, 8H, C$H_2$), 1.29 (m, 48H, C$H_2$). IR (KBr, cm-1): 1725, 1748 (C=O), 1245, 1170 (C-O). $T_m$: 156-157 °C.

mPEG-OH (5.0 kDa) (7.3 g, 1.5 mmol) was dehydrated by azeotropic distillation in toluene (30 ml), then **10a** (4Br-MA6) (4.0 g, 4.4 mmol) and DPTS (0.31 g, 1.0 mmol) in methylene chloride (30 ml) were added at room temperature. After 10 min under nitrogen, DCC solution (1.0 M in methylene chloride, 4.5 ml) was added dropwise. After twenty-four hours, the by-product was removed by filtration. The filtrate was washed with brine (20 ml), dried over magnesium sulfate, and evaporated to dryness. The crude product was purified by precipitation into diethyl ether (100 ml) from methanol (5 ml), then dried under vacuum oven. Product **11a** was obtained as a light yellish, waxy solid: 5.1 g, 78% yield. $^{1}$H NMR ($CDCl_3$) ($\delta$): 5.72 (d, H, C*H*), 5.62 (d, H, C*H*), 5.17 (s, H, C*H*), 5.05 (s, H, C*H*), 3.60 (m, ~460H, C$H_2$), 3.36 (m, 8H, C$H_2$), 2.43 (t, 4H, C$H_2$), 2.31 (t, 4H, C$H_2$), 1.64 (m, 8H, C$H_2$), 1.42 (m, 4H, C$H_2$), 1.33 (m, 4H, C$H_2$). IR (KBr, cm-1): 1755 (COOR), 1728 (COOH), 1242, 1147 (C-O). $T_m$: 58-59 °C.

The synthesis of **11b** followed the same method as **11a** above. **11b** was obtained as a yellow solid: 4.2 g, 71% yield. $^{1}$H NMR ($CDCl_3$) ($\delta$): 5.77 (d, H, C*H*), 5.65 (d, H, C*H*), 5.25-5.16 (m, H, C*H*), 5.08 (d, H, C*H*), 3.60 (m, ~460H, C$H_2$), 3.37 (m, 8H, C$H_2$), 2.39

(t, 4H, C$\underline{H_2}$), 2.31 (t, 4H, C$\underline{H_2}$), 1.64 (m, 8H, C$\underline{H_2}$), 1.44 (m, 4H, C$\underline{H_2}$), 1.27 (m, 48H, C$\underline{H_2}$). IR (KBr, cm-1): 1752 (COOR), 1730 (COOH), 1240, 1151 (C-O). $T_m$: 55-56 °C.

$NaN_3$ (0.11) g was dissolved in 10 ml DMF and added into a 10 ml DMF solution of **11a** (0.963 g). The reaction mixture was stirred for 18 hours at room temperature. The reaction mixture was then diluted by $CH_2Cl_2$ (150 ml), washed by water (50 ml x 6) and brine (50ml). The organic portion was dried over $MgSO_4$, concentrated and precipitated by ethyl ether (100 ml). Product **12a** was obtained as white solid: 0.72 g, 75% yield. $^1$H NMR ($CDCl_3$) ($\delta$): 5.70 (d, H, C$\underline{H}$), 5.59 (d, H, C$\underline{H}$), 5.18 (s, H, C$\underline{H}$), 5.03 (s, H, C$\underline{H}$), 3.60 (m, ~460H, C$\underline{H_2}$), 3.22 (m, 8H, C$\underline{H_2}$), 2.4 (t, 4H, C$\underline{H_2}$), 2.28 (t, 4H, C$\underline{H_2}$), 1.64 (m, 8H, C$\underline{H_2}$), 1.40 (m, 4H, C$\underline{H_2}$), 1.36 (m, 4H, C$\underline{H_2}$). IR (KBr, cm-1): 1751 (COOR), 1730 (COOH), 1233, 1150 (C-O). $T_m$: 60-61 °C. GPC: Mw: 5520; PDI: 1.1.

The synthesis of **12b** followed the same method as **12a** above. **12b** was obtained as white solid, 0.34 g, 69% yield: $^1$H NMR ($CDCl_3$) ($\delta$): 5.78 (d, H, C$\underline{H}$), 5.62 (s, H, C$\underline{H}$), 5.55-5.18 (m, H, C$\underline{H}$), 5.10, 5.08 (d, H, C$\underline{H}$), 3.60 (m, ~460H, C$\underline{H_2}$), 3.37 (m, 4H, C$\underline{H_2}$), 3.22 (m, 4H, C$\underline{H_2}$), 2.41 (t, 4H, C$\underline{H_2}$), 2.26 (t, 4H, C$\underline{H_2}$), 1.58 (m, 8H, C$\underline{H_2}$), 1.38 (m, 4H, C$\underline{H_2}$), 1.21 (m, 48H, C$\underline{H_2}$). IR (KBr, cm-1): 1750 (COOR), 1735 (COOH), 1243, 1150 (C-O). $T_m$: 59 °C. GPC: Mw: 5980; PDI: 1.1.

### 5.3.3 Future Work

Hydrophobic drug molecules bearing hydroxyl functional groups (e.g. camptothethin) may be coupled onto the triazide-modified AScMs. As is shown in Scheme 5-6, the

hydroxyl groups can be converted to alkynes, which then react to form triazoles in a large range of chemical/physical environments. Because the drug-conjugated amphiphilic polymers remain amphiphilic, the conjugated polymer may act as an enhanced unimer to form micelles in aqueous solution and load even more drug molecules via oil/water emulsion method. Although the solubility of the whole micelle may decrease, the weight percentage of drug loading and loading efficiency are expected to improve. Drug molecules with free carboxylic acids may also be modified as shown in Scheme 5-6. In this example, the triazide functionalization is applied to amphiphilic star-like macromolecules (ASMs) by placing the bromine-terminated mucic acid derivatives on the hydrophobic core first before converting to triazide. In this way, novel unimolecular micelles, with higher drug loading capacity may be generated, as shown in Scheme 5-6.

**5.4 References**


1. Bailey, B. and.Gregery, F., Folate metabolism and requirements. *J. of Nutrition,* **1999.** *129*: p. 779-782.
2. Kisliuk, R., Folates. *Encyclopedia of Life Sciences.* Vol. DOI: 10.1038/npg.els.0003924. 2006, Chichester, UK: John Wiley & Sons, Ltd.
3. Hilgenbrink, A. and Low, P., Folate receptor-mediated drug targeting: From therapeutics to diagnostics. *J. Pharm. Sci.,* **2005**. *94*: p. 2135-2146.
4. Low, P. and Anthony, A., Folate receptor-targeted drugs for cancer and inflammatory diseases. *Adv. Drug Del. Rev.*, **2004**. *29*(8): p. 1055-1058.
5. Zhao, X.and Lee, R., Tumor-selective targeted delivery of genes and antisense oligodeoxyribonucleotides via the folate receptor. *Adv. Drug Del. Rev.,* **2004**. *29*(8): p. 1193-1204.
6. Gabizon, A., Shmeeda , H., Horowitz, A. and Zalipsky, S., Tumor cell targeting of liposome-entrapped drugs with phospholipid-anchored folic acid PEG conjugates. *Adv. Drug Del. Rev.*, **2004**. *29*(8): p. 1177-1192.
7. Tian, L., Yam, L., Zhou, N., Tat, H. and Uhrich, K., Amphiphilic scorpion-like macromolecules (AScMs): Design, synthesis and characterization. *Macromolecules*, **2004**. *37*(2): p. 538-543.
8. Chnari, E., Nikitczuk, J., Wang, J., Uhrich, K. and Moghe, P., Engineered polymeric nanoparticles for receptor targeted blockage of oxidized low density lipoprotein uptake and atherogenesis in macrophages. *Biomacromolecules*, **2006**. *7*(6): p. 1796 -1805.
9. Kaiser, E., Colescott, R., Bossinger, C. and Cook, P., Color test for detection of free terminal amino groups in the solid phase synthesis of peptides. *Anal. Biochem.,* **1970**. 34: p. 595-598.
10. Schartl, W., Crosslinked spherical nanoparticles with core shell topology. *Adv. Mater.*, **2001**. *12*(24): p. 1899 - 1908.
11. Torchilin, V., Structure and design of polymeric surfactant-based drug delivery systems. *J. Control. Rel.,* **2001**. *23*: p. 137-172.
12. Watson, P., Jones, A. and Stephens, D., Intracellular trafficking pathways and drug delivery: fluorescence imaging of living and fixed cells. *Adv. Drug Del. Rev.,* **2005.** *57*: p. 43-61.
13. Jones, A., Gumbelton, M. and Duncan, R., Understanding endocytic pathways and intracellular trafficking: a prerequisite for effective design of advanced drug delivery systems. *Adv. Drug Del. Rev.,* **2003**. *55*: p.:1353-1357.
14. Duncan, R., Ringsdorf, H. and Satchi-Fainaro, R., Polymer therapeutics polymers as drugs, conjugates and gene delivery systems: past, present and future opportunities. *Adv. Polym. Sci.,* **2006**. *192*: p. 1-8.
15. Zhao, H., Lee, C., Sai, P., Choe, Y., Boro, M., Pendri, A., Guan, S. and Greenwald, R., 20-O-acylcamptothecin derivatives: evidence for lactone stabilization. *J. Org. Chem.*, **2000**. *65*(15): p. 4601-4606.
16. Greenwald, R., Annapurna, P., Conover, C., Lee, C., Choe, Y., Gilbert, C., Martinez, A., Xia, J., Wu, D. and Hsue, M., Camptothecin-20-PEG ester transport forms:

the effect of spacer groups on antitumor activity. *Bioorg. Med. Chem.*, **1998**. *6*: p. 551-562.
17. Maeda, H., Greish, K. and Fang, J., Exploiting the enhanced permeability and retention effect for tumor targeting. *J. Adv. Polym. Sci.*, **2006**. *193*: p. 103.
18. Altintas, O., Yankul, B., Hizal, G. and Tunca, U., A3 type star polymers via click chemistry. *J. Polym. Sci.: Part A: Polym. Chem.,* **2006**. *44*(21): p. 6458-6465.
19. Zhu, Y., Huang, Y., Meng, WD., Li, H. and Qing, F., Novel perfluorocyclobutyl (PFCB)-containing polymers formed by click chemistry. *Polymer,* **2006**. *47*(18): p. 6272-6279.
20. Vogt, A. and Sumerlin, B. An efficient route to macromonomers via ATRP and click chemistry. *Macromolecules*, **2006**. *39*(16): p. 5286-5292.

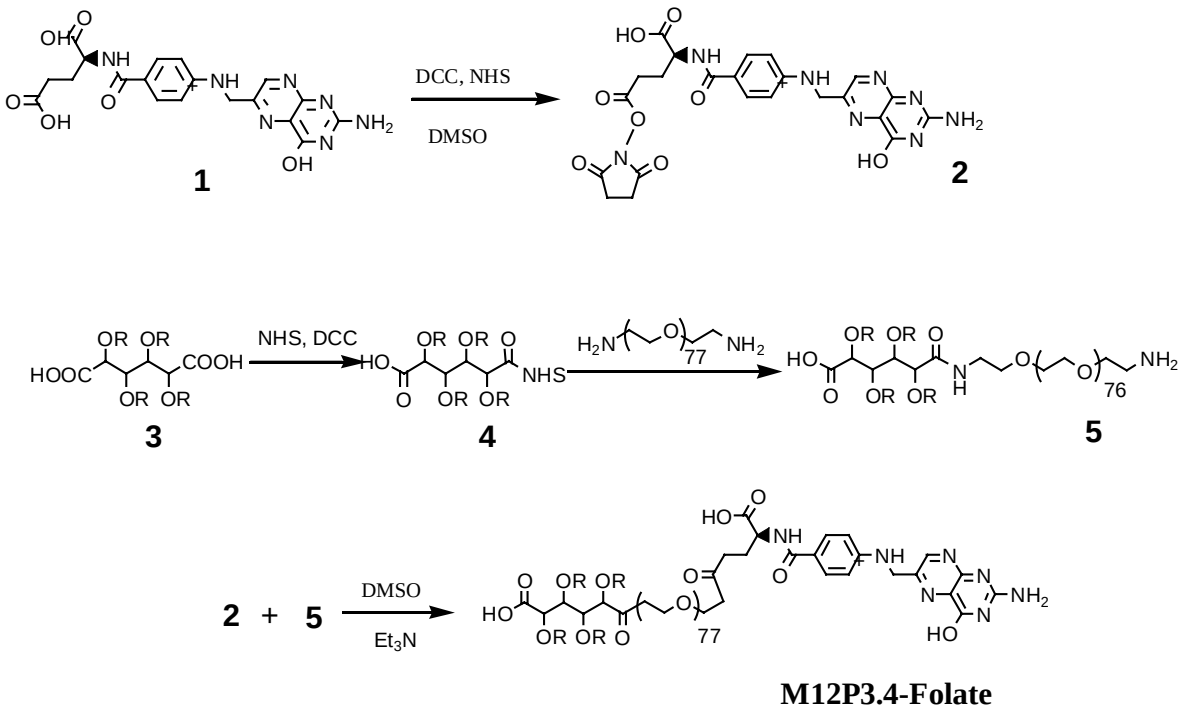


Scheme 5-1: Coupling of folic acid on the hydrophilic end of AScM.

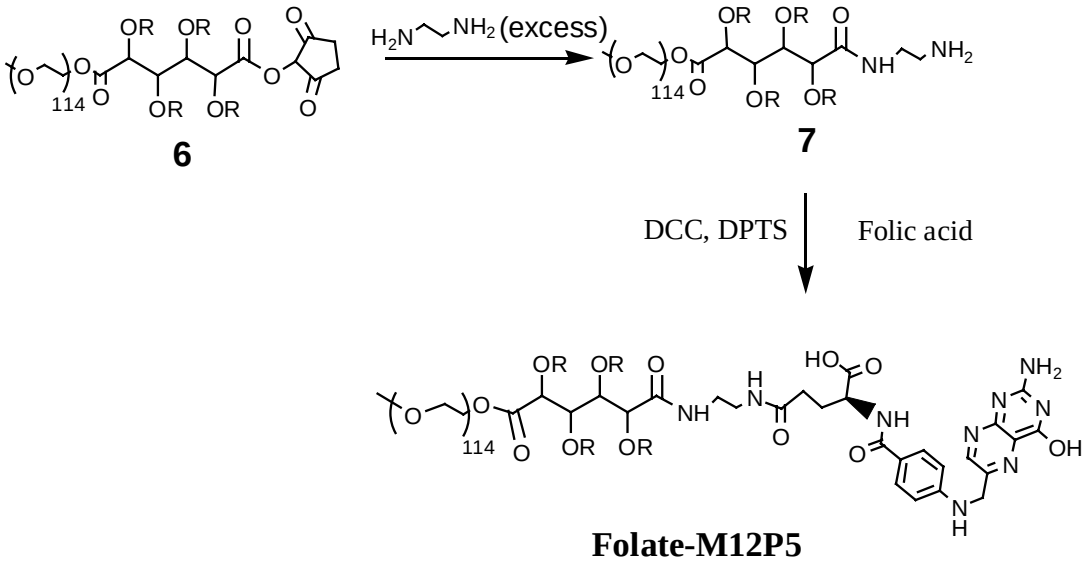


Scheme 5-2: Coupling of folic acid on the hydrophobic end of AScM.

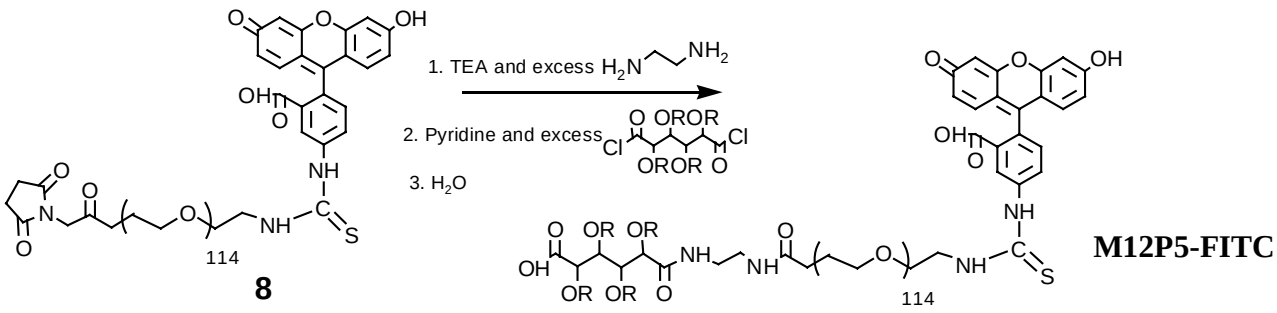


Scheme 5-3: Coupling of FITC on the hydrophilic end of AScM.

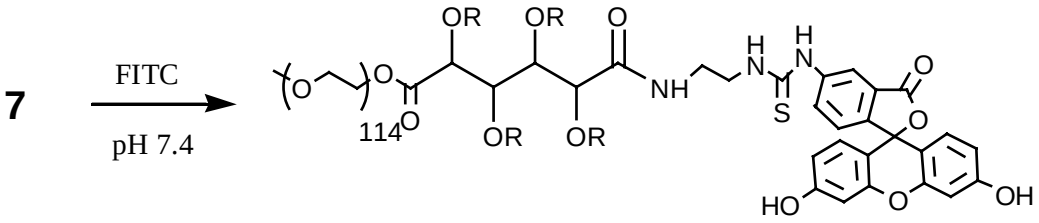


**FITC-M12P5**

Scheme 5-4: Coupling of FITC on the hydrophobic end of AScM.

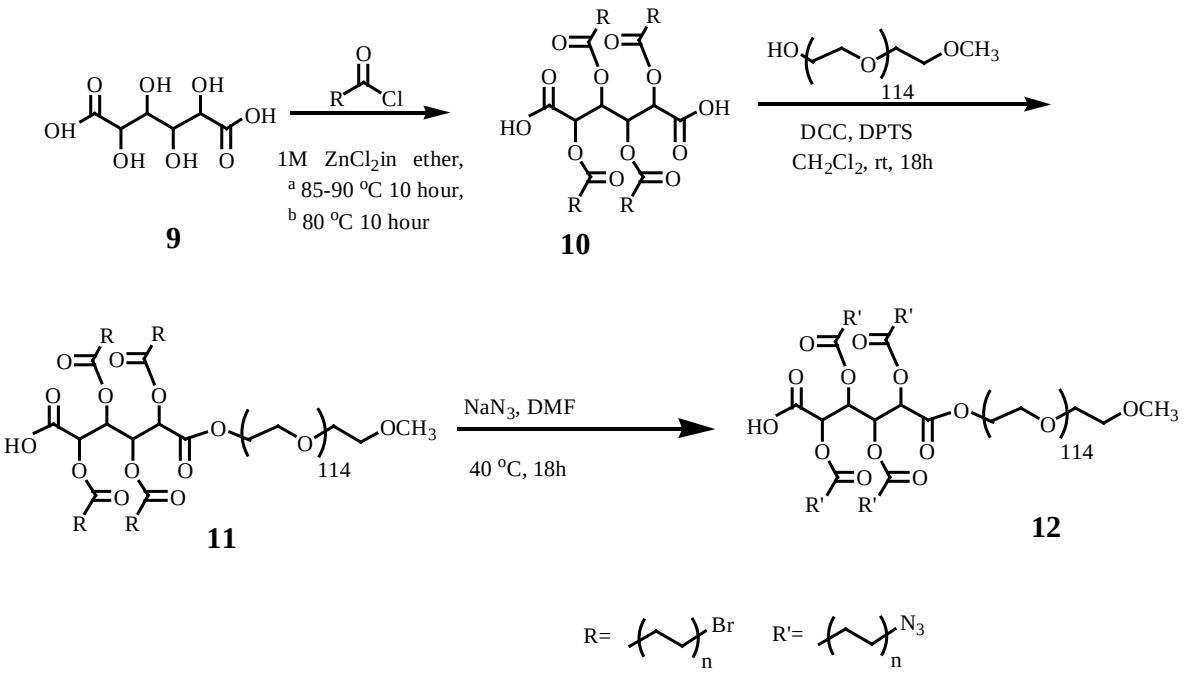


Scheme 5-5: Functionalization of hydrophobic terminal, where **a** is n=2 and **b** is n=5

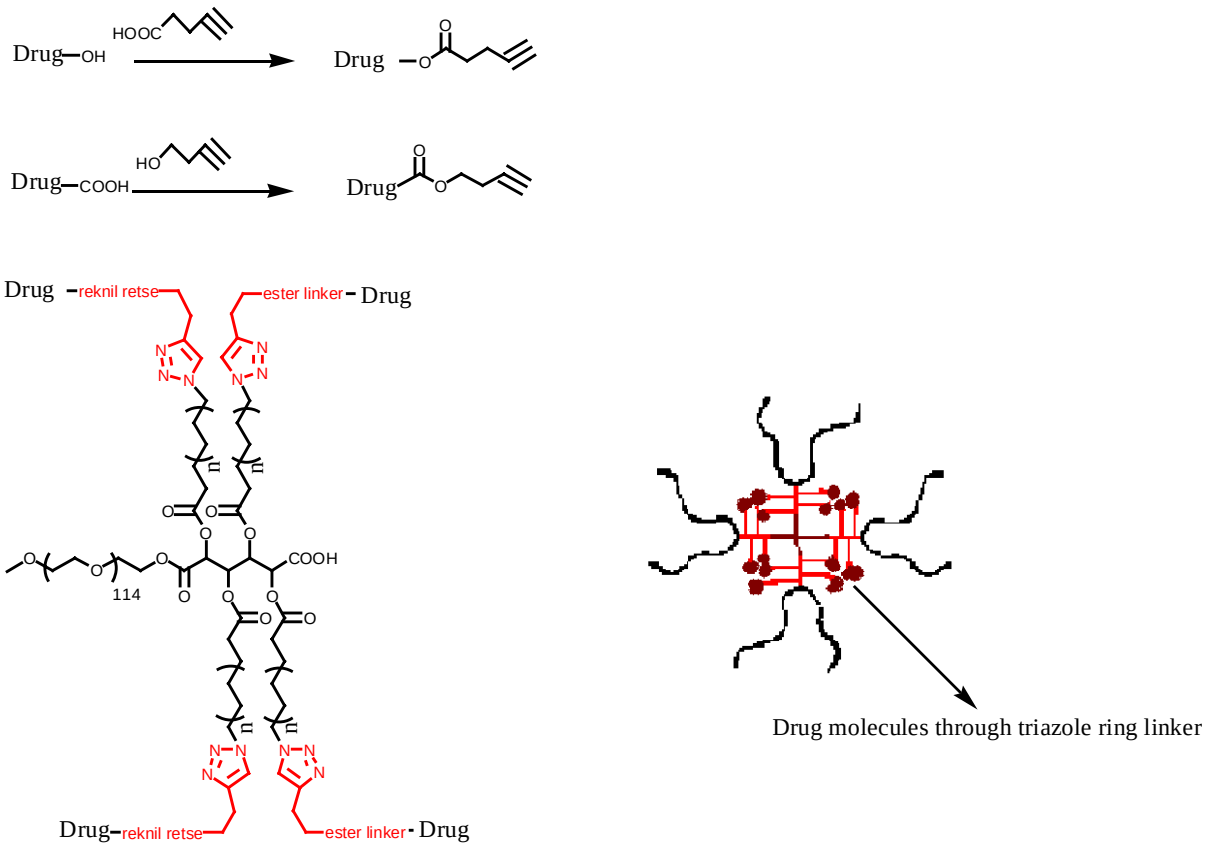


n=1 & 4.

Scheme 5-6 Future works for AScM-drug conjugation through click chemistry

# CURRICULUM VITA

## Jinzhong Wang

### EDUCATION

09/2002-10/2007 PhD, Polymer Chemistry
Department of Chemistry and Chemical Biology
Rutgers University, New Brunswick, NJ, USA
Advisor: Professor Kathryn Uhrich
Co-Advisor: Professor Prabhas Moghe

09/1998-05/2002 B.S., Chemistry
Department of Polymer Chemistry
Peking University, Beijing, China
Advisor: Professor Gaoyuan Wei

### RESEARCH EXPERIENCE

06/2007 –08/2007 Summer Internship
Research Engineering
ExxonMobil, Clinton, NJ, USA
Advisor: Dr. Ahbi Patil

09/2002 –05/2007 Research Assistant
Department of Chemistry and Chemical Biology
Rutgers University, New Brunswick, NJ, USA

### TEACHING EXPERIENCE

09/2004-12/2006 Mentored to undergraduate research students: Andrew Wu, Steven Linguito, Angela Bae, Anthony Argenti, Eric Wydra and Julius Johnson

09/2002 –05/2004 Teaching Assistant
Department of Chemistry and Chemical Biology
Rutgers University, New Brunswick, NJ, USA

### JOURNAL PUBLICATIONS

- **Wang, J**; Plourde, N; Iverson, N; Moghe, PV and Uhrich, KE "Design and Evaluation of Nanoparticles in Inhibiting Highly Oxidized Low Density Lipoproteins Uptake by Macrophages-with Varied Number and Location of Carboxylates" *International Journal of Nanomedicine* (In Press, September 2007) [invited].
- Steege, K. E; **Wang, J**; Uhrich, KE and Castner Jr. EW "Local Polarity and Microviscosity in the Hydrophobic Core of Amphiphilic Star-like and Scorpion-like Macromolecules" *Macromolecules,* **2007**, *40*, 3739-3748.
- **Wang, J**; Argenti, A and Uhrich, KE "Nanoscaled Amphiphilic Star-like Macromolecules with

Carboxyl-, Methoxyl- and Amine-terminated Chain Ends" *Journal of Bioactive and Compatible Polymers*, **2006**, *21*, 297-312.

- Chnari, E; Nikitczuk, JS; **Wang, J**; Uhrich, KE and Moghe, PV "Engineered Polymeric Nanoparticles for Receptor-targeted Blockage of Oxidized Low Density Lipoprotein Uptake and Artherogenesis in Macrophages" *Biomacromolecules,* **2006**, *7(6)*, 1796-1805.
- Tian, L; Yam, L; **Wang, J**; Tat, H and Uhrich, KE "Core Crosslinkable Polymeric Micelles from PEG-lipid Amphiphiles as Drug Carriers." *Journal of Materials Chemistry*, **2004**, *14(14)*, 2317-2324.

**PATENTS/APPLICATIONS**

- Chnari, E; **Wang, J**; Moghe, PV and Uhrich, KE "The role of Chemical Architecture of Nanoparticles in Blocking of Cellular Clearance of LDL" Application No: 60/706.373. Rutgers ID: 06-016
- Uhrich, KE; **Wang, J** and Moghe, PV "Micelle Assemblies" (Filed February 9, 2007).